

# **Battery Cage Mechanics for the Renewable Energy Vehicle Project**

**Christian A. Tietzel**

10415074

School of Mechanical Engineering, The University of Western Australia

**Supervisor: Associate Professor Kamy Cheng**

School of Mechanical Engineering, The University of Western Australia

**Co-Supervisor: Professor Thomas Braunl**

School of Electrical, Electronic and Computer Engineering, The University  
of Western Australia

**Final Year Project Thesis**

**School of Mechanical Engineering**

**The University of Western Australia**

**Submitted: October 26<sup>th</sup>, 2009**

## **Project Summary**

In Australia there is growing recognition of the need for actions to address the increasing effects of global warming. There is therefore a greater requirement for renewable energy technologies. Australia has a heavy dependence on automobile transportation which produces large amounts of green house gases and hence requires an alternative solution. In 2009 the Renewable Energy Vehicle team from The University of Western Australia converted a Lotus Elise sports car into an electric drive system whilst striving to maintain its performance characteristics and road worthiness. A Hyundai Getz commuter vehicle which was converted in 2008, was analysed throughout 2009, and upgraded where necessary to maximise performance efficiency and comfort. The vehicle is now undergoing approval from the Department for Planning and Infrastructure.

This project is responsible for the placement, design and construction of the battery cages for the Lotus Elise. The placement depends upon many factors such as the centre of gravity and axle loadings which will also affect the performance of the vehicle. The design is required to adhere to the rules set out in the national guidelines for the installation of electric drives in motor vehicles which must be read in conjunction with other relevant codes and standards. The battery cages were designed and analysed with the aid of SolidWorks and ANSYS Workbench. They were then constructed and installed predominantly by the UWA Electrical Engineering workshop and are currently operational.

The Hyundai Getz battery cage enclosure was sealed and temperature tested, and an active venting system was designed and installed to maximise the efficiency and lifetime of the batteries. The system is currently operational and automatically controlled by a thermostat.

**Letter of Transmittal**

Christian A. Tietzel  
169 Broome Street  
Cottesloe, WA, 6011

26<sup>th</sup> October, 2009

Professor David Smith  
Dean  
Faculty of Engineering, Computing and Mathematics  
The University of Western Australia  
35 Stirling Highway  
Crawley, WA, 6009

Dear Professor Smith

I am pleased to submit this thesis, entitled “**Battery Cage Mechanics for the Renewable Energy Vehicle Project**”, as part of the requirement for the degree of Bachelor of Engineering.

Yours Sincerely

Christian A. Tietzel  
10415074

### **Acknowledgements**

This project would not have been successfully completed without the continual support and guidance from many personnel. I would firstly like to thank my mechanical engineering supervisor, Kamy Cheng, for his continual advice and guidance on all topics explored in my project. Secondly to thank my co-supervisor, Thomas Braunl, who has managed the REV team throughout 2009 to produce a safe working vehicle.

I would like to thank the Electrical Engineering workshop for their patience and time spent fabricating and installing the components designed. In particular I would like to mention Ken Fogden, who has also given continual advice in all design aspects of the vehicle. Similarly, thanks to the Mechanical workshop, particularly Derek Goad, for fabrication of individual components. I would also like to thank Jeremy Leggoe for his advice on thermodynamic topics covered in the design of the venting system for the Hyundai Getz.

To all the members of the REV team and all the additional people that have contributed in some way, I would like to say thank you, as this project has largely been a team effort which would not have been completed without the input from all members and associates.

## Contents

|     |   |    |
|-----|---|----|
| 1   | Introduction.....                                       | 1  |
| 1.1 | Background.....   | 1  |
| 1.2 | Project Objectives.....                                 | 3  |
| 2   | Literature Survey.....                                  | 4  |
| 2.1 | Chapter Overview.....                                   | 4  |
| 2.2 | Battery Cage Location.....                              | 4  |
| 2.3 | Lithium-Ion Batteries.....                              | 7  |
| 2.4 | Battery Cage Codes and Standards.....                   | 8  |
| 3   | Battery Cage Ventilation System for Hyundai Getz.....   | 10 |
| 3.1 | Overview.....   | 10 |
| 3.2 | Design.....   | 10 |
| 3.3 | Results & Discussion.....                               | 23 |
| 4   | Battery Restraint System for Lotus Elise.....           | 27 |
| 4.1 | Overview.....   | 27 |
| 4.2 | Design Process.....                                     | 27 |
| 4.3 | Results & Discussion.....                               | 34 |
| 5   | Manufacture and Implementation Safety Requirements..... | 54 |
| 6   | Conclusion & Future Work.....                           | 55 |
| 7   | References.....   | 57 |
| 8   | Appendices.....   | 60 |

## Nomenclature

|                           |   |
|---------------------------|---|
| $A_c$                     | Minor diameter area   |
| $A_c$                     | Cross sectional area  |
| $a_e$                     | Minimum distance from the edge of a hole to the edge of a ply measured in the direction of the component of a force plus half the bolt diameter |
| $A_s$                     | Surface area  |
| $A_s$                     | Tensile stress area   |
| $d_f$                     | Diameter of the bolt  |
| $D_h$                     | Hydraulic diameter  |
| $E$                       | Young's modulus   |
| $f$                       | Friction factor   |
| $F_{\text{Front impact}}$ | Front impact force  |
| $f_{uf}$                  | Minimum tensile strength  |
| $g$                       | Gravitational acceleration  |
| $h$                       | Convection heat transfer coefficient  |
| $k$                       | Thermal conductivity  |
| $l$                       | Length of bar   |
| $L$                       | Length of tube  |
| $L_c$                     | Characteristic length   |
| $L_t$                     | Thermal entry length  |
| $m$                       | Mass  |
| $n$                       | Number of routes  |
| $N_{tf}$                  | Nominal tensile capacity  |
| $Nu$                      | Nusselt number  |
| $p$                       | Perimeter   |
| $P$                       | Pitch   |
| $Pr$                      | Prandtl number  |
| $q$                       | Flow rate   |
| $\dot{Q}$                 | Heat transfer rate  |
| $R$                       | Thermal resistance  |
| $Ra_L$                    | Rayleigh's number   |
| $Re$                      | Reynolds number   |
| $T$                       | Temperature   |
| $T_{\text{avg}}$          | Average temperature   |
| $t_p$                     | Thickness of ply  |
| $T_{\infty}$              | Ambient Temperature   |
| $V_{\text{avg}}$          | Average velocity  |
| $V_b$                     | Nominal bearing capacity  |
| $V_f$                     | Nominal shear capacity  |
| $\beta$                   | Volume expansivity  |
| $\Delta l$                | Elongation distance   |

|                      |                       |
|----------------------|-----------------------|
| $\Delta P_L$         | Pressure loss         |
| $\Delta T$           | Change in temperature |
| $\varepsilon$        | Strain                |
| $\varepsilon_{\max}$ | Maximum strain        |
| $\nu$                | Kinematic viscosity   |
| $\rho$               | Density               |
| $\sigma_y$           | Yield strength        |

## **1 Introduction**

### 1.1 Background

Australia and the world are becoming more aware and responsive to the effects of climate change. The Intergovernmental Panel on Climate Change found in their fourth assessment report 2007, that there is a 90% chance that global warming is caused by greenhouse gas emissions (Pachauri & Reisinger 2007). With these realisations, and also given the limited supply of oil, Australia ratified the Kyoto Protocol in December 2007 and requires immediate research and development for renewable energy technologies. Of the 576 million tonnes of carbon dioxide emitted in Australia in 2006, 14% was due to transportation (Department of Climate Change 2008). As a result of Australia's small population and large land mass there is a high reliance on automobile transportation. Hence there is high demand in the car industry for zero emission vehicles to be available to the public. These cars must have the performance, luxuries and comparative costs to be a competitive viable option for everyday users.

The Renewable Energy Vehicle (REV) team at The University of Western Australia (UWA) was re-started in 2008 by Professor Thomas Braunl and Associate Professor Kamy Cheng with an aim to develop renewable energy vehicle technologies, that is, ways of powering a vehicle without relying on petrol or diesel. The REV team precursor project had looked at hydrogen technologies but with electric vehicles being far simpler, cost effective and easier to charge from a standard plug point (Braunl 2009), the focus was changed. Although an electric vehicle must be charged from the power grid, the equivalent level of CO<sub>2</sub> emissions per kilometre are still less than the level of emissions for the most recent technology petrol vehicles. For example the new electric MINI, MINI-E, when charged from an Australian outlet produces the equivalent of approximately 14.6kg of CO<sub>2</sub> per 100km (see Appendix A for calculation) compared to the petrol MINI Cooper which produces 16.1kg of CO<sub>2</sub> per 100km (MINI 2009b). However as electricity generating renewable energy technologies rapidly grow this gap will widen. To confirm this point, the REV team charges it's vehicles from solar cells located on the roof of the UWA Electrical Engineering building. Furthermore, future electric vehicles will generally be used to commute by day and charge up overnight on low-peak electricity. This won't affect dirty coal power stations as they will be running to cover the base load requirement and it will be a long time until there are enough electric cars to increase this requirement (Marshall 2009). To demonstrate the viability

of renewable energy transportation, everyday commuter and performance vehicles are used for conversion. If these cars can be converted at a low cost without sacrificing performance characteristics and practical features, they will be a competitive alternative for public users.

In 2008 the UWA REV team converted a Hyundai Getz, five-seater commuter vehicle into an electric drive vehicle. In 2009 the REV team aims to convert a Lotus Elise S2, two seater performance vehicle into electric drive. The aims of this project it to work closely with the REV team whilst managing the Lotus mechanical students to achieve completion of the vehicle by the end of 2009, and assist in upgrading the Hyundai where necessary. The main focus is on the design and construction of the battery cages for the Lotus, as well as analysis and design of a venting system for the Hyundai.

## 1.2 Project Objectives

This project focuses on battery cages for the REV team in 2009. The major task of this project is to complete the structural designs of battery cages and necessary mountings for the 2002 model Lotus Elise in accordance with the Australian Design Rules for modification of production and individually constructed vehicles. A total of 100 lithium-ion batteries or as close to must be housed in the vehicle. In designing the battery cages, particular consideration must be given to the affects the battery placements have on the overall performance of the vehicle. This must be done in conjunction with members of the REV team who are focusing on the drive mechanics, suspension, analysis of the weight distribution and cooling systems for the Lotus Elise.

The second focus of this project is on the ventilation of the currently operating battery cage for the 2008 model Hyundai Getz. The current Hyundai Battery Cage adhered to the relevant Australian Design Rules at the time of construction but the batteries are reaching temperatures above which their life expectancy is reduced. The batteries or connections are also unexpectedly releasing an irritating odour intermittently. Hence there is a requirement for a sealed ventilation system for the battery cage. This project will focus on the mechanical designs for the system to overcome these issues.

As the REV team aims to promote the electric car as a practical alternative to the common petrol powered vehicle, both cars must be aesthetically pleasing in all aspects. This report will initially focus on the Hyundai Getz ventilation system followed by the methodology for design of the battery cages for the Lotus Elise in 2009.

## **2 Literature Survey**

### 2.1 Chapter Overview

This chapter explores the various considerations that be must be made when designing a battery cage for an automotive vehicle and briefly describes the impacts they can have on the overall performance of the vehicle. The effects of operating conditions on lithium-ion batteries are also discussed as well as the relevant guidelines that must be adhered to in conjunction with the Australian Design Rules for modification of production and individually constructed vehicles

### 2.2 Battery Cage Location

Particular considerations must be given to the placement of the battery cages due to the relatively large weight they add to the vehicle. Altering the weight distribution of the vehicle can change the ride height and centre of gravity, affecting the handling of the car. The total weight of the vehicle also affects the acceleration and top speed. Therefore suitable placements of the batteries must be found that have minimal effects on these characteristics, whilst being structurally safe.

#### *2.2.1 Weight Implications*

For directional stability when driving an automotive vehicle, understeer is preferred, that is it tends to travel in a straight line, as oppose to oversteer where the car tends to spin. A way of understanding the directional stability of the vehicle is to consider the position of the neutral steer point (NSP) in relation to the position of the horizontal centre of gravity (COG) and the centre of pressure (COP), see Figure 1 below. The NSP is the point at which a laterally applied force would cause a vehicle to move sideways without yawing. To achieve understeer, the NSP must be behind the COG, hence during a turn the tyre forces act at the NSP and the inertia forces at the COG, the combined forces tend to yaw the car out of the bend and into a straight line. However if the car is subject to side winds, the wind force will act at the COP which is generally located in front of the COG, coupling this force with the forces acting on the tyres at the NSP, the car will tend to yaw away from the wind (Bastow 2004). Therefore it is desired that the NSP is kept behind the COG but the distance between the NSP and COP is kept at a minimal.

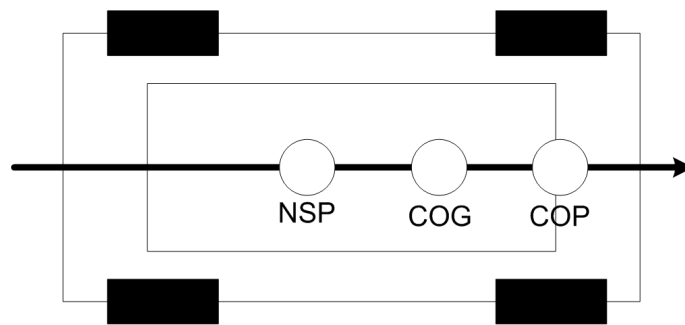


**Figure 1:** Relative Positions of NSP, COG and COP on a vehicle (Bastow 2004).

Similarly to the horizontal COG, the vertical COG should also be kept constant or otherwise lower. A low COG is desirable as it is generally associated with fewer driving dynamic problems and increased vehicle performance during cornering and braking (Reimpell 2001).

Altering the overall weight of the vehicle can have significant affects on the acceleration and top speed. From Newton's second law, it is clear that the acceleration varies directly with mass for a given force, even when incorporating the added inertia of the vehicles rotating parts, the acceleration for a given accelerating force is still inversely proportional to the mass of the vehicle. Similarly for speed and range of the vehicle with a fixed amount of energy, the weight is inversely proportional (Leitman & Brant 2009).

By altering the weight distribution and overall weight of the vehicle the ride height can also be changed. The ride height of a vehicle can be defined as the distance between the chassis of a vehicle and level ground. Changes in the ride height of the vehicle can significantly affect the suspension and handling, for example it can alter the roll axis of the vehicle and for ride height differences from side to side it can effect torque steer (Bastow 2004). Changing the ride height can also affect things such as the headlamp dip angle and vehicle ground clearance.

Hence it is vitally important, when selecting positions to place parts in an electric vehicle conversion that all the above factors are taken into account. It is ideal to keep the weight distribution, total weight and ride height the same as before conversion but not at the cost of safety.

### 2.2.2 *Current Electric Vehicles*

As seen with the Hyundai Getz converted by the REV team in 2008, there has to be a balance of practicality, aesthetics and vehicle performance. The battery cage in the Hyundai Getz (see Figure 2) was located in the rear boot of the vehicle. This was an obvious place to put the forty five lithium-ion batteries as there was inadequate room in the front engine bay and it was discouraged to sacrifice a passenger seat. However this did cause weight distribution issues with the Department for Planning and Infrastructure (DPI) who conveyed their concerns for overloading of the rear axle. An adequate solution was found by the 2009 REV team of upgrading the rear axle springs. This was approved by a professional automotive engineer. Therefore although identical performance issues were avoided in the Hyundai Getz, the advantages of each design must be prioritised and dealt with accordingly. For the Hyundai Getz, overloading of the rear axle was unavoidable without sacrificing a passenger seat.

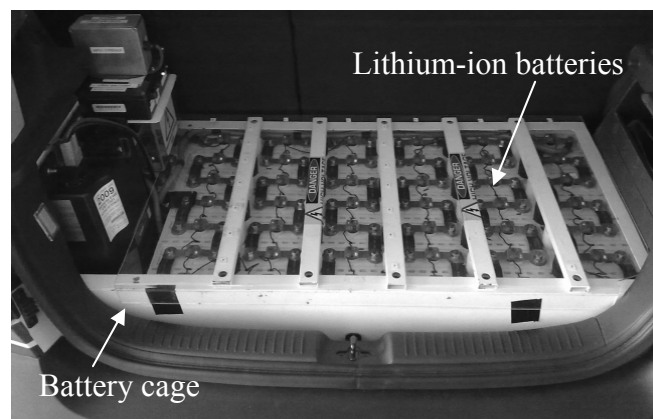


**Figure 2:** Hyundai Getz Battery Cage in the boot.

Current electric vehicle designs and concept models were also studied for ideas on battery placements. To maintain the COG and ride height, most cars have the batteries located as low and central as possible in the vehicle, for example the Holden Volt and MINI-E (see Figure 3) for reasons discussed previously. For vehicles designed and built initially as electric drives, all components can be fitted and designed compactly around the battery packs which demand a large space. As opposed to the constraints imposed on the REV team who must convert purpose built petrol vehicles using the available space left from the removal of petrol engine components for battery placements.

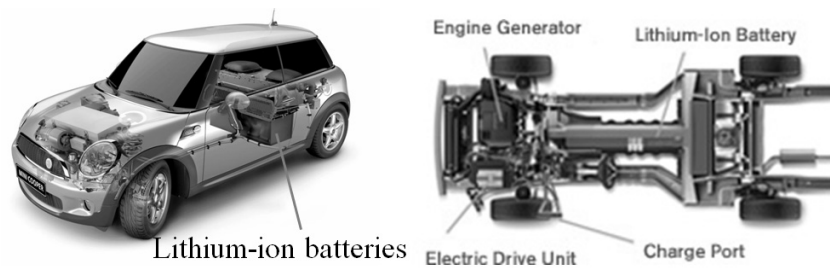


**Figure 3:** MINI-E (MINI 2009a) & Holden Volt (Holden 2009) battery placements respectively.

### 2.3 Lithium-Ion Batteries

Both the Hyundai Getz and Lotus Elise are powered by Thunder Sky lithium-ion batteries, models TS-LFP90AHA and TS-LFP60AHA respectively. Lithium-ion batteries are now the standard for electric vehicles due to their high power and energy density, and long life cycle compared to lead-acid and nickel metal hydride batteries, although this performance comes at a relatively large cost (Siguang 2009). Lithium-ion batteries produce the same amount of energy as nickel metal hydrides but they are typically forty percent smaller and half the weight (Dhameja 2001). This is essential in an electric vehicle as the total weight and distribution are the critical factors in determining the number of batteries stored on board.

The safe operating temperature for these batteries is displayed as anywhere from  $-25^{\circ}\text{C}$  to  $75^{\circ}\text{C}$  although to prolong the usable life and maximise performance of these batteries, the temperature must be monitored. For lithium-ion batteries the immediate performance is increased for higher temperatures. For increased temperature the discharge capacity of each cell is increased (see Figure 4). Essentially the available energy lost internally in each cell is decreased as the higher temperature lowers the batteries internal resistance.

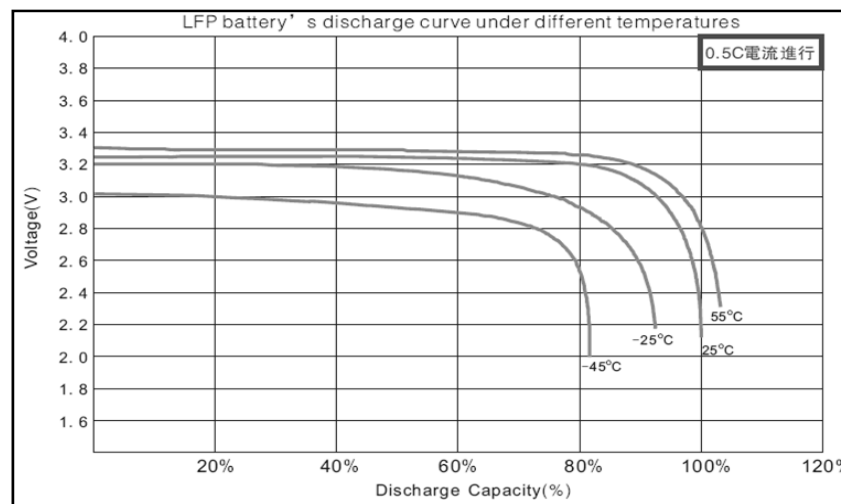


**Figure 4:** Discharge capacity vs. Voltage for various temperatures (Thunder Sky 2007)

However at elevated temperatures, the battery cells life time is reduced (Garche & Jossen 2000). A study on the life of lithium-ion batteries for back up applications kept them on continuous float charge with periodic discharging. It found that the cell degradation is significantly accelerated at elevated temperatures, a 15°C increase in temperature cuts the cell life in half (Asakura, Shimomura & Shodai 2003). Therefore there must be a compromise between battery performance and battery lifetime during discharging. However temperatures should be kept as low as possible for charging.

#### 2.4 Battery Cage Codes and Standards

As both the Hyundai Getz and Lotus Elise must be registered and roadworthy, they must comply with the Australian Design Rules (ADRs) for modification of production and individually constructed vehicles (ICVs). Both vehicles are classified as a passenger car, code MA. Section LO *Vehicle Standards Compliance* of the *National Code of Practice for Light Vehicle Construction and Modification* (NCOP) outlines the minimum requirements for the assessment and certification of compliance with the ADRs for ICVs. The vehicles must also comply with the specific regulations of NCOP14 *National Guidelines for the Installation of Electric Drive in Motor Vehicles* (Australian Motor Vehicle Certification Board Working Party 2006), of which the relevant battery cage codes and standards will be outlined further.

NCOP14 stipulates that the vehicle batteries must be fixed in position and housed in a battery restraint system which can adequately withstand vehicle crash accelerations set out in Table 1, for example for front impact they must withstand twenty times gravity, times the battery mass.

|                            |      |
|----------------------------|------|
| Front Impact               | 20 g |
| Side Impact                | 15 g |
| Rear Impact                | 10 g |
| Vertical (rollover) Impact | 10 g |

**Table 1:** Acceleration requirements that battery restraint system must withstand.

All batteries that contain liquid or give off gases must be sealed from the vehicle interior so neither liquid nor gas can leak into the vehicle. Depending on the batteries, they can be individually sealed and externally vented directly to the atmosphere, or the battery cage must be fully enclosed in a sealed compartment. Following further discussions with the DPI about sealed batteries, this regulation is only applicable for lead acid batteries as they can give off hydrogen in sufficient quantities to cause an

explosion. Furthermore the battery restraint system must be constructed of corrosion resistant material or adequately coated.

Should a ventilation system for gases be required, the inlet and outlet openings should be external to the vehicle. They should also be placed where the local pressure favours the required air flow direction. The air flow rate should be adequate to remove gas formation, and the inlets and outlets should be placed at opposite ends of the enclosure. A forced ventilation system may be required depending on the type and size of the vents, particularly for lead acid batteries. The system should operate automatically and extract gas from the battery compartment and not blow air in, as to avoid blowing gas into the interior of the vehicle through leaks in the compartment.

There are several other miscellaneous regulations that the vehicle must comply with or consider, including clear labelling of the battery compartment with the appropriate hazard symbols and an indication of the voltage likely to be encountered. It is also recommended that the vehicle be designed for prolonged operation in Australia's wide range of climatic conditions including ambient temperatures from  $-10^{\circ}\text{C}$  up to  $50^{\circ}\text{C}$ . The regulations also advise on considering the overall weight supported by the vehicle and the specific weight on each component due to the addition of the electric motor and batteries. The total weight could be less but the weight distribution could be significantly different, overloading individual components. When performing these calculations, the weight of the laden vehicle must be taken into consideration allowing at least 68kg per passenger plus 13.6kg of luggage for each. All regulations stated above must be adhered to in conjunction with any other relevant sections of the NCOP.

### **3 Battery Cage Ventilation System for Hyundai Getz**

#### 3.1 Overview

The Hyundai Getz battery cage does not require sealing or venting in accordance with the ADRs as sealed lithium-ion batteries are used. However the batteries in the battery cage which was designed in a previous year (Ip 2008) have been reaching temperatures above which the life expectancy is reduced during charging and discharging. Hence there is a requirement for an active venting system. The batteries or connections are also unexpectedly creating an irritating odour in the car cabin intermittently once every few weeks. It is suspected that this is from the heating of their casings or the cabling as the batteries are individually sealed and not meant to release gases (Thunder Sky 2007). The gas was tested several times for safety by the UWA chemistry lab and returned each time to be unknown, containing standard air properties. Therefore for the comfort and safety of the driver and passengers, removal of this gas is required by sealing the battery cage.

#### 3.2 Design

##### *3.2.1 Design Requirements*

1. To actively vent the cage for cooling purposes, a fan(s) is required to provide a constant airflow throughout. The optimal temperature for the batteries during discharging to increase its discharge capacity is 75<sup>0</sup>C, the maximum safe limit of the batteries. However, as discussed in section 2.3 *Lithium-Ion Batteries*, this can dramatically decrease the operating life of the batteries. As a compromise, a maximum discharging temperature of 60<sup>0</sup>C was agreed upon by the REV team. During charging the batteries should also be kept at a relatively low temperature to increase their operating life. It was agreed that it should only rise by a maximum of 5<sup>0</sup>C above ambient temperature to prolong the life. Hence an appropriate fan(s) must be sought to operate under these requirements.
2. To conceal the odour from the batteries, the cage must be sealed air tight. As an active venting system is required for cooling, the air flow must have an inlet and an outlet to the outside of the vehicle.

### 3.2.2 *Testing and Constraints*

To measure the level of cooling required throughout the vehicle during discharging, temperatures throughout the cage were taken whilst performance testing the car. The maximum temperature reached during discharging was 55<sup>0</sup>C, however this temperature was reached on a cool winter's day when the ambient temperature was only 23<sup>0</sup>C. If designing to the maximum ambient temperature of 50<sup>0</sup>C set out in NCOP14, the batteries would easily rise above the maximum limit of 60<sup>0</sup>C. Hence a maximum temperature rise of 10<sup>0</sup>C is taken as a worst case scenario for discharging.

Readings of the battery temperatures were also taken during charging. The maximum temperature reached throughout the cage during charging was 38<sup>0</sup>C when the ambient temperature was 16<sup>0</sup>C. As vehicle charging is normally done overnight, when ambient temperatures are low and usually reach no more than 25<sup>0</sup>C, the system is design so the batteries rise to a maximum of 30<sup>0</sup>C. Hence a maximum 5<sup>0</sup>C temperature rise is taken as a worst case scenario for charging.

The cage has been built previously to adhere to the guidelines set out in NCOP14, one of which is a strength requirement. Therefore the active venting system and sealing of the battery cage must be done whilst not altering any of the structural members. Due to the limited room in the boot of the Hyundai Getz, the entire floor space has been utilised, leaving no room for a fan(s) or duct inlets or outlets on the sides of the cage (see Figure 2 above). Hence the spare tyre wheel well underneath the cage is used for housing the fan(s) and allowing for inlet and outlet ducts into the cage. These ducts will then run to the bottom of the well to the outside of the vehicle. This also adds to the aesthetics of the vehicle. The wheel well is 200mm deep, also limiting the dimensions of the fan(s) choice. The only available power source during charging and discharging is 12 volts, hence also limiting appropriate fans. This must all be completed at a relatively low cost, with the total cost of the fan(s) amounting to less than \$200.

### 3.2.3 *Fan Technical Requirements*

The two critical factors in selecting the correct fan(s) are the required airflow and the pressure loss. These were calculated using equations and theories from Chapters 16 to 20 and constants from Appendix 1 of Thermal-Fluid Sciences (Cengel 2008) and are referred to in the following sections 3.2.3.1 *Required Airflow* and 3.2.3.2 *Pressure Loss*.

### 3.2.3.1 Required Airflow

The initial step in determining the required airflow is to calculate the rate of heat generated from the batteries ( $\dot{Q}$ ) which is equal to the total rate of heat transfer from the batteries. The transfer of heat from the batteries can be assumed to be primarily from conduction and convection, see Figure 5 below.

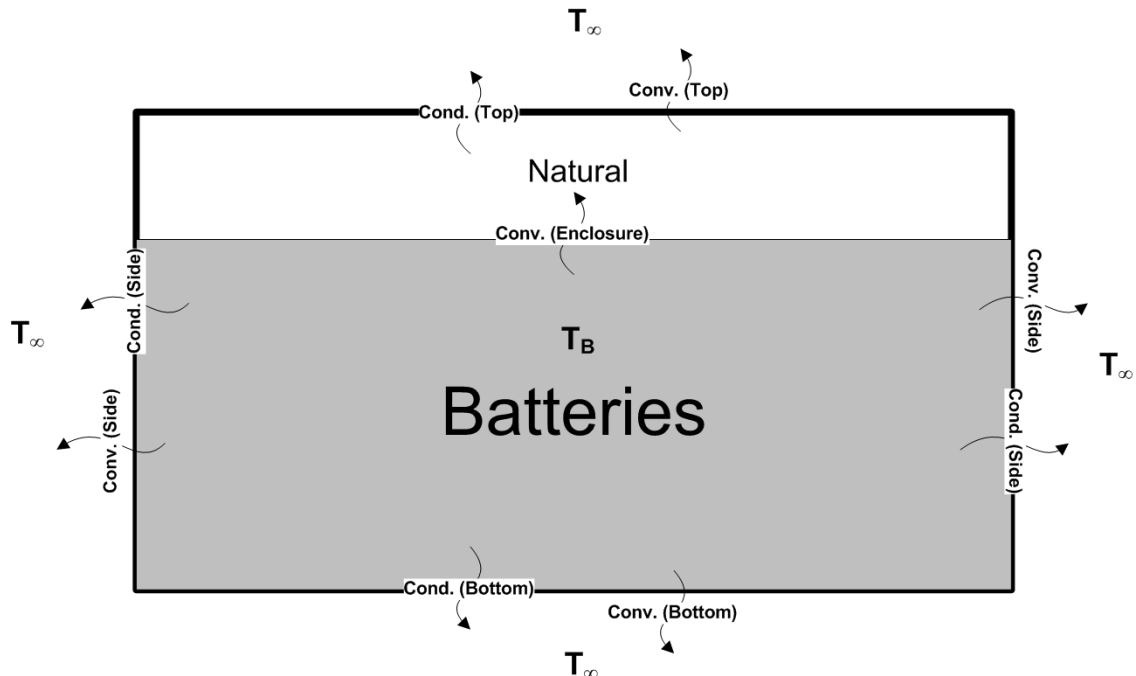


**Figure 5:** Diagram of heat flow from Hyundai Getz batteries.

This diagram can be summarised into a thermal circuit (Figure 6) to assist in calculations. The sides and bottom of the batteries are against thin aluminium which is an excellent conductor of heat, the resistance due to conduction through these walls can therefore be assumed to be zero as the temperature difference from one side to the other is negligible. A thermal circuit is analogous to an electrical circuit where the thermal resistance corresponds to the electrical resistance, the temperature difference corresponds to the voltage difference and the rate of heat transfer corresponds to the electrical current. Therefore the rate of heat transfer through the top path in Figure 6 can be assumed to be constant through each resistor. Hence the rate of heat transfer only needs to be calculated through one resistor for the top path. The total rate of heat generated from the batteries can be calculated by adding the three paths rate of heat transfer together.

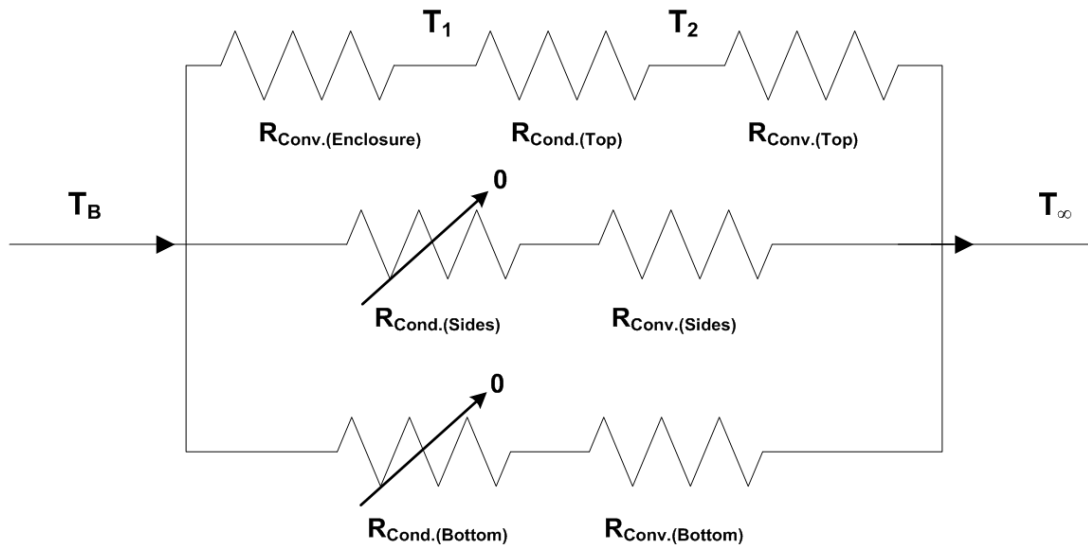


**Figure 6:** Thermal circuit for Hyundai Getz batteries.

To calculate the rate of heat transfer through the top path ( $\dot{Q}_{Top}$ ), equations for natural convection of a horizontal enclosure with a hot bottom surface and isothermal walls is used. Hence it is assumed that  $T_1$  equals  $T_2$ , the temperatures on the inner and outer surface of the thin perspex cover of the cage. Initially Rayleigh's number must be determined for an enclosure (equation 3.1) using the constants set out in Table 2 including the temperature  $T_1$  of the perspex which was measured during testing.

|   | <b>Discharging</b>                       | <b>Charging</b>                          |
|---|--|--|
| Battery temperature ( $T_B$ )                     | 55°C                                     | 38°C                                     |
| Perspex temperature ( $T_1$ )                     | 40°C                                     | 28°C                                     |
| Change in temperature ( $\Delta T$ )              | 15°C                                     | 10°C                                     |
| Average temperature ( $T_{avg}$ )                 | 47.5°C                                   | 33°C                                     |
| Volume expansivity ( $\beta$ )                    | 1/(320.5K)                               | 1/(306K)                                 |
| Prandtl number (Pr)                               | 0.7228                                   | 0.7268                                   |
| Thermal conductivity (k)                          | 0.02735W/mK                              | 0.02625W/mK                              |
| Kinematic viscosity ( $\nu$ )                     | 1.798x10 <sup>-5</sup> m <sup>2</sup> /s | 1.655x10 <sup>-5</sup> m <sup>2</sup> /s |
| Surface area ( $A_s$ )                            | 0.4437m                                  |  |
| Distance between top and bottom surface ( $L_c$ ) | 0.05m                                    |  |

**Table 2:** Various constants for calculation of free convection of enclosure.

Note: For the appropriate constants, values are taken at the average temperature.

$$Ra_L = \frac{g\beta\Delta TL_c^3}{\nu^2} Pr \quad (3.1)$$

Following this Nusselt's number (Nu) can be calculated using equation 3.2, which is the dimensionless convection heat transfer coefficient specific to the flow regime. It can then be transferred into equation 3.3 to give a rate of heat transfer through the top path. The calculation results are summarised in Table 3.

$$Nu = 1 + 1.44 \left[ 1 - \frac{1708}{Ra_L} \right]^+ + \left[ \frac{Ra_L^{1/3}}{18} - 1 \right]^+ \quad (3.2)$$

$$\dot{Q}_{conv} = kNuA_s \frac{\Delta T}{L_c} \quad (3.3)$$

|                 | Discharging | Charging |
|-----------------|-------------|----------|
| Ra <sub>L</sub> | 128,316     | 106,335  |
| Nu              | 4.223       | 4.049    |
| $\dot{Q}_{Top}$ | 15.37W      | 9.43W    |

**Table 3:** Summary of calculations for natural convection of top enclosure.

Next the rate of heat transfer through the bottom surface and side surfaces must be calculated using natural convection over horizontal and vertical plate equations. For these calculations the values from Table 4 are used and firstly inserted into equation 3.4 to calculate Rayleigh's number (Ra<sub>L</sub>) for the bottom and side surfaces separately.

|   | Discharging                              | Charging                                 |
|---|--|--|
| Battery temperature (T <sub>B</sub> )   | 55 <sup>o</sup> C                        | 38 <sup>o</sup> C                        |
| Ambient temperature (T <sub>∞</sub> )   | 23 <sup>o</sup> C                        | 16 <sup>o</sup> C                        |
| Average temperature (T <sub>avg</sub> ) | 39 <sup>o</sup> C                        | 27 <sup>o</sup> C                        |
| Volume expansivity (β)                  | 1/(312K)                                 | 1/(300K)                                 |
| Prandtl number (Pr)                     | 0.7255                                   | 0.7296                                   |
| Thermal conductivity (k)                | 0.02662W/mK                              | 0.02551W/mK                              |
| Kinematic viscosity (ν)                 | 1.702x10 <sup>-5</sup> m <sup>2</sup> /s | 1.562x10 <sup>-5</sup> m <sup>2</sup> /s |

|   | Bottom Surface              | Side Surfaces   |
|---|-----------------------------|-----------------|
| Perimeter of bottom surface (p)                           | 2.982m                      | Not Applicable  |
| Surface area (A <sub>s</sub> )                            | 0.4437m                     | 0.6560m         |
| Characteristic length of bottom surface (L <sub>c</sub> ) | 0.1488m (A <sub>s</sub> /p) | 0.220m (Height) |

**Table 4:** Constants for calculation of free convection of bottom and side surfaces.

Note: For the appropriate constants, values are taken at the average temperature.

$$Ra_L = \frac{g\beta(T_B - T_\infty)L_c^3}{\nu^2} Pr \quad (3.4)$$

Given the calculated Raleigh numbers, they are inserted into equations 3.5 and 3.6 for bottom and side surfaces respectively to calculate Nusselt's number. Following this the rate of heat transfer can be calculated using equation 3.7, see Table 5 for a summary of the calculated values.

$$Nu_{Bottom} = 0.27Ra_L^{1/4} \quad (3.5)$$

$$Nu_{Side} = \left\{ 0.825 + \frac{0.387Ra_L^{1/6}}{[1 + (0.492/Pr)^{9/16}]^{8/27}} \right\}^2 \quad (3.6)$$

$$\dot{Q}_{conv} = kNuA_s \frac{(T_B - T_\infty)}{L_c} \quad (3.7)$$

|           | Bottom Surface |           | Side Surface |            |
|-----------|----------------|-----------|--------------|------------|
|           | Discharging    | Charging  | Discharging  | Charging   |
| $Ra_L$    | 8,302,167      | 7,087,646 | 26,831,858   | 22,906,632 |
| $Nu$      | 14.49          | 13.93     | 41.57        | 39.73      |
| $\dot{Q}$ | 36.81W         | 23.31W    | 105.59W      | 66.49W     |

**Table 5:** Summary of calculations for natural convection of bottom and side surfaces.

Now that the rate of heat transfer through each path has been calculated, they can be added up for discharging and charging to obtain the total rate of heat transfer from the batteries which is equal to the total rate of heat generated ( $\dot{Q}_{Total}$ ) from the batteries. This gives 157.77W and 99.23W respectively. For both discharging and charging the allowable maximum temperature rise of the batteries from ambient is known as 10°C and 5°C respectively, therefore to achieve these constraints, the allowable total thermal resistance ( $R_{Total}$ ) for the thermal circuit can be calculated using equation 3.8 and gives 0.06338K/W and 0.05039K/W.

$$R_{Total} = \frac{\Delta T}{\dot{Q}_{Total}} \quad (3.8)$$

Since the battery cage is going to be cooled from ducts beneath, the air will flow up through the batteries, over the top of the enclosure and back down through the batteries. Hence there will be heat transferred from the batteries from forced convection through the gaps between the batteries and forced convection over the top of the enclosure (Figure 7). Note that due to the small size of the gaps between the batteries, the effects of natural convection were previously ignored.

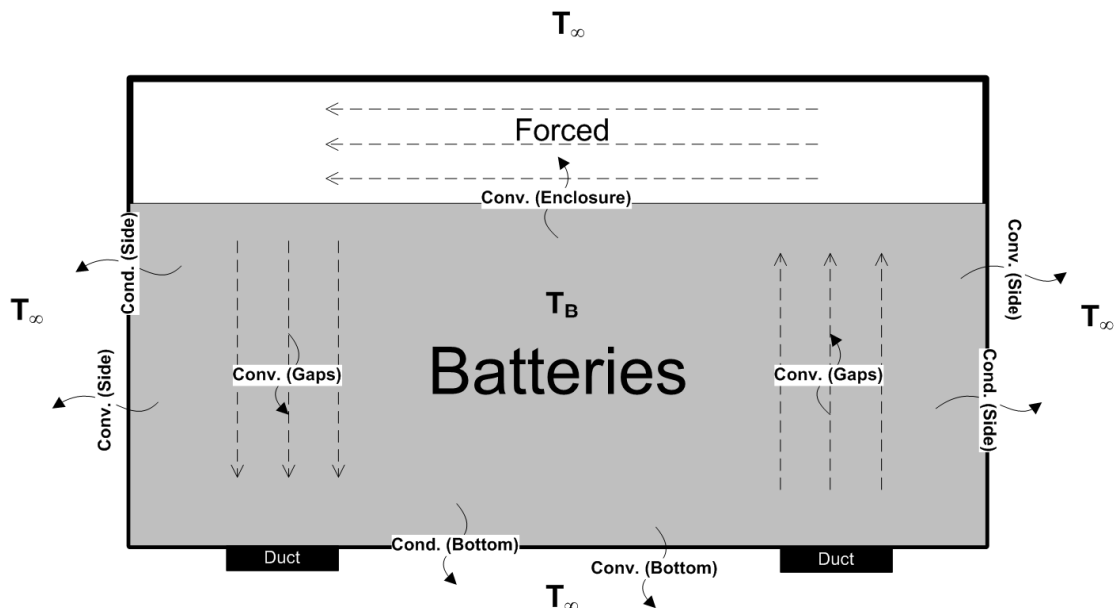


**Figure 7:** Diagram of heat flow from Hyundai Getz batteries with forced convection.

Therefore the thermal circuit can be summarised in Figure 8 below. Note that heat transferred through the top of the enclosure can now be assumed to be negligible as the airflow will remove this heat.

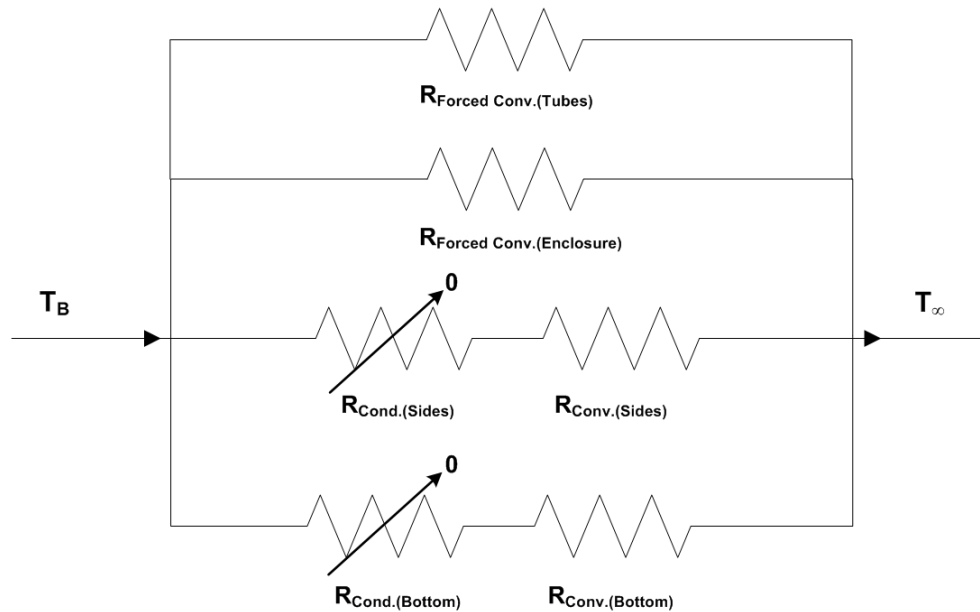


**Figure 8:** Thermal circuit for Hyundai Getz batteries with forced convection.

The thermal resistance through the side surfaces and the bottom will remain constant, so the total resistance from forced convection must be low enough to achieve the total required thermal resistance for the system. The thermal resistance through the sides and bottom can be determined from equation 3.9 and then used in equation 3.10 with the total required thermal resistance to determine the required thermal resistance from forced convection ( $R_{\text{Forced Conv}}$ ). The resulting values are 0.08827K/W for discharging and 0.06344K/W for charging, see Table 22 of Appendix B for summary of thermal resistance values. Note that if forced convection wasn't required, the thermal resistance from natural convection of the enclosure would be less than the calculated values for  $R_{\text{Forced Conv}}$ . This is not the case, refer to Appendix C for the calculated values.

$$R_{\text{Conv}(Bottom/Sides)} = \frac{L_c}{kNuA_s} \quad (3.9)$$

$$\frac{1}{R_{\text{Total}}} = \frac{1}{R_{\text{Conv}(Bottom)}} + \frac{1}{R_{\text{Conv}(Sides)}} + \frac{1}{R_{\text{Forced Conv}}} \quad (3.10)$$

The undetermined and required variable in the system to achieve this overall resistance is the flow rate through the battery cage to achieve forced convection. The total flow rate through the gaps must equal the flow rate over the top of the enclosure at steady state. Therefore a system of equations can be set up to determine the flow rate. Firstly  $R_{\text{Forced Conv}}$  can be split into its components as seen in equation 3.11.

$$\frac{1}{R_{Forced\ Conv}} = \frac{1}{R_{Forced\ Conv(Top)}} + \frac{1}{R_{Forced\ Conv(Tubes)}} \quad (3.11)$$

Firstly to determine the thermal resistance for forced convection over the top of the batteries ( $R_{Forced\ Conv(Top)}$ ), a series of equations for flow through a tube can be used to obtain an equation in terms of the flow rate ( $q$ ) and other known variables. The flow is assumed as tube flow as this is the most relevant flow regime over the top of the batteries, however instead of using the surface area ( $A_s$ ) of the entire tube,  $A_s$  is assumed to equal the area on top of the batteries which is within the flow path. As these equations are developed for a circular tube, the diameter is taken as the hydraulic diameter ( $D_h$ ) equal to four times the cross sectional area divided by the perimeter. Note an iterative approach was used to determine the type of flow present, laminar or turbulent. Reynolds number ( $Re$ ) for all cases was calculated to range from 750 to 1490 which is less than 2300 where the flow becomes transitional, therefore the flow is assumed laminar. Reynolds number over the top is so low because of the low flow velocity due to the large cross sectional area. Next the thermal entry length ( $L_t$ ) can be calculated in equation 3.12 to range from 2.57m to 5.14m which is much longer than the total length of the tube, therefore the flow can be assumed to be thermally developing laminar flow.

$$L_t = 0.05RePrD_h \quad (3.12)$$

For thermally developing laminar flow, the Nusselt number can be calculated using equation 3.13. Using this and the other relevant basic flow equations set out in Appendix D, they can be substituted into each other to give the final equation 3.14.

$$Nu = 3.66 + \frac{0.065\left(\frac{D_h}{L}\right)RePr}{1+0.04\left[\left(\frac{D_h}{L}\right)RePr\right]^{2/3}} \quad (3.13)$$

$$\frac{1}{R_{Forced\ Conv(Top)}} = \frac{kA_s}{D_h} \left[ 3.66 + \frac{0.065\frac{qD_h^2Pr}{A_c v L}}{1+0.04\left(\frac{qD_h^2Pr}{A_c v L}\right)^{2/3}} \right] \quad (3.14)$$

Table 6 below states the various constants that need to be inserted into equation 3.14 to achieve final equations 3.15 for discharging and 3.16 for charging.

|   | Discharging                              | Charging                                  |
|---|--|---|
| Prandtl number (Pr)                             | 0.7228                                   | 0.7296                                    |
| Thermal conductivity (k)                        | 0.02735W/mK                              | 0.02551W/mK                               |
| Kinematic viscosity (v)                         | 1.798x10 <sup>-5</sup> m <sup>2</sup> /s | 1.562 x10 <sup>-5</sup> m <sup>2</sup> /s |
| Wetted perimeter of duct (p)                    |  | 1.84m                                     |
| Cross sectional area (A <sub>c</sub> )          |  | 0.0435m <sup>2</sup>                      |
| Hydraulic diameter of tube (D <sub>h</sub> )    |  | 0.0946m                                   |
| Length of tube (L)                              |  | 0.340m                                    |
| Surface area within tube flow (A <sub>s</sub> ) |  | 0.2958m <sup>2</sup>                      |

**Table 6:** Constants to determine equations for forced convection over the top.

Note: For the appropriate constants, discharging values are taken at 50°C and 25°C for charging.

$$\frac{1}{R_{Forced\ Conv(Top)}} = 0.08552 \left[ 3.66 + \frac{1581q}{1+0.04(24324q)^{\frac{2}{3}}} \right] \quad (3.15)$$

$$\frac{1}{R_{Forced\ Conv(Top)}} = 0.07977 \left[ 3.66 + \frac{1837q}{1+0.04(28263q)^{\frac{2}{3}}} \right] \quad (3.16)$$

If one fan is used to cool the system, given the 77mm diameter ducting to be used, there are twelve different directions in which the air can flow to the top of the batteries, directly up, forward then up and back then up, see Figure 9. Similarly the air can flow down to the outlet duct in a similar fashion. If two fans were used there would be twice the number of routes. Hence the thermal resistance is calculated for one rectangular tube, assuming equal flow rate through each tube equal to the total flow rate (q) on the number of routes (n).

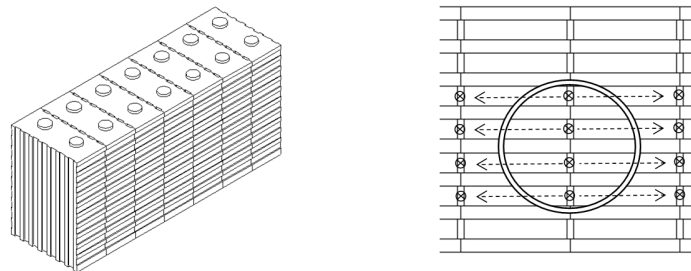


**Figure 9:** One row of batteries (left) and inlet duct with flow directions (right)

To determine the thermal resistance for forced convection through one gap to the top of the batteries and back down ( $R_{Forced\ Conv(1\ Tube)}$ ), a series of equations were used for turbulent flow in tubes. Although the air flows up through a gap, over the top and then back down a gap, the total length of the gaps are combined and analysed as one tube with their total surface areas combined, this is acceptable as all other variables are equal. For these paths the flow was initially assumed turbulent. For turbulent flow, the hydrodynamic and thermal entry lengths can be assumed to equal ten times the

hydrodynamic diameter. Since the length of the tubes are much longer than this, entrance effects can be presumed negligible, therefore assuming fully developed turbulent flow in the entire tube. Given fully developed turbulent flow, Nusselt's number can be determined using equation 3.17. Using this and the other relevant basic equations for tube flow set out in Appendix D, formula 3.18 can be determined in terms of the appropriate constants.

$$Nu = 0.023Re^{0.8}Pr^{0.4} \quad (3.17)$$

$$\frac{1}{R_{Forced\ Conv(1\ Tube)}} = \frac{0.023A_s k \left(\frac{qD_h}{nA_c v}\right)^{0.8} Pr^{0.4}}{D_h} \quad (3.18)$$

Table 7 below states the various constants that need to be inserted into equation 3.18 to achieve the final equations, 3.19 for discharging and 3.20 for charging.

|  | Discharging                              | Charging                                  |
|--|--|---|
| Prandtl number (Pr)                          | 0.7228                                   | 0.7296                                    |
| Thermal conductivity (k)                     | 0.02735W/mK                              | 0.02551W/mK                               |
| Kinematic viscosity (v)                      | 1.798x10 <sup>-5</sup> m <sup>2</sup> /s | 1.562 x10 <sup>-5</sup> m <sup>2</sup> /s |
| Wetted perimeter of duct (p)                 |  | 0.032m                                    |
| Cross sectional area (A <sub>c</sub> )       |  | 5.50x10 <sup>-5</sup> m <sup>2</sup>      |
| Hydraulic diameter of tube (D <sub>h</sub> ) |  | 6.88x10 <sup>-3</sup> m                   |
| Total length of tube (L)                     |  | 0.429m                                    |
| Surface area within tube (A <sub>s</sub> )   |  | 0.0137m <sup>2</sup>                      |

**Table 7:** Constants to determine equations for forced through one duct.

Note: For the appropriate constants, discharging values are taken at 50<sup>0</sup>C and charging at 25<sup>0</sup>C.

$$\frac{1}{R_{Forced\ Conv(1\ Tube)}} = 1.100 \times 10^{-3} \left(\frac{6,957,225q}{n}\right)^{0.8} \quad (3.19)$$

$$\frac{1}{R_{Forced\ Conv(1\ Tube)}} = 1.030 \times 10^{-3} \left(\frac{8,008,381q}{n}\right)^{0.8} \quad (3.20)$$

The total thermal resistance due to flow through the batteries (R<sub>Forced Conv(Tubes)</sub>) can then be found using the parallel resistance equation to give equations 3.21 for forced convection through the tubes for discharging and 3.22 for charging.

$$\frac{1}{R_{Forced\ Conv(Tubes)}} = \frac{n}{R_{Forced\ Conv(1\ Tube)}} = n \times 1.100 \times 10^{-3} \left(\frac{6,957,225q}{n}\right)^{0.8} \quad (3.21)$$

$$\frac{1}{R_{Forced\ Conv(Tubes)}} = \frac{n}{R_{Forced\ Conv(1\ Tube)}} = n \times 1.030 \times 10^{-3} \left(\frac{8,008,381q}{n}\right)^{0.8} \quad (3.22)$$

Using equation 3.11 and substituting in the relevant formulas, the equation can be solved for total flow rate values for charging and discharging and for one or two fans, see Appendix E for formulas. These values are summarised in Table 8 below.

|  | <b>Discharging</b>                                  | <b>Charging</b>                                     |
|--|---|---|
| Required total flow rate with 1 fan (q)  | $7.35 \times 10^{-3} \text{ m}^3/\text{s}$ (7.4L/s) | $10.7 \times 10^{-3} \text{ m}^3/\text{s}$ (11L/s)  |
| Required total flow rate with 2 fans (q) | $6.22 \times 10^{-3} \text{ m}^3/\text{s}$ (6.2L/s) | $9.00 \times 10^{-3} \text{ m}^3/\text{s}$ (9.0L/s) |
| -Required flow rate for each             | $3.11 \times 10^{-3} \text{ m}^3/\text{s}$ (3.1L/s) | $4.50 \times 10^{-3} \text{ m}^3/\text{s}$ (4.5L/s) |

**Table 8:** Required total flow rates for discharging and charging.

Therefore the critical required fan flow rates are 4.5L/s with two fans and 11L/s with one fan, both from charging.

### 3.2.3.2 Pressure Loss

To find the appropriate fan that can support the calculated flow rates, the corresponding pressure loss ( $\Delta P_L$ ) must be determined for each. All pressure loss is assumed to be from flow between the batteries, flow over the large area on top of the batteries is assumed negligible in comparison. As previously described, the flow rate through each tube can be approximated to equal, the total flow rate (q) divided by the number of paths (n) and since these paths are in parallel, the pressure loss across each can be assumed equal and equal to the total pressure loss. Modelling one tube between the batteries with average velocities calculated from equation 8.5 and Reynolds number from 8.4 of Appendix D, a corresponding friction factor using a Moody chart for a smooth tube can be determined. The pressure loss can then be calculated using equation 3.23, these values are summarised in Table 9. All other relevant variables were taken from Table 7.

$$\Delta P_L = f \frac{L}{D_h} \frac{\rho V_{avg}^2}{2} \quad (3.23)$$

|                                | <b>1 Fan</b>           | <b>2 Fans</b>          |
|--------------------------------|------------------------|------------------------|
| Density ( $\rho$ )             | $1.184 \text{ kg/m}^3$ | $1.184 \text{ kg/m}^3$ |
| Average velocity ( $V_{avg}$ ) | 16.21m/s               | 6.82m/s                |
| Reynolds number (Re)           | 7141                   | 3004                   |
| Friction factor (f)            | 0.033                  | 0.043                  |
| Pressure loss ( $\Delta P_L$ ) | 320Pa                  | 73.8Pa                 |

**Table 9:** Calculated pressure losses for critical required flow rates

Note Reynolds number was determined to equal 7141 and 3004 for the critical values of a one and two fan system respectively remembering that the flow was assumed turbulent between the batteries. Tube flow is said to generally be transitional from 2300 to 4000, the one fan system can clearly be assumed turbulent although the two fan system flow is theoretically transitional. However due to fluctuations in flow from an intended thermostat controlled system, vibrations in the vehicle and especially increases

and decreases in natural flow from driving, the flow can be assumed turbulent for calculations of the Nusselt number.

Therefore the technical requirements for each 12V fan in a one or two fan system can be summarised in Table 10 below.

|              | <b>One Fan</b> | <b>Two Fans</b> |
|--------------|----------------|-----------------|
| q            | 11L/s          | 4.5L/s          |
| $\Delta P_L$ | 320Pa          | 73.8Pa          |

**Table 10:** 12 volt Fan(s) technical requirements.

### 3.2.4 *Concealment of Battery Cage*

To seal the battery cage to prevent gases leaking into the car cabin, the walls parallel to the side of the car had to be covered which previously were not. The plate in the bottom of the battery cage also had to be redesigned to accommodate the duct inlets and outlets of the venting system. As the inlet and outlet ducts are also located underneath the vehicle it is possible for large amounts of water to be propelled inside, therefore guards overlapping the entire duct were required for prevention. Additionally, filters to prevent any moist air entering the battery cage are required.

SolidWorks 2008 SP4.0, a computer aided drafting (CAD) software package was used to design components. This provided easy alterations of designs and clear drawings for fabrication. Fabrication of the sheet metal was prepared by the UWA Electrical Engineering workshop, and installed in the vehicle in G50 of the UWA Electrical Engineering building with assistance.

### 3.2.5 *Design Safety*

There were various considerations which had to be taken into account in designing the active venting system, with the key risks outlined below.

Initially components within the battery cage were leaking gases every now and then which could be hazardous. These gases were tested by the UWA Chemistry Laboratory several times and came back each time containing general air properties, not containing anything harmful. However, as a safety precaution and to mitigate the risk these gases are required to be vented to the outside of the vehicle. Therefore during installation it is important to ensure that every air gap is sealed air tight.

Risk 1: Hazardous gases (assuming they are hazardous) contained in the vehicle with passengers (Table 11):

|                          | Consequence | Likelihood | Risk |
|--------------------------|-------------|------------|------|
| <b>Before Mitigation</b> | Severe      | Likely     | High |
| <b>After Mitigation</b>  | Severe      | Rare       | Low  |

**Table 11:** Risk 1 Values

The second reason for the active venting system is to prevent the batteries from exceeding 60°C. If the batteries exceed 150°C, although unlikely, they can rupture, releasing hydrogen fluoride and hydrogen phosphide (Thunder Sky 2007). Having a venting system in place mitigates the possibility of this happening.

Risk 2: Batteries exceeding 150°C and rupturing releasing hazardous gases (Table 12):

|                          | Consequence | Likelihood | Risk   |
|--------------------------|-------------|------------|--------|
| <b>Before Mitigation</b> | Severe      | Unlikely   | Medium |
| <b>After Mitigation</b>  | Severe      | Rare       | Low    |

**Table 12:** Risk 2 Values

The main concern when designing the venting system is the prevention of water from the exterior of the vehicle entering the interior of the battery cage and touching the live 144 volt system. This could conduct electricity through the battery cage and the rest of the vehicle. Several safety measures are in place to mitigate this risk. Firstly guards underneath the vehicle will prevent any water entering the ducts and if they do, each individual duct tubing inlet and outlet is offset from each other, further preventing the flow of water. Additionally, as previously mentioned, each duct contains a filter, this is at the top of each duct to prevent any moist air entering the cage, this will also prevent small amounts of water proceeding into the cage if it penetrates the previously mentioned measures.

Risk 3: Water entering the battery cage and conducting electricity through the vehicle (Table 13):

|                          | Consequence | Likelihood | Risk   |
|--------------------------|-------------|------------|--------|
| <b>Before Mitigation</b> | Severe      | Possible   | Medium |
| <b>After Mitigation</b>  | Severe      | Rare       | Low    |

**Table 13:** Risk 3 Values

Note: Please see Appendix F for the risk matrix used to determine the level of risk before and after mitigation.

### 3.3 Results & Discussion

#### *3.3.1 Fan Selection*

A large number of electronic and computer shops were investigated to find a fan(s) which met the appropriate technical requirements, size and costs. Although most fans found at dedicated computer shops were all less than \$30, they barely met the required flow rate for zero pressure loss, under the systems calculated pressure loss these fans did not operate.

No fan found met the requirements for a one fan system, to sustain the high pressure loss of 320Pa, the size of the fans were too large to fit in the wheel well of the vehicle. For a two fan system only two manufacturers were found with fans that met the requirements, Mirconel and ebmpapst. Comparatively, the Micronel fan, model D604T was more appropriate as it had a circular end to attach a duct (see Figure 10).

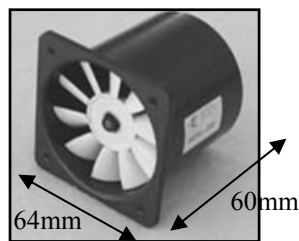


**Figure 10:** Micronel fan D604T (Micronel 2009).

However once the manufacturer was contacted about this product, they disclosed that in some cases the fan vanes cracked, they suggested a different brushless model, D604Q, which retailed at \$598.13. This was much more than the allowable budget. Therefore the ebmpapst models were further investigated. There were several appropriate models, the 3212 range, and the 8212 range of models. The determining features between these models were availability, price and sound level, the chosen model was 8212JN. As seen from Figure 11 below the operating conditions are well within the fans capabilities. For fan dimensions see Appendix G.

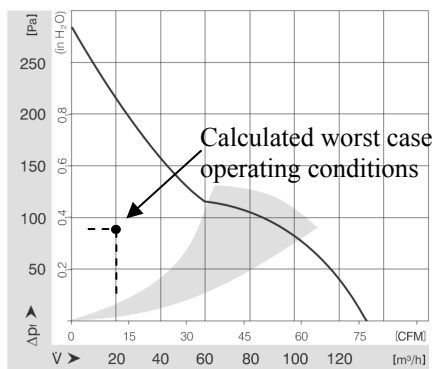


**Figure 11:** Graph of pressure loss versus airflow for 8212JN fan (ebm-papst 2009).

### 3.3.2 Final Design & Installation

The final design of the sheet metal walls and floor to conceal the battery cage is displayed in Figure 12, for fully dimensioned drawings see Appendix H. As can be seen, ducts from the base of the battery cage have to run to the bottom of the wheel well to exhaust the air to the outside of the vehicle. For this, ducts used to cool computer CPU's were used as they fitted perfectly around the outside of the 80mm square fan casings.

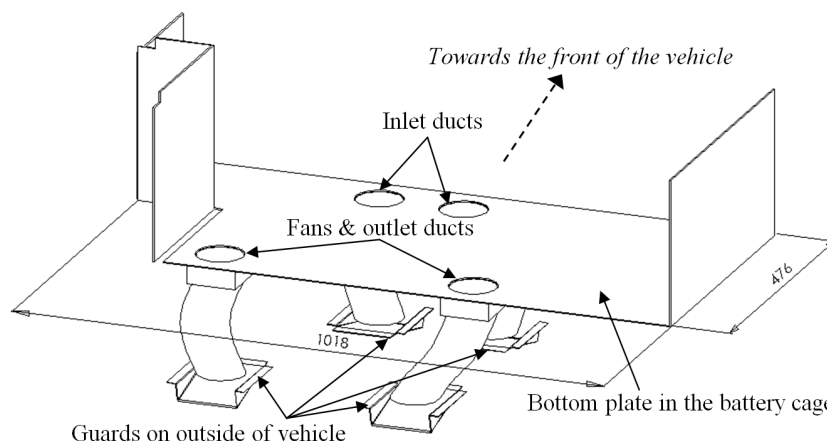


**Figure 12:** Final design of additional components made for the venting system (mm).

Sheet metal guards were created to be placed underneath the vehicle (Figure 12) to prevent water entering the ducts. Note the guards at the front face forward to create a positive pressure to force air through the ducts and the ducts at the rear face backwards to create a negative pressure to assist in pulling the air out of the ducts. Each duct also contains a plastic guard to prevent any objects entering the cage and also a filter to prevent moist air and water entering.

Once the system was installed, electrical engineering members of the REV team inserted a thermostat into the battery cage to automatically operate the fans when

necessary. Therefore if the temperature inside the battery cage reaches  $5^{\circ}\text{C}$  above ambient temperature when charging, the fans switch on, and if the temperature inside ever exceeds  $60^{\circ}\text{C}$  then the fans also switch on. To assist in removing any odours from leaking into the cabin, the fans switch on for one minute every hour to extract the air.

Concealing the cage was exceptionally difficult as none of the structural members could be altered as this would affect its strength. Therefore to prevent any air gaps around the sheet metal, the edges were covered with a weather proof rubber to form a tight seal and all other gaps were filled with adhesive foam.

### 3.3.3 Testing

Once the system was completely installed the battery temperatures were tested. The batteries were charged in different ambient temperatures to test whether the cells would exceed  $5^{\circ}\text{C}$  above ambient. Figure 13 displays the range of temperatures taken from the batteries during different ambient temperatures.

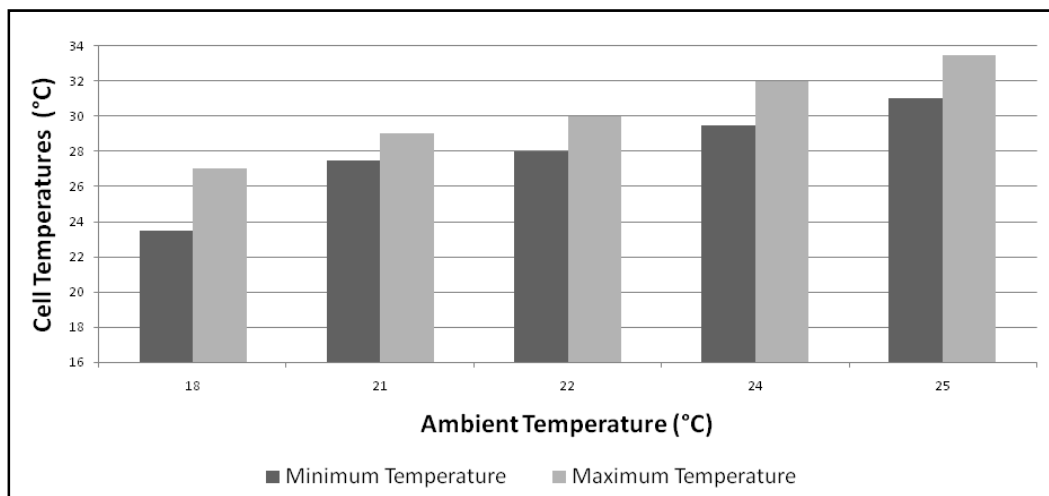


**Figure 13:** Maximum and minimum cell temperatures during charging.

As can be seen the battery temperatures maximum and minimum vary markedly. This is because the higher temperature batteries are more centrally located where limited air flows around the cells which do not have a duct placed underneath or close to them. The average minimum temperature increase above ambient is  $5.9^{\circ}\text{C}$  and the average maximum temperature increase is  $8.3^{\circ}\text{C}$ . Although the cell temperatures are slightly exceeding the specified  $5^{\circ}\text{C}$  above ambient, this is acceptable as the key purpose was to minimise the temperature rise during charging. This is clearly viewable as the maximum

temperature rise recorded during initial testing was 22°C when ambient was 16°C, far more than any recordings after installation.

Valuable testing data is limited for discharging as the batteries rarely exceed 60°C without extreme ambient temperatures. As this project was completed before the summer months commenced, only one day experienced in late October had an ambient temperature above 30°C. The ambient temperature on this day was 37°C, and although the vehicle was driven until the batteries went flat, they did not exceed 55°C. This is because the guards underneath the vehicle at the duct inlets and outlets are orientated to favour the direction of flow, creating a natural airflow through the battery cage whilst driving, hence negating the need for fans up to this temperature. Although limited data was recorded during discharging, this is acceptable as the critical technical requirements for the system were determined from charging. Therefore if the system is operating as expected during charging, it is safe to assume that it will also during discharging.

#### *3.3.4 Discussion*

The entire venting system is operating as required although temperatures are slightly exceeding 5°C above ambient during charging due to the limited flow around some batteries. This could be improved by placing smaller inlet and outlet ducts and more of them underneath the battery cage to get a more even flow around each cell. However this is not necessary, as the initial goal was to reduce the temperature rise during charging which has been achieved. Temperature rises of 5°C to 10°C above ambient are acceptable.

If the initial designs of the battery cage had considered the need for a venting system, it could have allowed for ducts on the sides of the battery cage above the batteries, or if aesthetics were not an issue, ducts could be attached on top of the battery cage. This would allow a fan to pull air in one side and out the other, creating a constant flow over the top of the batteries. Although the air would not have flowed in the gaps between the batteries, the pressure loss over the top would have been minor in comparison. From the investigations done to find an appropriate fan, it was evident that the fans ability to operate at a high pressure corresponded to its cost. Therefore if only a small pressure loss was present across the top, a high flow rate fan would be available at a much lower cost and perhaps only one would be necessary, significantly decreasing the overall costs of the system.

## 4 Battery Restraint System for Lotus Elise

### 4.1 Overview

The Lotus Elise (Figure 14) must house a large number of lithium-ion batteries to supply energy to the high performance electric motor. This project focuses on the battery cages that hold these batteries in place; they must have several practical capabilities and also adhere to the relevant ADRs. This chapter details the requirements and methodology followed for development of the battery cages.



**Figure 14:** The REV team's 2002 model Lotus Elise.

### 4.2 Design Process

#### 4.2.1 *Battery Cage Design Requirements*

1. The Lotus must house as close to one hundred lithium-ion batteries as possible to power the 400V electric motor. Leaving out a few batteries due to space is satisfactory although considerably reducing the number would have significant performance effects on the electric motor and hence the car.
2. The battery cages must be as easily accessible as possible. This is to aid in removing failing cells during operation and assist the electrical engineers for frequent alterations to the electronics within the battery cages.
3. The batteries must be held tight in place but have at least a 20mm clearance above the batteries for a battery management system applied to each cell and connections between the cells.
4. The battery cages must be sealed from the cabin to prevent any release of gases to the passengers as was experienced in the Hyundai Getz.
5. Similarly to the Hyundai Getz, the Lotus Elise is not required to be vented in accordance with the ADRs as lithium-ion batteries are being used. However to

maximise performance and operating life of the batteries, a venting system will be required. An analysis and design of a venting system for the Lotus was performed under guidance by a colleague of the REV team, Timothy Wallace. Hence the battery cages must be designed to assist in an efficient cooling system.

6. The battery cages must be placed in positions to achieve as similar weight distribution as possible to the original specifications. If not this can affect the ride height, COG and in turn driving characteristics as detailed in section 2.2.1 *Weight Implications*.

#### 4.2.2 Constraints

1. As outlined in section 2.4 *Battery Cage Codes and Standards*, the cages must adhere to the standards set out in NCOP14 to comply with the ADRs. The most critical requirement for design of the battery cages is the required forces they must withstand of 20g times the battery mass for front impact, 15g for side impact and 10g for rear and vertical impact (Australian Motor Vehicle Certification Board Working Party 2006).

2. An obvious but critical determinant of battery placement is available space in the vehicle with all the petrol engine components removed. Figure 15 displays the original petrol components that were removed from the vehicle.

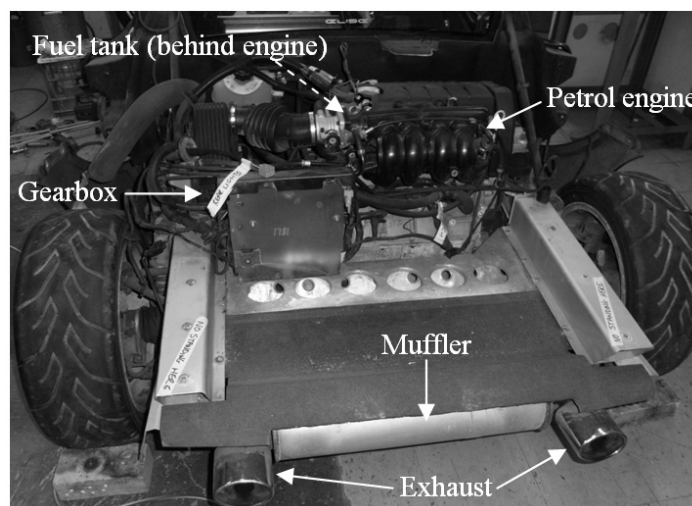


**Figure 15:** Lotus Elise with original petrol components.

Replacing these components with the electric motor and suitable drive mechanics is a priority. Certain parts within the Lotus are also unmodifiable, for example initially it was hoped that the crumple zone in the front of the vehicle would be modifiable to store

batteries (Figure 16) whilst still performing as required. However after discussions with the Department for Planning and Infrastructure (DPI) they conveyed their concerns as it would alter the safety of the vehicle and would have to be rebuilt, analysed and certified by a professional engineer. Due to the limited resources and time constraints on the REV team, this was not an option. Likewise, the firewall behind the seats in the vehicle is unmodifiable without similar problems (Figure 16). See Appendix I for a full schematic of the 2002 model Lotus Elise chassis.



**Figure 16:** Lotus Elise crumple zone (left) and rear firewall behind seats (right).

3. As the electric vehicle is attempting to mimic the performance characteristics of the Lotus petrol vehicle, none of the performance enhancing features can be altered. For example although the front crumple zone is unmodifiable due to safety constraints, it is also preferred that this and the fibre glass shell around the crumple zone are unchanged as this area has air flowing through it to create a downwards force on the front of the vehicle, which is highly desired for a rear heavy vehicle (Figure 16). Clearly the stereotypical streamline characteristics of the Lotus Elise are desired to be kept constant as well.

4. When choosing the appropriate placement for the batteries it is also important to consider the vehicle structure adjacent to support the batteries. Every attempt was made to reuse existing mounts and bolt holes.

5. The battery cages must be completed at a relatively low cost of labour and material and be easy to manufacture within a short period of time due to the number of battery cages that would be required.

#### 4.2.3 Battery Specifications

The energy sources for the electric motor are lithium-ion phosphate batteries by Thunder Sky, model TS-LFP60AHA, with a nominal voltage of 3.2V. These batteries are individually sealed and weigh 2.106kg each. The batteries must be stored upright or flat on the largest face, however the former is preferred. The dimensions of the batteries are displayed in Figure 17.

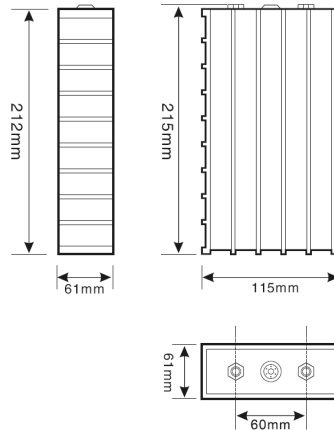


**Figure 17:** Individual lithium-ion battery dimensions (Thunder Sky 2007).

#### 4.2.4 Material

A suitable material was chosen for the battery cages to meet the following key requirements:

- Readily available to the workshop
- Low cost
- High yield strength
- Easily weldable
- Easily modifiable for changes at later stages.

The two materials which best meet these requirements were aluminium and mild steel, with the major differences in density and strength, see Table 14 for details. However once analysing preliminary designs of the battery cages with aluminium, its strength properties were too low for the requirements of the ADRs given the available space. Therefore as a sacrifice for weight, mild steel was chosen as the most suitable candidate with intent to use as little as possible.

|                          | Aluminium (AS1866 6060/T5) | Steel (AS3679.1 Grade 300) |
|--------------------------|----------------------------|----------------------------|
| Density                  | 2700kg/m <sup>3</sup>      | 8050kg/m <sup>3</sup>      |
| Minimum Yield Strength   | 110MPa                     | 320MPa                     |
| Minimum Tensile Strength | 150MPa                     | 440MPa                     |

**Table 14:** Properties of aluminium (Standards Australia 1997) and steel (Standards Australia 1996) materials.

#### 4.2.5 Computer Aided Drafting Modelling and Analysis

All conceptual and final designs were built in the CAD software SolidWorks 2008 SP4.0. SolidWorks provides an easy to use platform for developing and modifying designs at a later stage.

Once designs were completed within SolidWorks they were imported into ANSYS Workbench 11.0 SP1 to perform a stress analysis. SolidWorks output files are compatible with ANSYS Workbench geometries. Therefore if structures did not pass the stress analysis in ANSYS Workbench they were easily modified within SolidWorks and imported again (see Figure 18).

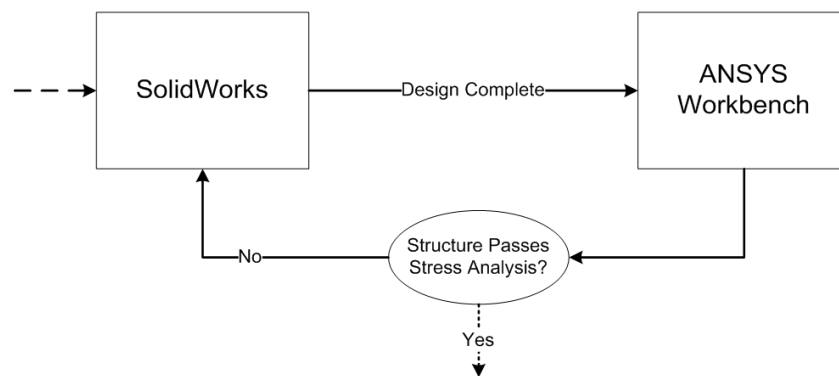


**Figure 18:** Interactive Process for design between SolidWorks and ANSYS Workbench.

#### 4.2.6 Design Methodology

The general process followed for the design of each battery cage can be summarised in the flowchart of Figure 19 below. Once the design requirements and constraints were defined, the battery cages could be developed in a SolidWorks model. Following, a mock battery cage was made from ply wood to test that it fitted in position and also logistically for removal. Once the cages passed these tests, a stress analysis was performed in ANSYS Workbench to check their adherence to the NCOP14 crash accelerations. To obtain an accurate result it is ideal that each mesh is refined to obtain a maximum stress which is converged to within 5%. If they did not pass, this process was repeated until a satisfactory design was developed. Although most cages were mounted on existing structural members and bolts, some cages required additional mounting designs. Where necessary these mount designs were analysed in a similar process. Feedback was continually sought from the UWA Electrical Engineering workshop for ease of manufacture to limit the number of workshop hours required. Once all designs were completed, they were approved by the appropriate REV team supervisors for

construction. The strength of all bolts used to secure the battery cages and mounts were also analysed in accordance with the Australian standards under the crash impact accelerations.

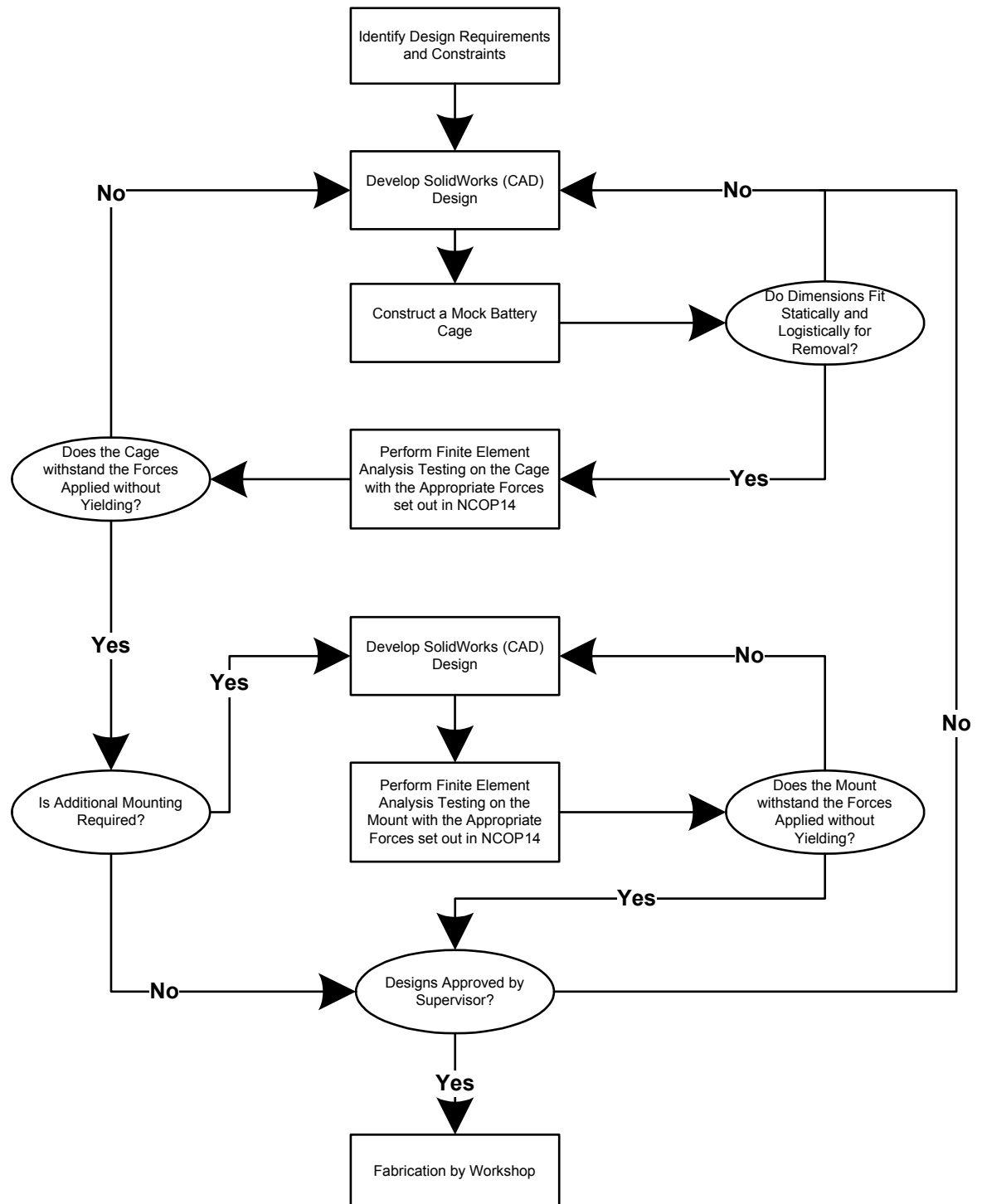


Figure 19: Flowchart of design process for battery cages.

4.2.7 Design Safety

The task for design and construction of the cages to house the batteries is based around safety. The key purpose of the cages is to restrain the batteries in place, with particular attention focused on their restraint during crash impacts. However the key risks considered in designs of the battery cages and their mounts are outlined below.

To adhere to the ADRs the battery cages must withstand the crash accelerations set out in NCOP14 to mitigate the risk of them coming loose in a crash. If they did not they could cause severe harm to passengers or bystanders.

Risk 1: Batteries braking free from the battery cage during a crash (Table 15):

|                   | Consequence | Likelihood | Risk |
|-------------------|-------------|------------|------|
| Before Mitigation | Severe      | Likely     | High |
| After Mitigation  | Severe      | Rare       | Low  |

**Table 15:** Risk 1 Values

It is possible that during a crash, the battery cage supports or bolts could fail, releasing the cages to be thrown throughout the vehicle and colliding with a passenger or bystander. To mitigate this risk they must also be designed to withstand the crash accelerations of NCOP14.

Risk 2: Battery cage braking free from the vehicle during a crash due to failure of the supports or bolts (Table 16):

|                   | Consequence | Likelihood | Risk |
|-------------------|-------------|------------|------|
| Before Mitigation | Severe      | Likely     | High |
| After Mitigation  | Severe      | Rare       | Low  |

**Table 16:** Risk 2 Values

As with Hyundai Getz venting system, particular attention must be taken to seal the battery cages from water to prevent it conducting the high voltages contained within, throughout the vehicle. Therefore each battery cage must be sealed water tight to mitigate this risk.

Risk 3: Water entering the battery cage and conducting electricity through the vehicle (Table 17):

|                   | Consequence | Likelihood | Risk   |
|-------------------|-------------|------------|--------|
| Before Mitigation | Severe      | Possible   | Medium |
| After Mitigation  | Severe      | Rare       | Low    |

**Table 17:** Risk 3 Values

When designing all new parts for the vehicle, they must be designed not to alter any of the chassis members in the vehicle to weaken their structural capacity, as well as any other safety components such as the crumple zone. If they have to be modified, adequate analysis must prove the capability of modified components, this will mitigate the risk of compromising the current vehicle structure.

Risk 4: Failure of the current vehicle structure from modifications (Table 18):

|                   | Consequence | Likelihood | Risk   |
|-------------------|-------------|------------|--------|
| Before Mitigation | Major       | Possible   | Medium |
| After Mitigation  | Major       | Rare       | Low    |

**Table 18:** Risk 4 Values

Note: Please see Appendix F for the risk matrix used to determine the level of risk before and after mitigation.

### 4.3 Results & Discussion

#### *4.3.1 Initial Battery Cage Locations*

There were several designs considered for the battery cages and drive system in the Lotus. As the drive system concepts and designs were developed, the battery cage designs also evolved and went through many changes to allow for modifications.

In an effort to maintain the initial weight distribution of the vehicle, as many batteries as possible were required to be placed forward of the rear axle. There was not any available space in the front of the vehicle without modifying the fibreglass shell or the crumple zone which should be avoided as previously described. Therefore the next available space moving backwards, is the previous location of the fuel tank, directly behind the seats (Figure 20).

Moving into the rear engine compartment, some decisions had to be made on the drive mechanics to identify the available space. After an analysis by REV team member, Frans Ho, it was realised that a single speed differential would be adequate to replace the gearbox and maintain the performance characteristics of the vehicle due to the relatively flat torque curve of the electric motor. This layout would remove the heavy and large gearbox and replace it with a smaller differential located between the wheels. There would then be adequate space forward of the rear axle to locate all the required batteries with two layers placed where the gearbox was located, see Figure 20 below.

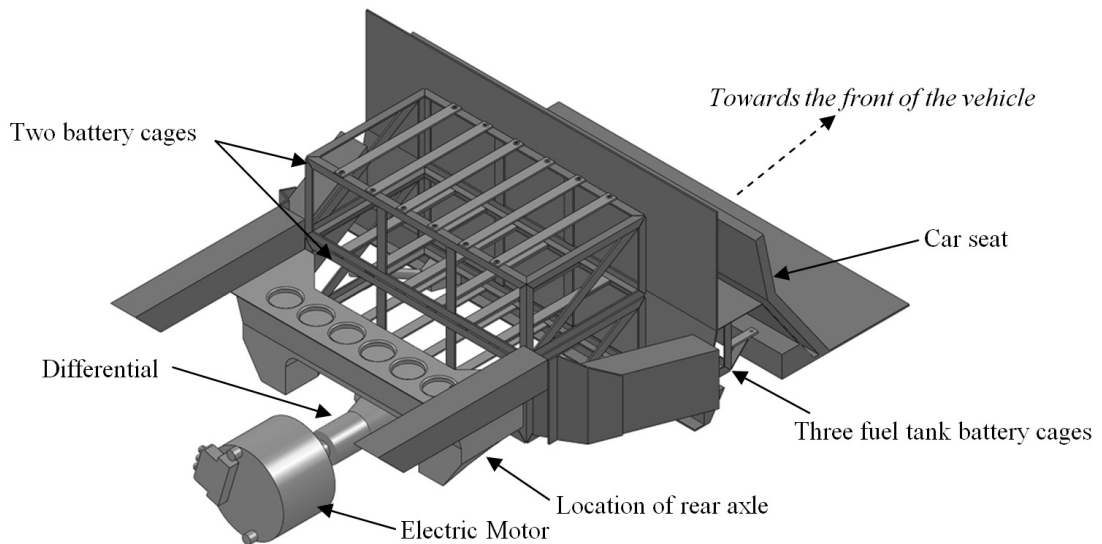


**Figure 20:** Isometric CAD drawing of the rear structure and components.

However after extensive research by the REV team, a suitable differential which met the size, cost and technical requirements could not be found by mid 2009. Therefore the existing gearbox had to be maintained onto which the electric motor was directly mounted.

#### 4.3.2 Final Battery Cage Locations and Designs

With the existing gearbox maintained, there were three positions chosen to place batteries, in the area where the fuel tank was located, one layer above the gearbox and motor, and under the boot in the rear of the vehicle. Placing batteries in the rear of the vehicle was not preferable, however due to the limited space this was unavoidable. Each final design which passed the acceleration requirements will be discussed further, however the stress analysis and reasons for selection of material dimensions will be presented in the following section.

As in the initial design, batteries were placed in the fuel tank area, as this is the available space farthest forward of the rear axle. Between the fuel tank and the cabin was only a thin sheet of aluminium, therefore to allow easy access to this area, this was removed with the intention of replacing it with a detachable cover, once the battery cages were installed. A single mock battery cage, initially three by nine batteries was constructed from ply wood to confirm it would fit in the space and could also be adequately removed. However it was quickly realised that there was only enough room for a battery cage two by nine and this would have to be broken into three separate cages in order to place and remove them due to protruding parts. This way one could be

slotted in either side and the centre one last (Figure 21). In this area there are two horizontal chassis members which the fuel tank was previously bolted to, these members were also used to mount the battery cages which slotted in between.

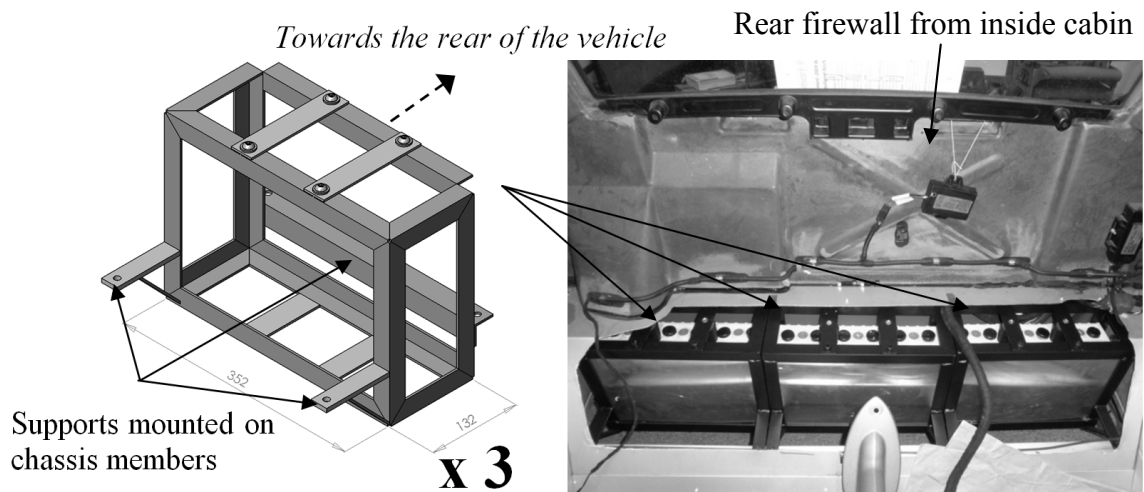


**Figure 21:** Final fuel tank battery cage design (left) and installed cages (right), (mm).

Unlike the other cages, the equal angle bar across the top at the rear is facing backwards. This is so the last battery can be inserted as it is only two batteries wide so each battery is butted up against a face. This fuel tank area is concealed from the cabin by a sheet metal cover bolted on and from underneath by the diffuser which runs under the vehicle. Therefore these battery cages did not need individual sealing to prevent water entering or gases escaping into the cabin. Each face is left open to assist airflow except the front face which is covered with sheet metal to assist in packing the batteries tightly together to avoid vibrations. The final fuel tank battery cage design is displayed in Figure 21. For fully dimensioned drawings see Appendix J.

Above the gearbox and motor a battery cage of 49 batteries, 7 by 7 was designed, see Figure 22. A mock battery cage was initially constructed as it was hoped more batteries could fit to lessen the load in the rear battery cage. However due to the car computer, motor, gearbox and their mounts, and the fibreglass cover, a maximum of 49 batteries could be fitted very tightly in between. There is less than a 10mm gap between the top of the battery cage and the fibreglass cover, therefore every bolt had to be countersunk flush with the top of the cage. Given this limited available space, modification of designs to strengthen the cage were restricted, this is discussed further in the following section. A separate mount was required to support the central battery cage and had to be designed so the above cage was sitting as low as possible (Figure 22). Therefore the top

surface of the mount/bottom of the battery cage is preferably at the same level as the highest point below, which is the gearbox/motor adapter plate. Therefore the mount passes over the gearbox at its lower points where adequate space had to be left to account for movement in the gearbox due to its damped mounting points. By lengthening the bolts, existing bolt holes from the vehicle were used to attach the mount so as to not modify the strength of the chassis by drilling new holes. For fully dimensioned drawings of the central battery cage see Appendix K and for the mount see Appendix L.

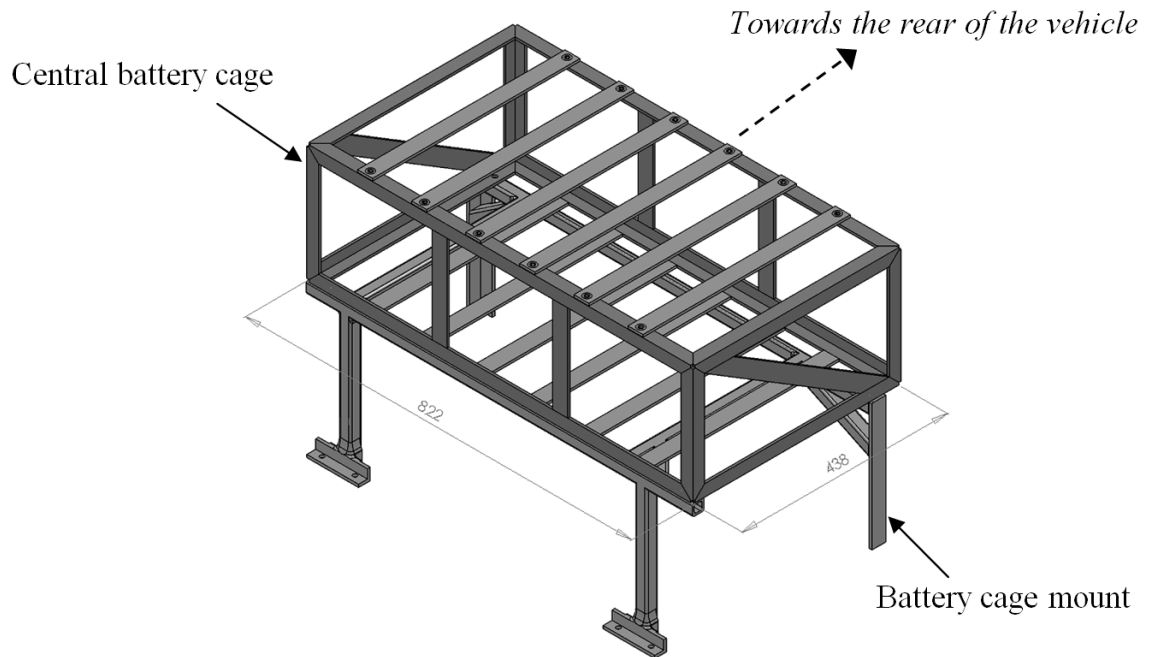


**Figure 22:** Final central battery cage and mount design (mm).

The last battery cage is located in the very rear of the vehicle, underneath the boot where the muffler and exhaust was situated. Although it is preferable not to place batteries this far back, this was unavoidable given the number of batteries required and available space. The battery cage is however kept as low as possible to maintain a low centre of gravity. The final rear battery cage contains 32 batteries, 8 by 4, see Figure 23 below. For fully dimensioned drawings see Appendix M.

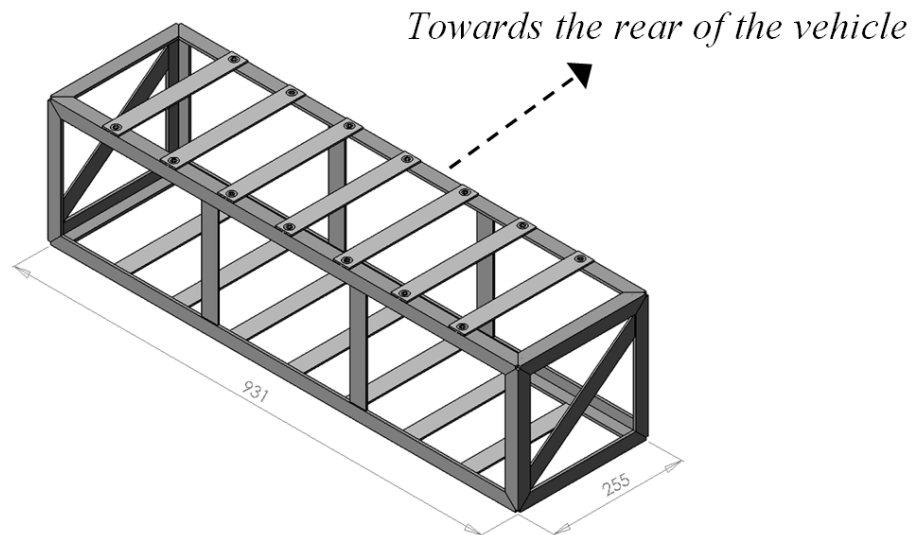


**Figure 23:** Final rear battery cage design (mm).

This battery cage is mounted to the car from above by rails used to support the boot. These rails however were only rated to support 50kg, therefore requiring strengthening. Under guidance this analysis was performed by REV team member, Adam Doster. Initially the rails were going to be replaced with thicker aluminium but due to a lack of appropriate sizes, 3mm thick mild steel was used. The original rails were also not a standard size, they have the outside bottom corners removed to allow movement in the suspension wishbones. This was overcome by using a smaller hollow tube to raise the larger rectangular steel tube to the original height, see Figure 24. The top of the battery cage however has to sit level with the top of a structural member in front of it. Therefore aluminium spacers were used to lower the cage to this height (Figure 25).

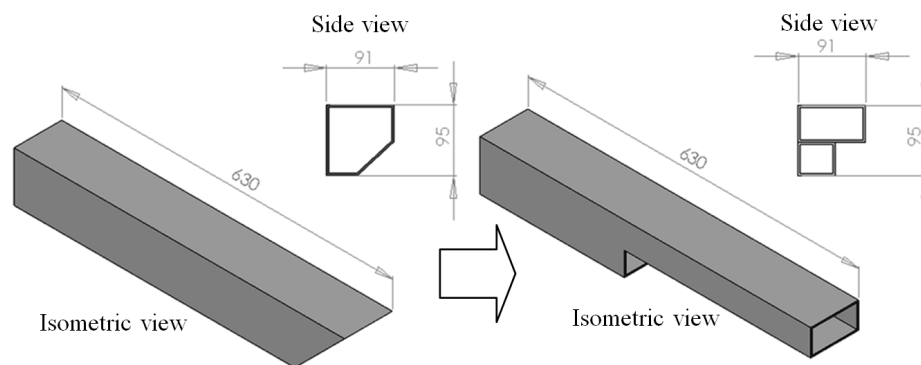


**Figure 24:** Original aluminium (left) and upgraded steel rails (right), (mm).

A CAD model rear of the seats of all the major components was created to aid in designing parts to be inserted in the vehicle. The final design of all components installed can be seen below in Figure 25.

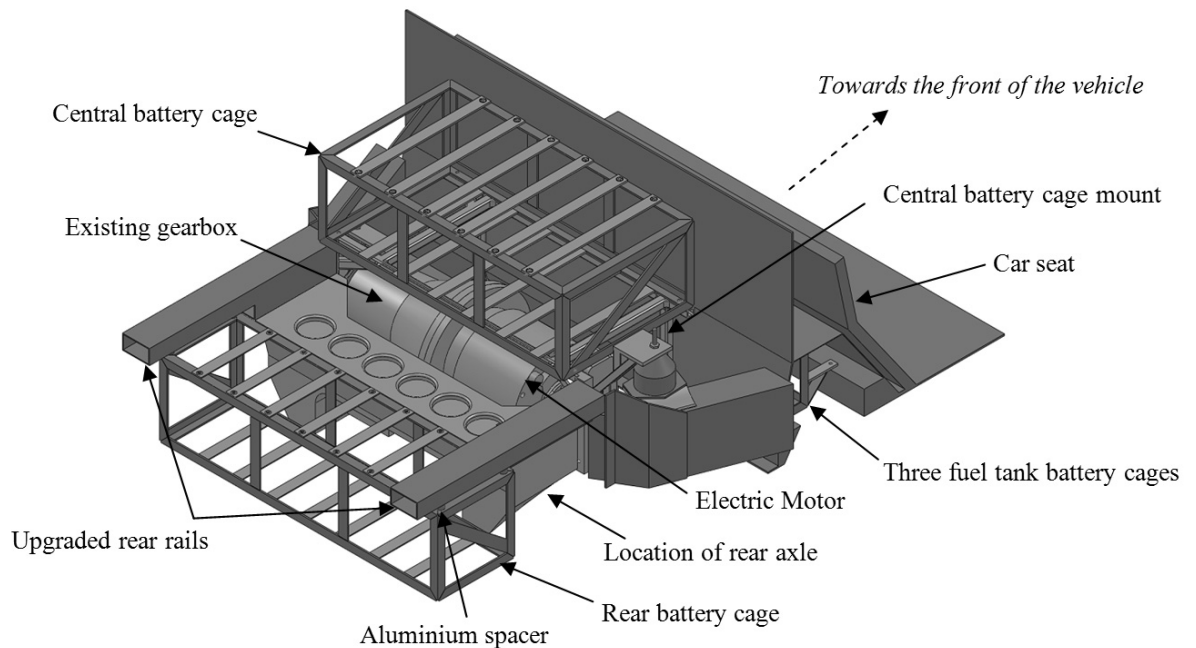


**Figure 25:** Isometric CAD drawing of the rear structure and components.

To be able to remove the batteries from the cages, each cage has bolted down flat rectangular steel straps across the top which can be easily removed. To hold the batteries tight, these straps have rubber door stoppers bolted underneath them every battery width, hence each battery is supported on all four corners. Plastic spacers were lathed to make sure every stopper is compressed by 3mm once the straps are bolted down so there is no movement, see Figure 26 below.

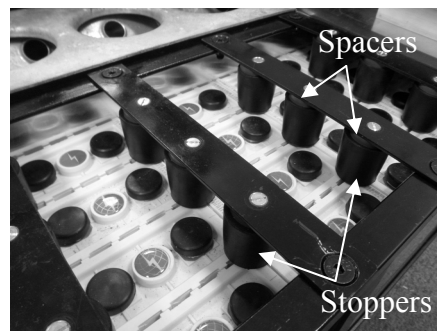


**Figure 26:** Stoppers and spacers securing batteries vertically.

All welds on the battery cages were produced using MIG welding. As all the cells within the cage have to sit flat to assist in connecting the batteries, all welds had to be ground flush. Therefore every bar welded had to be chamfered to ensure full penetration of the weld so grinding the weld back would not remove its strength. As described in section 4.2.7 *Design Safety*, each battery cage has to be sealed water tight. As previously stated the fuel tank battery cages are concealed as oppose to the central and

rear cages. The Lotus Elise does have a diffuser running under the entire length of the vehicle, therefore preventing the majority of water entering the vicinity of the rear and central battery cages. However to be certain, every vertical and bottom face of these battery cages was covered with sheet metal and sealed with an adhesive. The top of the central cage was covered with perspex with weather proof rubber edges which fold over the sides to prevent any water entering. The perspex allows easy inspection of the batteries and also adds to the aesthetics of the vehicle. The top of the rear battery cage is sealed by an aluminium plate which supports the motor controller directly on top. As there will be little water contacting the battery cages, coating the steel with paint was adequate to prevent corrosion and the sheet metal contains an anodized layer increasing its corrosion resistance.

To secure each battery cage in place, high tensile M8 bolts (grade 12.9) were used, see the following section for stress analysis. Additionally all nuts used were nylon inserted “nylock” nuts to prevent the nut working loose.

#### *4.3.3 Stress Analysis*

A stress analysis of the proposed battery cage designs was carried out using ANSYS Workbench. As outlined in section *2.4 Battery Cage Codes and Standards*, they must withstand 20g for front impact, 15g for side impact and 10g for rear and vertical impact. The mounts and bolts used were also checked for their adherence to these forces.

Once importing the SolidWorks models into ANSYS Workbench, the appropriate supports and forces were applied. A simulation was then run obtaining a safety factor for the yield strength of the material against the maximum equivalent (von-Mises) stress. Each component was designed to a minimum safety factor of 1. This is because of the allowance the DPI has already built into their large acceleration requirements. The maximum equivalent stress on every component was converged to within 5% by means of refining the mesh, discussed in section *4.3.3.2 Analysis Refinement*.

##### *4.3.3.1 Battery Cages Applied Forces*

Depending on the size of each battery cage, the required forces it must withstand vary. They can be calculated by the required acceleration times the total battery mass ( $m$ ), i.e. for front impact ( $F_{\text{Front impact}}$ ) see equation 4.1 below. The required forces for each battery cage are summarised in Table 19.

$$F_{Front\ impact} = 20 \times 9.81 \times m \quad (4.1)$$

|                                   | Fuel tank battery cage | Central battery cage | Rear battery cage |
|-----------------------------------|------------------------|----------------------|-------------------|
| <b>Number of batteries</b>        | 6                      | 49                   | 32                |
| <b>Total battery mass, m (kg)</b> | 12.64                  | 103.19               | 67.39             |
| <b>Total force (N)</b>            |                        |                      |                   |
| Front impact                      | 2,479                  | 20,247               | 13,222            |
| Side impact                       | 1,859                  | 15,185               | 9,917             |
| Rear impact                       | 1,240                  | 10,123               | 6,611             |
| Vertical impact                   | 1,240                  | 10,123               | 6,611             |

**Table 19:** Required forces each battery cage must withstand.

As the batteries are rigidly fixed in place, there would be minimal movement of the batteries within the cage during a crash. Therefore force from movement of the batteries within the cage is assumed negligible. Additionally, as the batteries have a thick plastic casing, there would be considerable deformation of the batteries when a force is applied across one face of the cage, therefore only transferring a partial load to the opposite inner face. For safety it is assumed that no force is transferred to the other side via the batteries, therefore the battery cages are over designed as essentially the face with the force applied is absorbing the entire force and only transferred through the battery cage structural members. Hence a separate static analysis is carried out applying each of the forces evenly across the appropriate face of each battery cage. As the cages are an assembly of several parts, within ANSYS Workbench multiple faces cannot be selected and a force evenly distributed across them. Therefore a pressure had to be calculated to apply to each part face for the appropriate side. The exposed area of each face is obtained, and the pressure to evenly distribute across each face can be calculated by dividing this into the force, these values are summarised in Table 24 of Appendix N.

#### 4.3.3.2 Analysis Refinement

The mesh of each structure was refined until the maximum stress converged to within 5%, as previously stated. Convergence was achieved by increasing the mesh relevance which increases the fineness of the mesh by increasing the number of elements and decreasing the element size. In the vicinity of critical locations, spheres of influence were used decreasing the element size to obtain a more accurate solution.

When converging the stress, care had to be taken with an understanding and awareness of the most likely failure points to be able to disregard unrealistic outputs from simulations. A common problem encountered was singular stresses around the fixed bolt holes used to mount the components. Originally these bolts holes were constrained by fixing the inside face of the hole, however this created singular stresses around the

edges, exaggerating the actual stress values. An example of this is displayed in Figure 27 below. Therefore to overcome this problem, as the bolt would be rigidly fixed it is similar to constraining the component at a point. Hence majority of the externally fixed bolt holes which were analysed were modelled as a fixed point. The bearing capacity of the steel around these bolt holes was also checked manually which will be discussed in section 4.3.3.7 *Bolt Stress Analysis*.

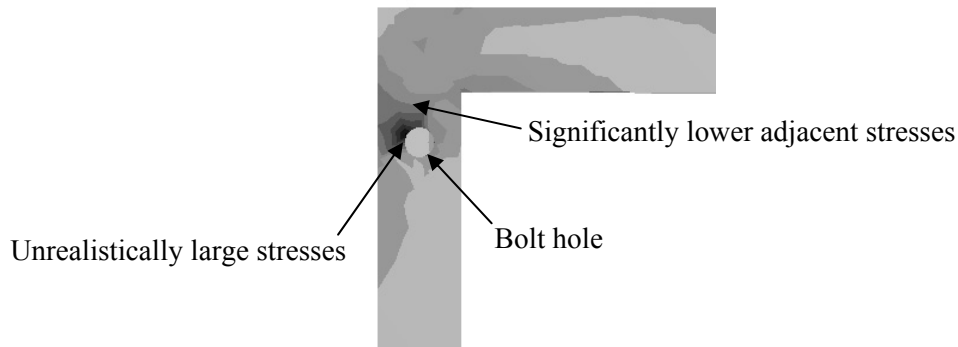


**Figure 27:** Singular stresses around a fixed bolt hole where the darker shades represent higher stresses.

The strain under loading was also manually calculated for several points to confirm its adherence to the materials properties. This was done by using the total deformation output from ANSYS Workbench and then calculating the strain at the most critical points and comparing this to the maximum allowable strain ( $\epsilon_{max}$ ) of 0.0016, calculated from the yield strength ( $\sigma_y$ ) and Young's modulus (E) (Australian Institute of Steel Construction 1999), see equation 4.2. An example of this is from the central battery cage where the total deformation is displayed in Figure 28.

$$\epsilon_{max} = \frac{\sigma_y}{E} = \frac{320MPa}{2 \times 10^5 MPa} = 0.0016 \quad (4.2)$$

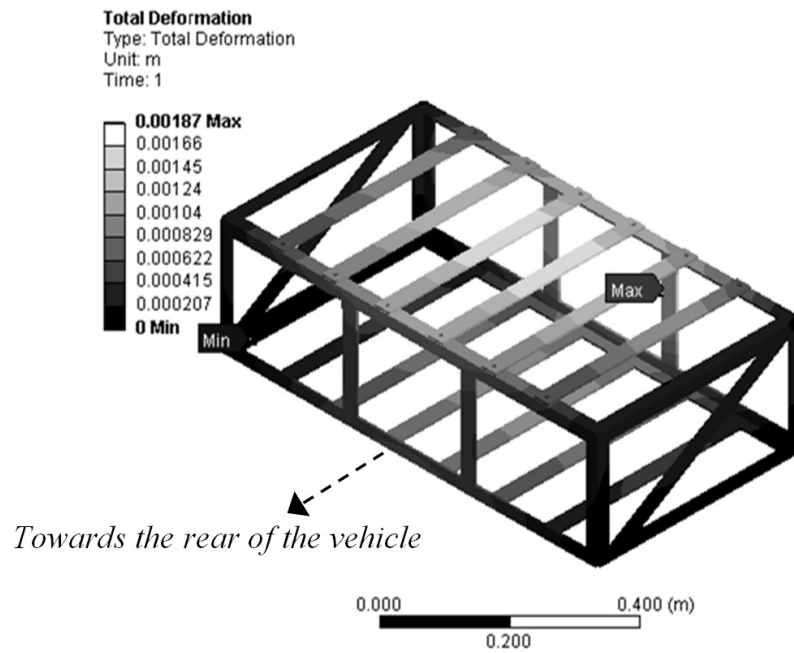


**Figure 28:** Total deformation (m) of the central battery cage from front impact.

Taking the maximum deformation point from the centre of the vertical flat bar of height ( $l$ ), an approximation of the elongation distance ( $\Delta l$ ) can be calculated to be 0.0344mm using Pythagoras' theorem on the drawing in Figure 29. Hence from equation 4.3 the calculated strain ( $\epsilon$ ) for this member is determined to be 0.000170, far less than  $\epsilon_{max}$ .

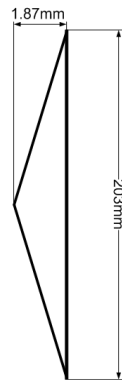


**Figure 29:** Approximation of elongation of vertical member of central battery cage.

$$\epsilon = \frac{\Delta l}{l} = \frac{0.0344}{203} = 0.000170 \quad (4.3)$$

This method was followed and the strain was calculated for several points on all simulated structures to verify results.

#### 4.3.3.3 Fuel Tank Battery Cage

The three identical fuel tank battery cages were analysed separately as they are individually mounted. It was originally hoped that the cage could be built from aluminium, however after running an analysis with the appropriate material properties it

was quickly realised this would not suffice the given forces. Due to the limited available space within the fuel tank area, using thicker or hollow section rectangular members to add strength was not an option. Therefore thin 3mm mild steel was used. As can be seen from Figure 30, with the structure fixed by the four bolt holes, it comfortably passes all acceleration requirements.

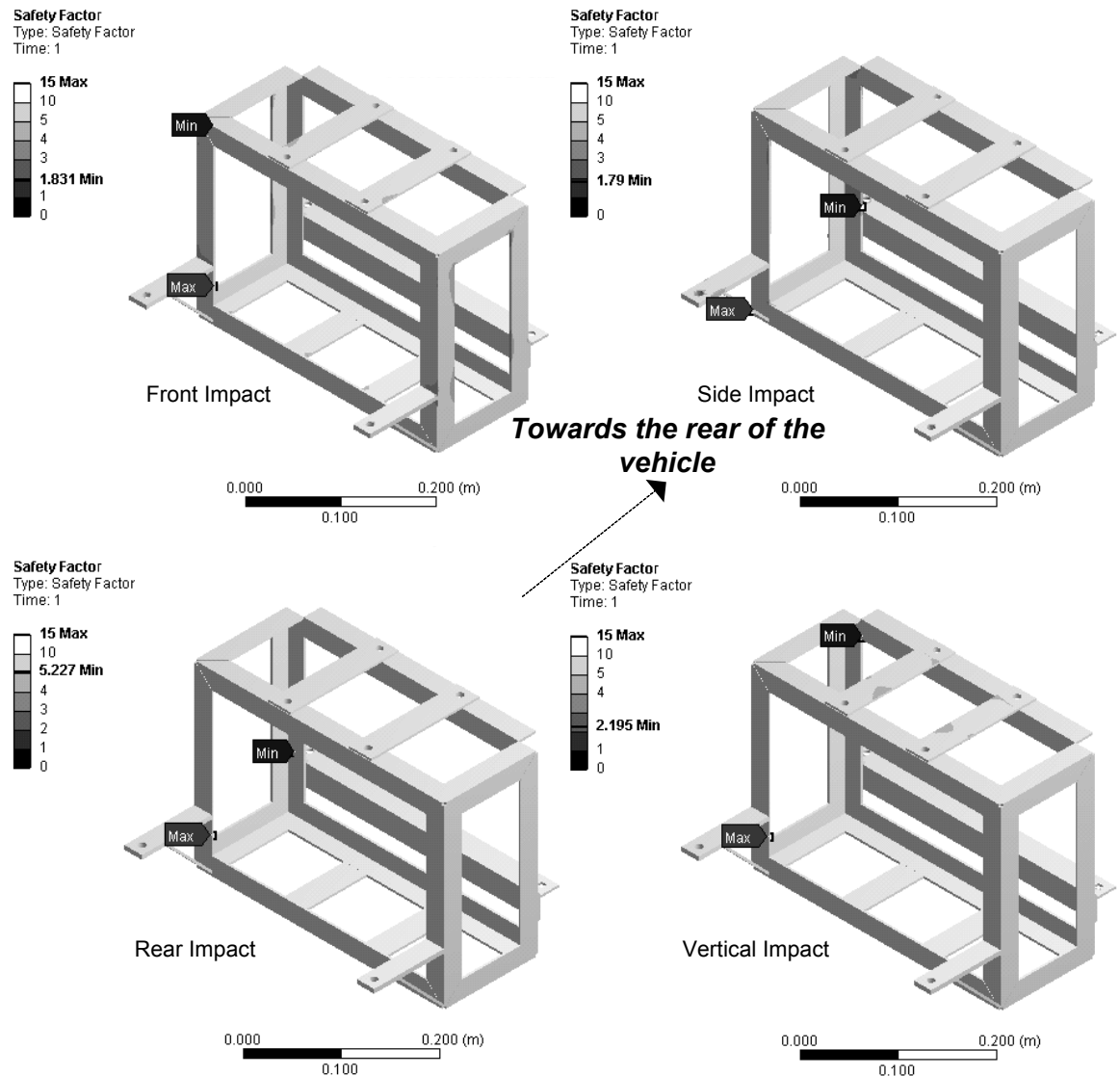


**Figure 30:** Fuel tank battery cage safety factor contours for front (top left), side (top right), rear (bottom left) and vertical (bottom right) impact accelerations.

#### 4.3.3.4 Central Battery Cage

The central battery cage is fixed for analysis by four points in the bottom corners of the battery cage where it is mounted. Following the analysis of the fuel tank battery cages it was clear that aluminium was not going to be adequate for the larger cages. Initially the cage was designed using all 3mm thick members, however after continual analysis every member was upgraded to 5mm. It would have been preferred to use rectangular

hollow sections 32mm wide, 13mm high and 1.6mm thick for the horizontal flat bars across the top and bottom. This would have prevented failure from bending when under the largest force from front impact. However this was not possible as it would have increased the overall height of the battery cage exceeding the height of the available space. The flat diagonal bars on the side of the cage were added to transfer the large front impact force from the top down to the corner bolted joints. This prevents the top of the cage translating in relation to the bottom. As displayed in Figure 31, the battery cage passes all impact accelerations with 5mm thick mild steel.

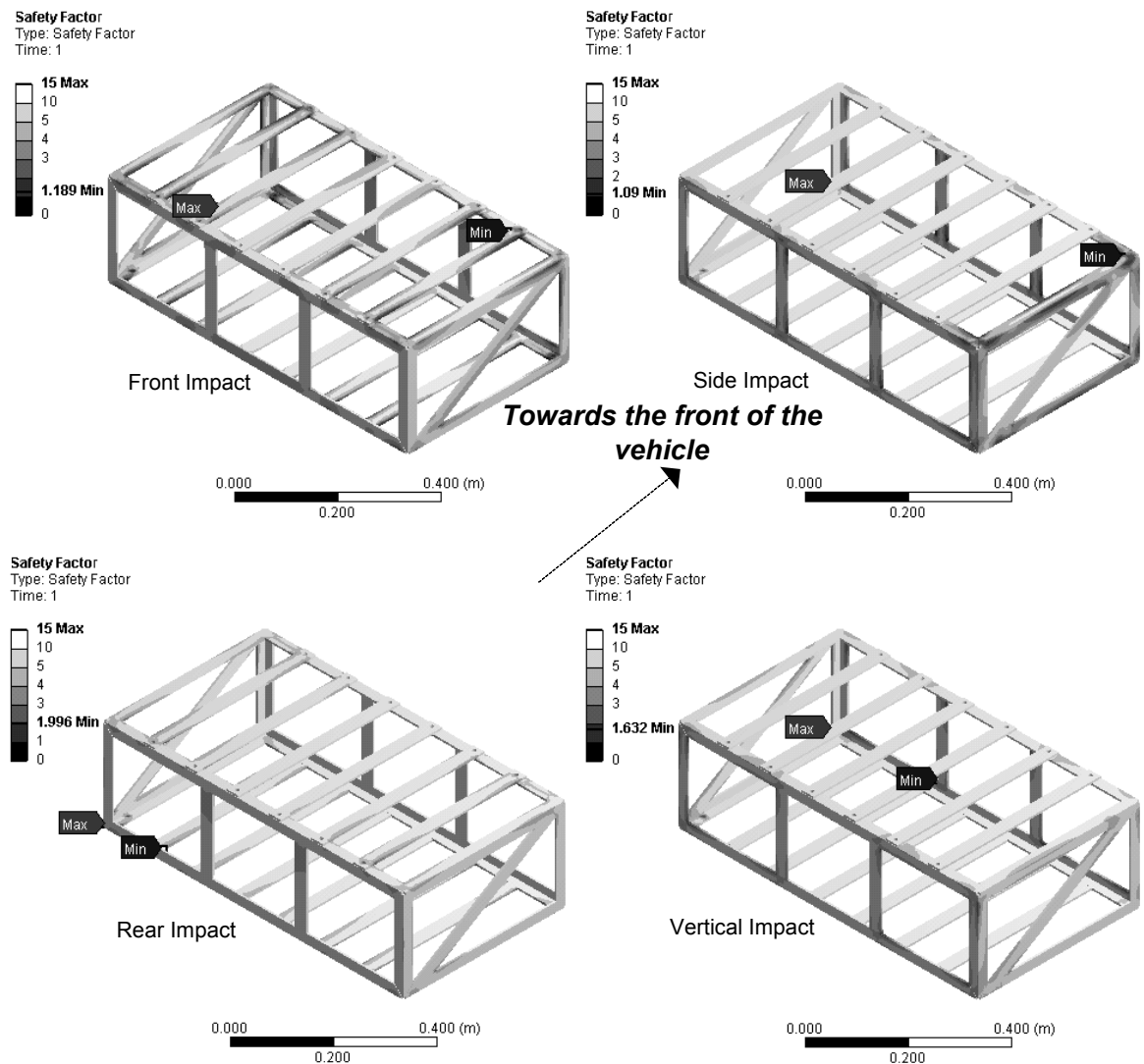


**Figure 31:** Central battery cage safety factor contours for front (top left), side (top right), rear (bottom left) and vertical (bottom right) impact accelerations.

#### 4.3.3.5 Rear Battery Cage

The rear battery cage is fixed by four points on top of the cage in the corners, where it is mounted to the rails on the back of the car. This cage was also initially analysed with

3mm thick members but this failed under the required accelerations. Therefore continual analysis was carried out upgrading different members to 5mm thick. The optimal solution was found using 5mm thick members for the equal angle bars and 3mm for the flat bars. Again, it would have been preferred to use hollow section members however due to height restrictions this was not possible. As with the central battery cage, diagonal side bars were added, however these face in the opposite direction to transfer the largest front impact force from the bottom to the bolted joints at the top. As displayed in Figure 32 the rear battery cage passes all impact acceleration requirements.

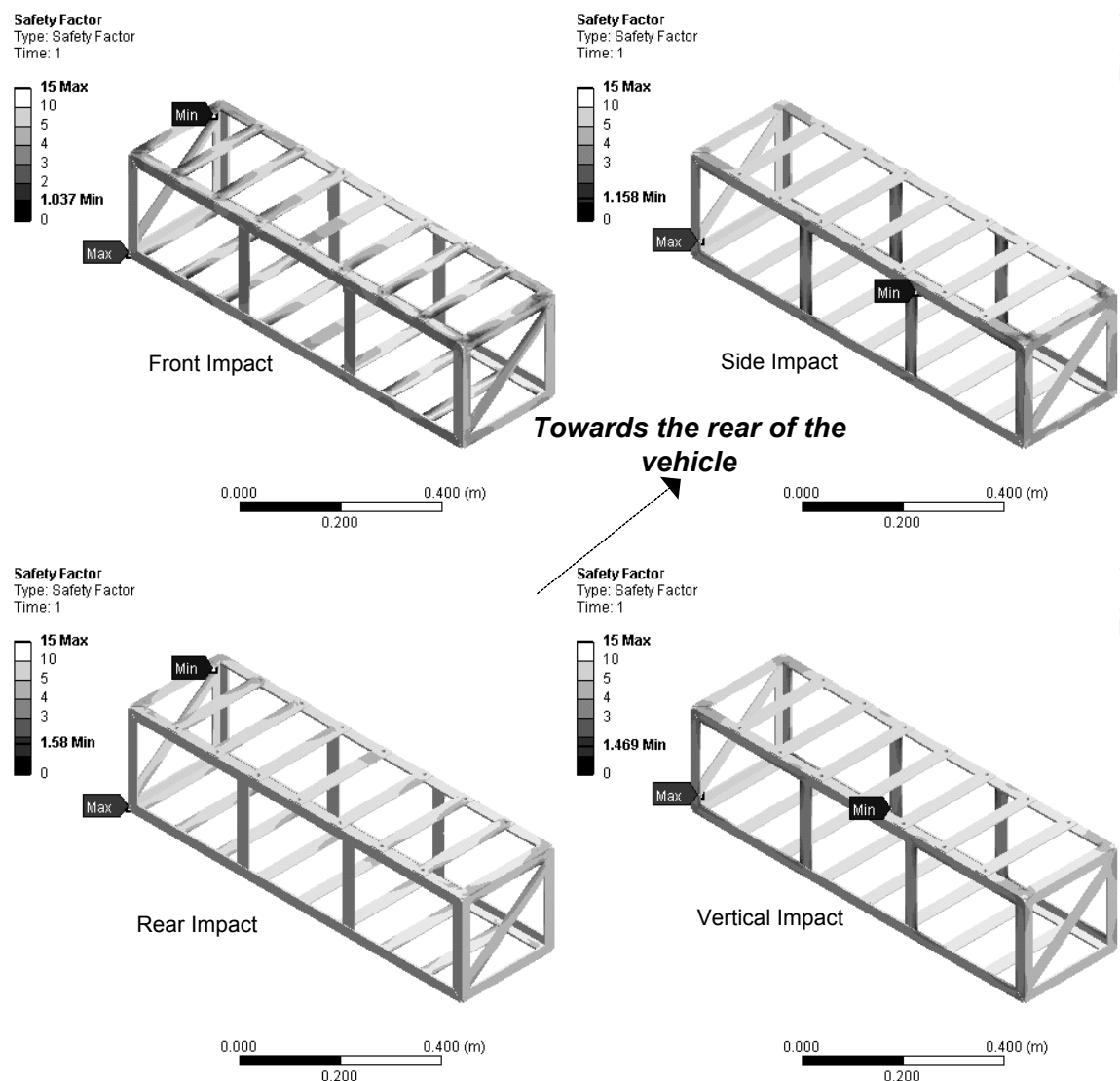


**Figure 32:** Rear battery cage safety factor contours for front (top left), side (top right), rear (bottom left) and vertical (bottom right) impact accelerations.

#### 4.3.3.6 Central Battery Cage Mount

The required forces the mount must withstand are the same forces applied to the central battery cage transferred through the joints. The horizontal forces i.e. the front impact, side impact and rear impact can be applied as point forces on the mount at the bolted joints (Figure 33). As the cage sits flat on top of the mount, the vertical force must be applied as a pressure force across the top surface area. This pressure equals 282,371Pa given an area of 0.03585m<sup>2</sup> and the vertical force of 10,123N. As opposed to the battery cages, the side force must be applied from both sides as the mount is not symmetrical. The mount has two bolts in each leg, these were treated as fixed points for analysis. The angle bar on the base of the two front legs is also resting on a structural chassis member of the vehicle, therefore this is treated as a compression only support vertically. Similarly the rear legs are butted up against a chassis member from behind, therefore this can also be treated as a compression only support horizontally (Figure 33).

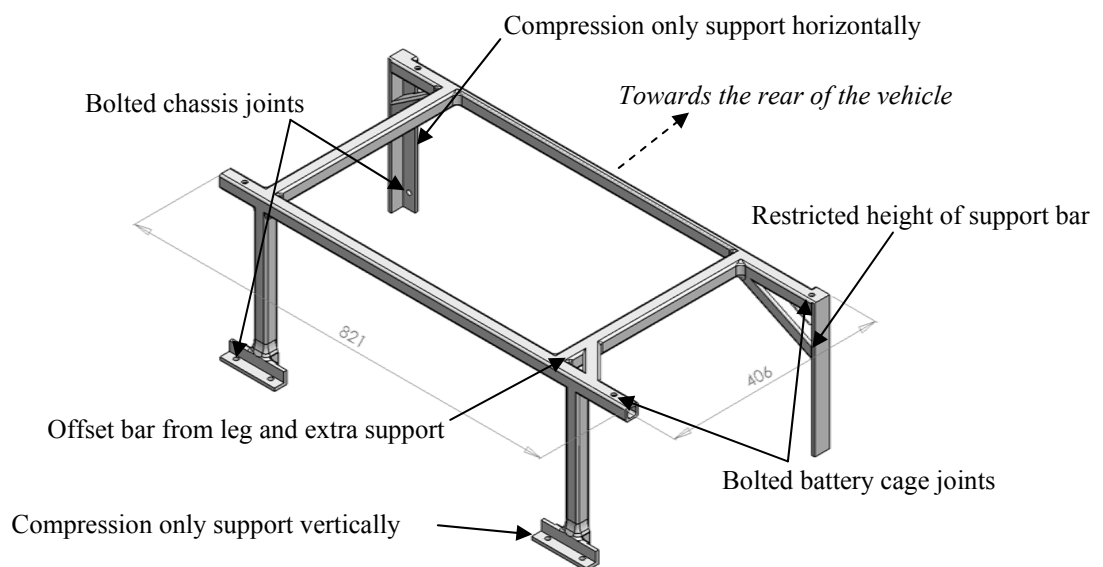


**Figure 33:** Central cage mount position of applied forces and supports (mm).

The central battery cage mount had to be designed so the above cage was sitting as low as possible, this restricted the available space to support the upper structure. This is the reason for the diagonal support bar being attached to the angle bar section at such a high point. For better support it would have been attached lower, however the gearbox was obscuring the path. Additionally the horizontal bar running length ways with the vehicle on the passenger side had to be offset from the mounted leg, see Figure 33. This created additional bending stresses where it intersects the front bar. Therefore to reduce the bending moment, an extra support bar was added transferring load directly to the support leg and effectively reducing the length of the offset bar, hence reducing the

bending moment. The final mount safety factor contours for the given impact accelerations whilst applying the discussed constraints are displayed in Figure 34.

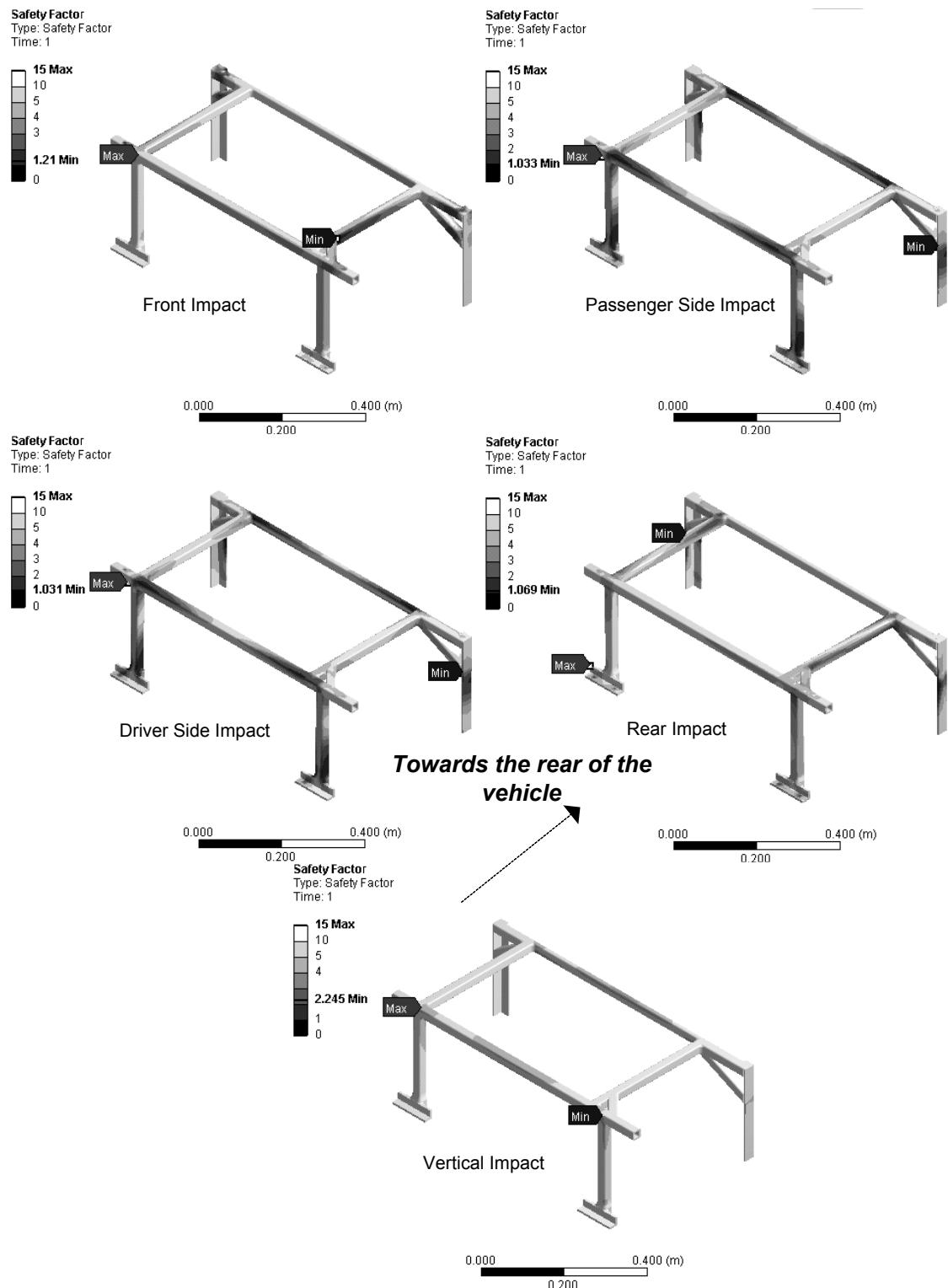


**Figure 34:** Central battery cage mount safety factor contours for front (top left), passenger side (top right), driver side (middle left), rear (middle right) and vertical (bottom) impact accelerations.

#### 4.3.3.7 Bolt Stress Analysis

All the cages and mounts are bolted down using M8 high strength structural bolts, grade 12.9. These bolts have a minimum tensile strength ( $f_{uf}$ ) of 1220MPa (Standards Australia 1995). The maximum shear and tensile forces applied to the bolts must be checked against the bolts capacity. The maximum bearing force, which is equal to the maximum shear force for all given cases as it is just one steel ply joined to another, is also checked against the structural steels capacity.

The nominal shear capacity ( $V_f$ ) can be calculated to be 26.25kN using equation 4.4 (Standards Australia 1998) given a basic minor diameter of 6.647mm (Standards Australia 1985) to produce a minor diameter area ( $A_c$ ) of 34.70mm<sup>2</sup>.

$$V_f = 0.62f_{uf}A_c \quad (4.4)$$

The nominal tensile capacity ( $N_{tf}$ ) of the bolt must also be determined. The tensile stress area ( $A_s$ ) must initially be calculated using equation 4.5 (Standards Australia 1985) given the pitch ( $P$ ) is 1.25mm and the diameter of the bolt ( $d_f$ ) is 8mm. It is determined to be 36.61mm<sup>2</sup>. Following  $N_{tf}$  can be calculated to be 44.66kN using equation 4.6 (Standards Australia 1998).

$$A_s = \frac{\pi}{4}(d_f - 0.9382P)^2 \quad (4.5)$$

$$N_{tf} = A_s f_{uf} \quad (4.6)$$

The nominal bearing capacity ( $V_b$ ) of the steel is the lesser of the two calculated values for local bearing failure (equation 4.7) and plate-tearout failure (equation 4.8) (Standards Australia 1998).

$$V_b = 3.2d_f t_p f_{up} \quad (4.7)$$

$$V_b = a_e t_p f_{up} \quad (4.8)$$

Where the minimum thickness ( $t_p$ ) of the steel used is 3mm and the minimum tensile strength of the steel is 440MPa. Equation 4.8 determines the nominal bearing capacity for the steel subject to a component of force acting towards an edge, therefore  $a_e$  is the minimum distance from the edge of a hole to the edge of the steel, measured in the direction of the component of a force, plus half the bolt diameter (Standards Australia 1998), which is 11mm for all cases. Therefore the nominal bearing capacities are calculated to be 33.79kN and 14.52kN with the lesser obviously being 14.52kN.

The design forces must all be less than the nominal capacities multiplied by their capacity factors (Standards Australia 1998), summarised in Table 20.

|                               | Nominal capacity | Capacity factor | Maximum design force |
|-------------------------------|------------------|-----------------|----------------------|
| <b>Shear force on bolt</b>    | 26.25kN          | 0.80            | 21.00kN              |
| <b>Tension force on bolt</b>  | 44.66kN          | 0.80            | 35.73kN              |
| <b>Bearing force on steel</b> | 14.52kN          | 0.90            | 13.07kN              |

**Table 20:** Maximum design forces for bolt shear and tension and bearing on the ply.

As previously stated, the maximum shear force on the bolts is equal to the maximum bearing force on the surrounding steel for all cases. Therefore failure from the bolts shearing can be neglected as the bearing capacity of the steel is less than the shear capacity of the bolt. Hence the steel around the bolt will fail from bearing forces through plate tear-out failure first.

The maximum tension and shear/bearing forces are assumed to be divided evenly between each bolt. Therefore for each battery cage the maximum shear/bearing force is assumed equal to the front impact force divided by four. The only battery cage which is in pure tension from impact is the rear cage where the vertical impact force is divided by four to obtain the maximum tension force on the bolts. The maximum forces are summarised in Table 21. The central battery cage mount is bolted down in 8 locations, four vertically and four horizontally using larger M10 high tensile bolts. It also has multiple compression only supports and as the forces applied to it are equal to the forces applied to the central battery cage, it can safely be assumed that failure to the battery cage bolts would occur first. Hence it is neglected from Table 21.

|                               | Maximum shear/bearing force | Maximum tension force |
|-------------------------------|-----------------------------|-----------------------|
| <b>Fuel tank battery cage</b> | 620N                        | -                     |
| <b>Central battery cage</b>   | 5062N                       | -                     |
| <b>Rear battery cage</b>      | 3306N                       | 1653N                 |

**Table 21:** Maximum shear/bearing and tension forces from impact accelerations applied to the bolts on each battery cage.

As can be seen, all shear/bearing forces are far less than 13.07kN and the tension force is less than 35.73kN, therefore failure under these conditions will not occur.

#### 4.3.4 Discussion

The steel structures of the battery cages were fabricated by various workshops. Initially it was intended that the UWA Electrical Engineering workshop would manufacture all cages, however due to the unexpected workload the entire vehicle placed on them, the UWA Mechanical Engineering workshop and a professional electric vehicle conversion company, EV Works, fabricated the central and rear battery cages respectively. All other sealing and components for keeping the batteries held tight were fabricated by the

author in the UWA Electrical Engineering workshop with close guidance on machinery such lathes. Figure 35 displays a picture of the fabricated central and rear battery cages installed in the vehicle.

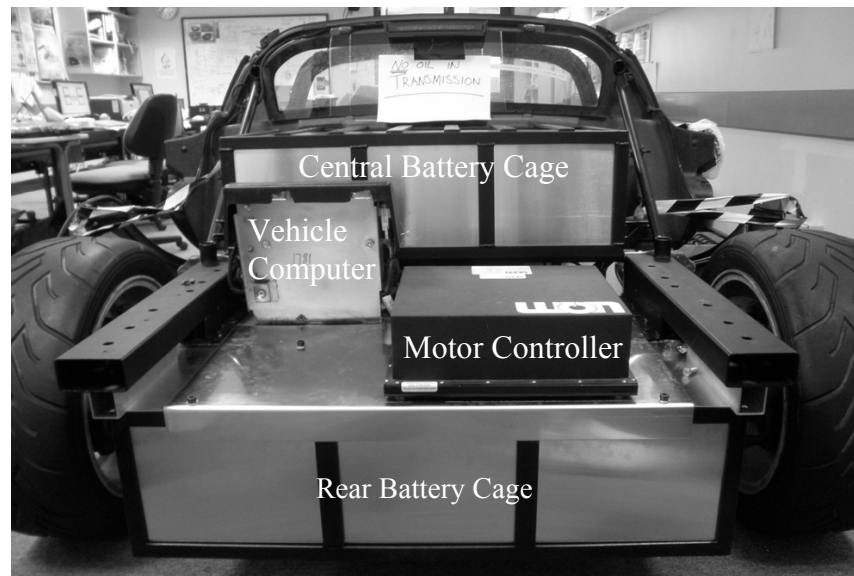


**Figure 35:** Central and rear battery cages installed in the vehicle.

Discussion and inspection of previously converted vehicles by EV works was carried out. They used the same material and similar designs for housing their batteries, confirming the suitability of designs optimised in this project. However there is a “grey” area in the impact acceleration requirements of NCOP14. The current standards do not specifically outline a method for treating the batteries contained in the battery cage. EV Works in the past have treated the batteries as rigid bodies, transferring load from one side of the battery cage to the other (Mr R Mason, 2009, pers. comm., 28 August). This adds significant strength to the battery cage, reducing the material thickness required for the larger cages. However as previously stated, the batteries used for this project are sealed in a plastic cover, therefore treating the batteries as rigid bodies for transferring load was deemed inappropriate. Therefore calculations performed without this consideration are a worst case scenario.

Testing the battery cages to verify results was investigated. Initially it was hoped that destructive testing could be carried out on the battery cages. However this required the fabrication of a second battery cage for each position. This was not financially viable for the REV team and there was also inadequate available staff within the UWA Electrical or Mechanical workshops to fabricate them in priority of other projects. If this

was possible, the cages would have been tested under the most critical load direction until destruction using the Instron machine within the UWA Civil Engineering workshop. This would verify the maximum load they could withstand. Secondly, strain gauge testing could be carried out on the battery cages verifying the stress results from ANSYS Workbench. However there was inadequate time available to do testing as the battery cages were not completed until early September and were installed straight in the vehicle. This was unavoidable as previously explained, the UWA Electrical Engineering workshop had insufficient staff to complete the cages earlier even though final designs were placed with them in late May, leading to external fabrication. However for the purpose of the vehicle and to meet the DPI requirements, physical testing is not required. The final battery cages meet all of the original objectives and DPI requirements.

A venting system analysis for the Lotus battery cages was carried out under guidance by REV team member Timothy Wallace. As the vehicle is not yet operating, testing could not be done to calculate the amount of heat generated from each battery cage. Therefore an assumption was made that the same amount of heat would be generated per volume of batteries for the Lotus Elise as for the Hyundai Getz, using the values calculated in this report. The final design incorporates a single required fan for each the central and rear battery cages mounted on the side at the top. Therefore there is little pressure loss as the air only flows across the top of the batteries, hence the requirement for only one fan per cage, as opposed to the Hyundai Getz which required two as they were mounted from underneath. The battery cages in the fuel tank area do not require an active venting system as the cages are not individually sealed and are only 2 batteries wide, therefore exposing a larger surface area to assist in heat flow. Additionally, the diffuser running under the fuel tank area has perforations in it to assist in air flow during driving. It was also preferable not to have fans directly underneath the passenger as this would cause additional noise.

The maximum number of batteries were placed forward of the rear axle, although due to the retainment of the original gearbox, there was little alternative choices available to fit up to 100 batteries, with the final arrangement containing 99. The placement of the rear battery cage had the largest impact on the weight distribution however this was unavoidable. The original front to rear weight distribution was 33/67 and with the modifications it is now 32/68 (Tang 2009), virtually identical, therefore only having

minimal effects on the handling of the vehicle. Although when taking into account the required passenger and luggage weights, the rear axle now exceeds its maximum limit by 34kg (Tang 2009) which is solely due to the compulsory allowance of 13.6kg of luggage per passenger. This luggage is placed rearward of the rear axle in the original boot, however as there is now no boot space available due to electronics, discussions with the DPI will have to be carried out to gain special consideration to remove the luggage allowance or move it forward in the passenger compartment. There have also been discussions with a professional automotive engineer who will have to approve the vehicle to the DPI, who believes that as the vehicle weight distribution is virtually identical, and hence the driving characteristics also, that the vehicle will be approved (Mr D Stevens, 2009, pers. comm., 8 October). If not further investigations will have to be carried out in upgrading the rear suspension and other necessary components.

Weight distribution issues were the critical determining factors in almost all mechanical designs by the REV team for conversion of the Lotus. However as this vehicle is converted as an example of a viable option from petrol vehicles, it should be noted that vehicles that are purpose built as electric drives can be designed to fit components around battery packs which demand a large space, and placed in more central locations. A purpose built electric car would not suffer the constraints imposed on the REV team who must convert a petrol vehicle using the limited space left after the removal of petrol engine components. This is reinforced by observing placement of the batteries in the electric Tesla Roadster (Figure 36) which is based on a Lotus Elise. All the batteries are placed centrally and low directly behind the seats.

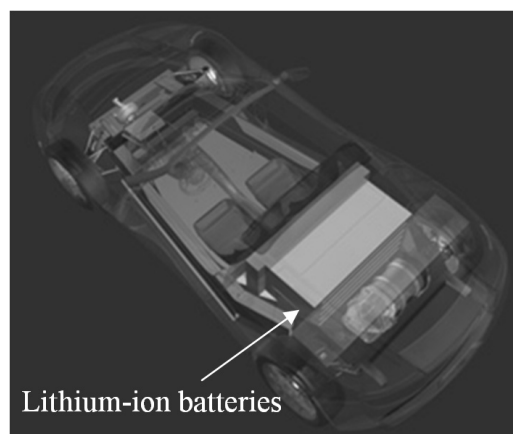


**Figure 36:** Battery placement in the Tesla Roadster (Tesla Motors 2009).

## **5 Manufacture and Implementation Safety Requirements**

Throughout construction and installation, the UWA Electrical and Mechanical Engineering workshops, and G50 laboratory of the UWA Electrical Engineering building were utilised. G50 stores the vehicles and is generally a place for the students to operate within where as the workshops provides additional machinery and staff assistance to fabricate components.

For access to the workshops and laboratory, a safety induction was performed to ensure a clean and safe working environment (School of Mechanical Engineering 2009). The safety induction outlines the rules and regulations for operating unsupervised within the workshops and laboratory. Upon completion of the safety induction, it is the student's responsibility to uphold these rules and regulations, which are outlined in Appendix O. As mechanical group leader for the Lotus Elise, the author was also responsible for ensuring each group member completed a safety induction, and also monitored the behaviour of students within the workshops and laboratory throughout the year.

The general safety inductions did not cover the safe operating procedures for particular machinery within the workshops. Therefore safe operating procedures were outlined by workshop technicians prior to use. Throughout this project, machinery that was required for operation during fabrication of components includes the sheet metal cutting guillotine, drill press and lathes. MIG welding was performed by the workshop staff on behalf of the author. These each have their own safe operating procedures (UWA Occupational Therapist 2001) outlined in Appendix P. One battery cage was fabricated by EV Works who used identical machinery requiring similar operating procedures.

Throughout fabrication and installation of components, care had to be taken to enforce the above safety requirements especially as group leader. Additionally, as there are high voltages within the battery cages, caution had to be taken towards electrical safety, ensuring a qualified technician disconnected the power before removal of any electrical components. When installing electrical wires, particular care was taken to ensure that the wires were sufficiently insulated and not resting on sharp edges which could potentially wear the wire down and become hazardous. All high voltages were clearly labelled with the appropriate hazard symbols. Care also had to be taken when installing the battery cages to follow proper lifting techniques and use of appropriate machinery as the battery cages filled with cells can weigh up to 125kg.

## **6 Conclusion & Future Work**

The Hyundai Getz currently contains a fully automatic temperature controlled active venting system. The system is sealed and vented to the exterior of the vehicle with two 12 volt fans. It will significantly improve the life expectancy of the expensive lithium-ion battery cells used to power the vehicle. It decreases the batteries temperature during charging and monitors the temperature during discharging to maintain an optimal level as a compromise between life expectancy and discharge capacity. As the system is sealed and vented to the exterior it also eliminates any gases released from within the battery cage moving around the cabin. To ensure the gases still do not leak into the cabin, the fans switch on briefly every hour to expel them to the outside.

The battery cages were completed to the specified requirements set out by the DPI, specifically the crash accelerations they must withstand. A thorough stress analysis was carried out using SolidWorks and ANSYS Workbench to obtain an optimal design. Although there were difficulties in determining the best placement for the battery cages to not modify the cars initial specifications and characteristics, the final result had little impact on the weight distribution of the vehicle. The installation of all the battery cages is currently complete and the REV team's electrical engineers are currently installing all electrical components, concluding the final tasks for completion of the vehicle. As viewed from the current installation of the battery cages, they will serve their purpose as expected, allowing relatively easy removal and inspection of the batteries as well as holding the batteries firmly down during operation.

Managing the Lotus Elise mechanical team provided an insight into the necessity for organised project management with particular emphasis on planning and time management. Although the car is not currently complete, significant effort was made to foresee the critical path of the project, so it was not delayed due to the design of parts by the mechanical team. Unfortunately difficulty with workshop availability led to a delay in completion of the project, which is now expected as mid November.

Upon the future completion of the vehicle, the REV team will require a professional automotive engineer to approve the vehicle and allow the DPI to inspect it for its adherence to the relevant ADRs. Particularly attention will be focused on the overloading of the rear axle; if it isn't immediately approved there will be a requirement for future REV team members to modify the rear of the vehicle by upgrading the

suspension. As in the Hyundai Getz, only the springs may be required to be modified for overloading of the rear axle. Once approved a vehicle license can be acquired.

NCOP14 *National Guidelines for the Installation of Electric Drive in Motor Vehicles* is currently under review with significant changes expected. Therefore should the battery cage crash accelerations be lowered or the method for analysis of the battery cages outlined further or altered, there may be a future requirement for the REV team to modify or rebuild the battery cages with a lighter or thinner material to improve the performance of the vehicle. Also if there is a future requirement for testing of the battery cages, this can also be performed by a future REV team member through strain gauge testing or destructive testing on the Instron machine if spare battery cages are fabricated.

The REV team aims to complete the Lotus Elise electric conversion whilst maintaining the original performance specifications. This will demonstrate an electric sports car as a viable option for future public users. Therefore to confirm this, the REV team will need to carry out appropriate performance testing on the vehicle at an approved race track once completed.

## 7 References

- Asakura, K, Shimomura, M & Shodai, T 2003, 'Study of life evaluation methods for Li-ion batteries for backup applications', *Journal of Power Sources*, vol. 119-121, pp. 902-905.
- Australian Institute of Steel Construction 1999, *Design Capacity Tables for Structural Steel*, 3rd edn, AISC, Sydney NSW.
- Australian Motor Vehicle Certification Board Working Party 2006, *National Guidelines for the Installation of Electric Drives in Motor Vehicles*, Department of Infrastructure, Transport, Regional Development and Local Government, Australia [31 March 2009].
- Bastow, D 2004, *Car suspension and handling*, Professional Engineering Publishing, Bury St. Edmunds.
- Braunl, T, *The REV Project*, The University of Western Australia. Available from: <http://therevproject.com/> [22 April 2009].
- Cengel, YA 2008, *Fundamentals of thermal-fluid sciences*, McGraw-Hill, Boston.
- Department of Climate Change 2008, *National Greenhouse Gas Inventory 2006*, Department of Climate Change, Canberra [31 March 2009].
- Dhameja, S 2001, 'The Li-ion Battery', in *Electric Vehicle Battery Systems*, Elsevier Newnes, p. 10.
- ebm-papst, 8212JN, ebm-papst. Available from: [http://www.ebmpapst.com/en/products/compact-fans/axial-compact-fans/axial\\_compact\\_fans\\_detail.php?pID=53943&PHPSESSID=edcwraol](http://www.ebmpapst.com/en/products/compact-fans/axial-compact-fans/axial_compact_fans_detail.php?pID=53943&PHPSESSID=edcwraol) [28 July 2009].
- Energy Task Force 2004, *Securing Australia's Energy Future*, Australian Government, Barton, ACT.
- Garche, J & Jossen, A 2000, 'Battery management systems (BMS) for increasing battery life time', in *Telecommunications Energy Special Conference, 2000*, p. 81.
- Holden, *The Electric Volt*, GM Holden Ltd. Available from: <http://www.holden.com.au/holden-innovation/volt> [27 March 2009].
- Ip, C 2008, *Battery Restraint System Design and Performance Evaluation for Renewable Energy Vehicle Project*, Final Year Project, The University of Western Australia.
- Leitman, S & Brant, B 2009, *Build your own electric vehicle*.
- Lotus Cars Ltd 2001, *Service Notes Elise*, Norfolk, England.
- Marshall, R 2009, 'GM Hollers for a Marshall', *Wheels*, vol. March 2009, p. 155.

Micronel, *SERIES D604T/Q*, Micronel. Available from:

<http://www.micronel.com/ProductPage-D.asp?pType=D604T/Q&pReset=y&pTitle=D604T%2FQ> [22 July 2009].

MINI, *MINI-E*, BMW Group Australia. Available from:

<http://www.mini.com.au/scripts/main.asp?PageID=29428> [1 April 2009].

MINI, *MINI Cooper*, BMW Group Australia. Available from:

<http://www.mini.com.au/scripts/main.asp?PageID=13589&LEVEL=2> [1 April 2009].

Pachauri, RK & Reisinger, A 2007, *Climate Change 2007 Synthesis Report*, Intergovernmental Panel on Climate Change, [31 March 2007].

Reimpell, J 2001, *The automotive chassis : engineering principles*, 2nd edn, Butterworth Heinemann, Oxford.

School of Mechanical Engineering 2009, *Project Safety Induction*, UWA, Perth.

Siguang, L 2009, 'Study on battery management system and lithium-ion battery', *Proceedings - 2009 International Conference on Computer and Automation Engineering, ICCAE 2009*, p. 222.

Standards Australia 1985, *AS 1275-1985 : Metric screw threads for fasteners*, SAI Global, Strathfield NSW.

Standards Australia 1995, *AS/NZS 4291.2:1995 : Mechanical properties of fasteners - Nuts with specified proof load values - Coarse thread*, SAI Global, Strathfield NSW.

Standards Australia 1996, *AS/NZS 3679.1:1996 : Structural steel - Hot-rolled bars and sections*, SAI Global, Strathfield NSW.

Standards Australia 1997, *AS/NZS 1866:1997 : Aluminium and aluminium alloys - Extruded rod, bar, solid and hollow shapes*, SAI Global, Strathfield NSW.

Standards Australia 1998, *AS 4100-1998 : Steel structures*, SAI Global, Strathfield NSW.

Tang, D 2009, *Suspension System for the Renewable Energy Vehicle Project*, Third Year Project, The University of Western Australia.

Tesla Motors, *Under the Skin*, Tesla Motors. Available from:

[http://www.teslamotors.com/design/under\\_the\\_skin.php](http://www.teslamotors.com/design/under_the_skin.php) [12 April 2009].

Thunder Sky, *Thunder Sky LiFeYPO4 Power Battery Specifications*, Thunder Sky Energy Group Limited. Available from: [http://www.thunder-sky.com/products\\_en.asp](http://www.thunder-sky.com/products_en.asp) [14 May 2009].

UWA Occupational Therapist, *Safety in Workshops*, UWA. Available from:

[http://www.safety.uwa.edu.au/policies/safety\\_in\\_workshops](http://www.safety.uwa.edu.au/policies/safety_in_workshops) [15th September 2009].

UWA Safety & Health Manager 2007, *UWA Electrical Safety Pamphlet*, UWA, Perth.

## 8 Appendices

### 8.1 Appendix A – MINI-E CO<sub>2</sub> emissions

Electricity delivered to households produces the equivalent of 950-1000kg of CO<sub>2</sub>/MWh (Energy Task Force 2004). Given a MINI-E consumes 0.15kWh/km (MINI 2009a), if the MINI-E was charged from a standard household plug point, it would be producing the equivalent of 14.2-15kg of CO<sub>2</sub>/100km or an average of 14.6kg of CO<sub>2</sub>/100km.

### 8.2 Appendix B - Thermal resistance values for Hyundai Getz battery cage

|                           | <b>Discharging</b> | <b>Charging</b> |
|---------------------------|--------------------|-----------------|
| R <sub>Total</sub>        | 0.06338K/W         | 0.05039K/W      |
| R <sub>Conv(Bottom)</sub> | 0.8694K/W          | 0.9437K/W       |
| R <sub>Conv(Sides)</sub>  | 0.3031K/W          | 0.3309K/W       |
| R <sub>Forced Conv</sub>  | 0.08827K/W         | 0.06344K/W      |

**Table 22:** Summary of thermal resistance values for Hyundai Getz battery cage.

### 8.3 Appendix C - Thermal Resistance of Natural Convection of Getz Enclosure

The thermal resistance from natural convection of the Hyundai Getz battery cage enclosure can be calculate using equation 8.1 to give 0.9757K/W for discharging and 1.0602K/W for charging. Note these values are greater than the required calculated values for forced convection, hence proving the requirement for a fan.

$$R_{Conv(Top)} = \frac{L_c}{kNuA_s} \quad (8.1)$$

### 8.4 Appendix D – Forced Convection over and between Getz batteries

The following equations, 8.2-8.6 were substituted into each other to obtain final equations 3.14 and 3.18 for tube flow.

$$R = \frac{1}{hA_s} \quad (8.2)$$

$$Nu = \frac{hD_h}{k} \quad (8.3)$$

$$Re = \frac{V_{avg}D_h}{\nu} \quad (8.4)$$

$$V_{avg} = \frac{q}{nA_c} \quad (8.5)$$

$$D_h = \frac{4A_c}{p} \quad (8.6)$$

8.5 Appendix E – Formulas for Required Flow Rate

$$\frac{1}{0.08827} = 3.911 \times 10^{-4} (2,033,071q)^{0.8} + n \times 1.272 \times 10^{-3} \left( \frac{6,768,232q}{n} \right)^{0.8} \quad (8.7)$$

$$\frac{1}{0.06344} = 3.659 \times 10^{-4} (2,340,245q)^{0.8} + n \times 1.191 \times 10^{-3} \left( \frac{7,790,832q}{n} \right)^{0.8} \quad (8.8)$$

8.6 Appendix F – Risk Matrix

Each risk can be classified as low, medium, high or extreme before and after mitigation using the risk matrix below (Table 23).

| Likelihood     | Consequence   |        |          |        |         |
|----------------|---------------|--------|----------|--------|---------|
|                | Insignificant | Minor  | Moderate | Major  | Severe  |
| Rare           | Low           | Low    | Low      | Low    | Low     |
| Unlikely       | Low           | Low    | Low      | Medium | Medium  |
| Possible       | Low           | Low    | Medium   | Medium | Medium  |
| Likely         | Low           | Medium | Medium   | High   | High    |
| Almost certain | Low           | Medium | Medium   | High   | Extreme |

Table 23: Risk Matrix

8.7 Appendix G – Dimension of 8212JN Fan for Hyundai Getz

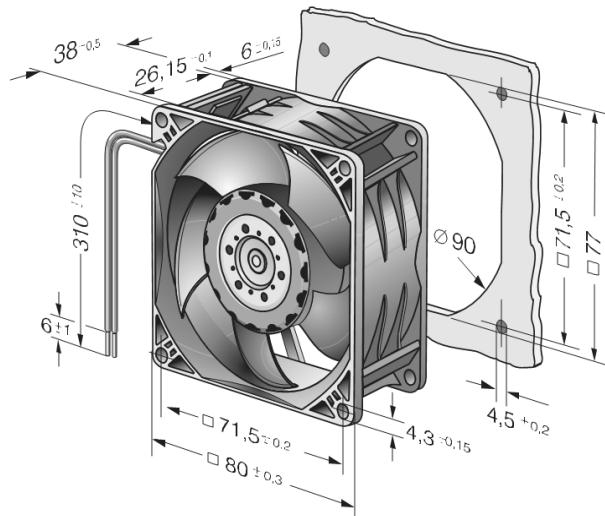
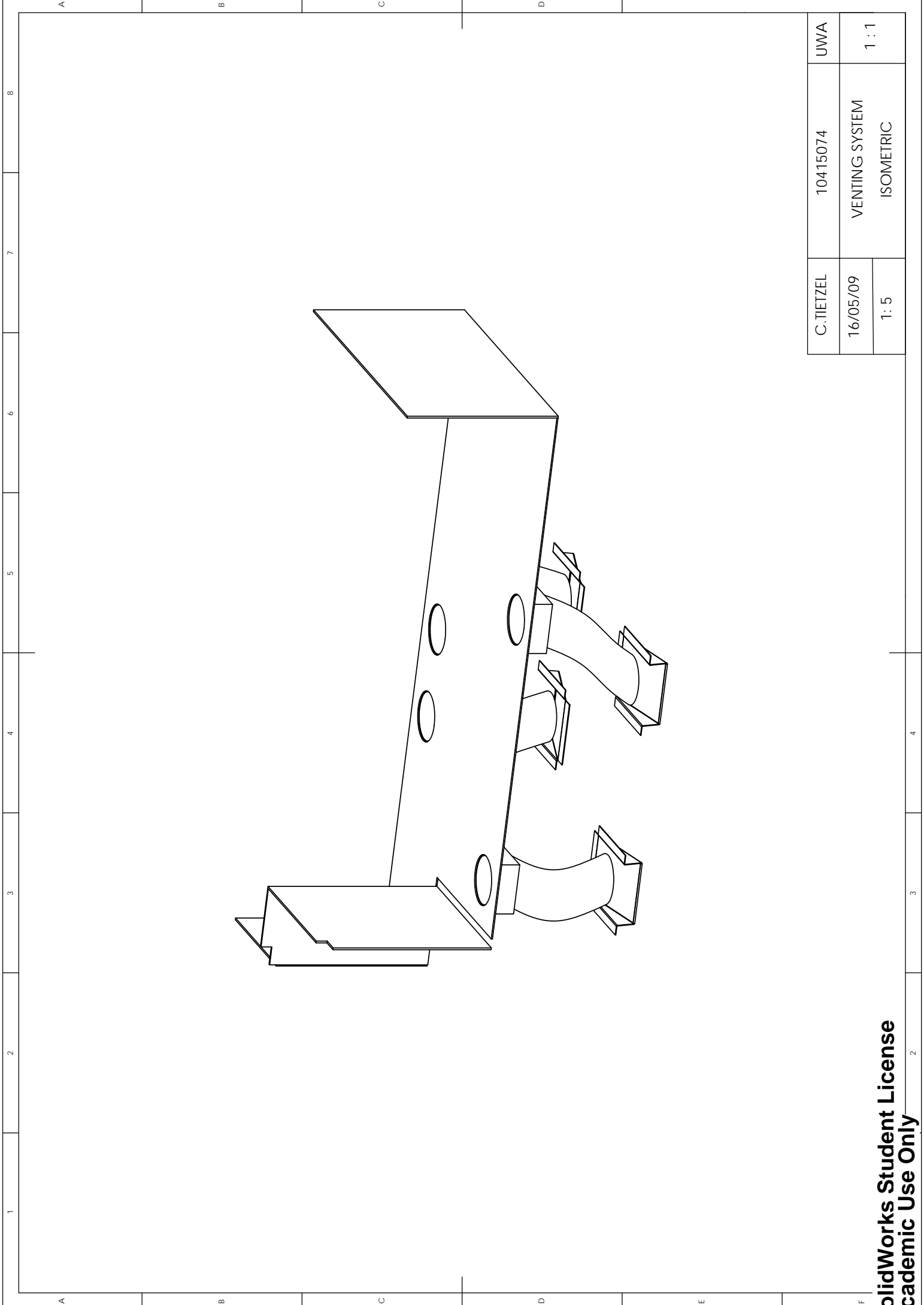


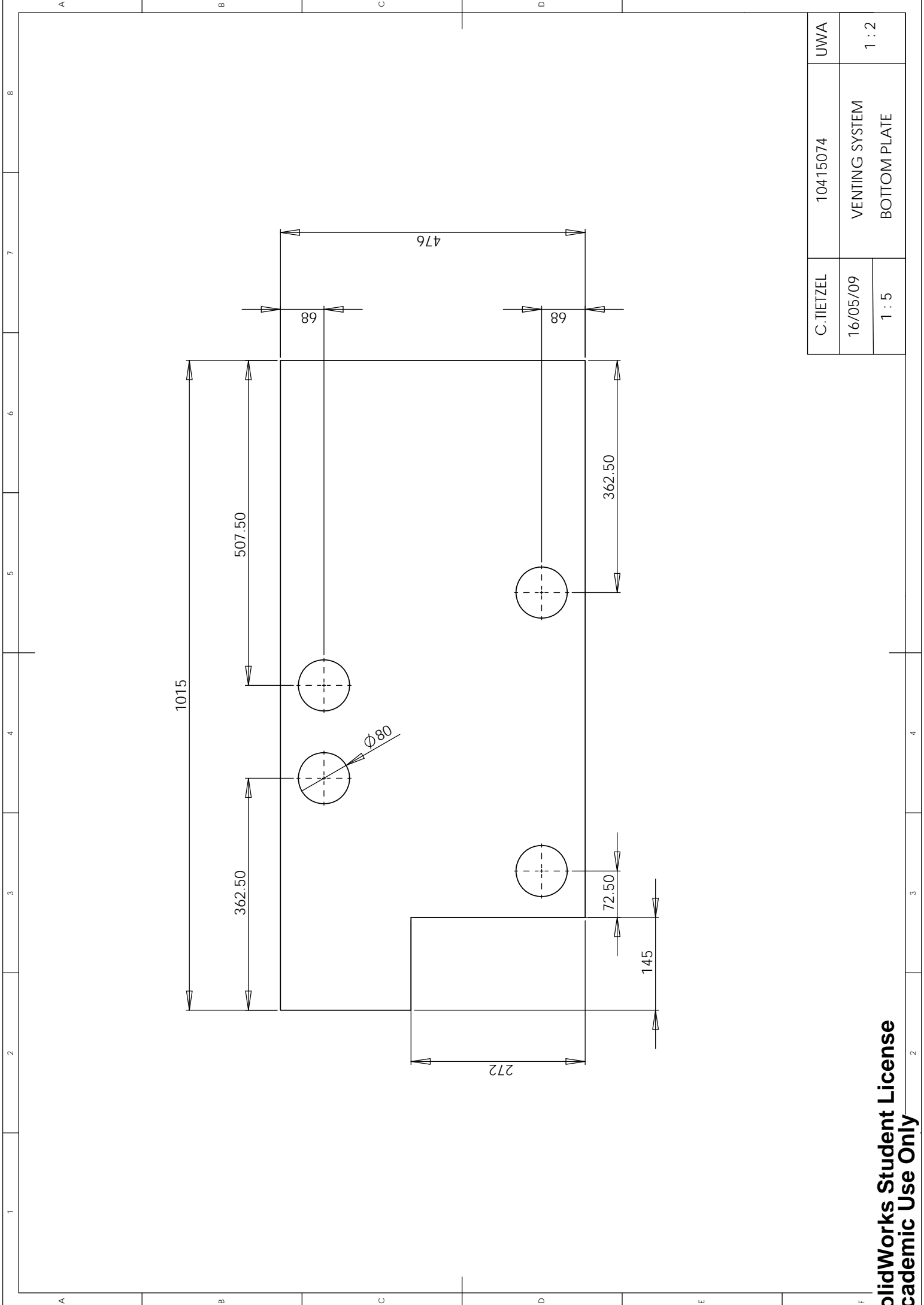
Figure 37: Dimensions of 8212JN fan for Hyundai venting system (ebm-papst 2009).

8.8 Appendix H – Hyundai Getz Venting System Drawings

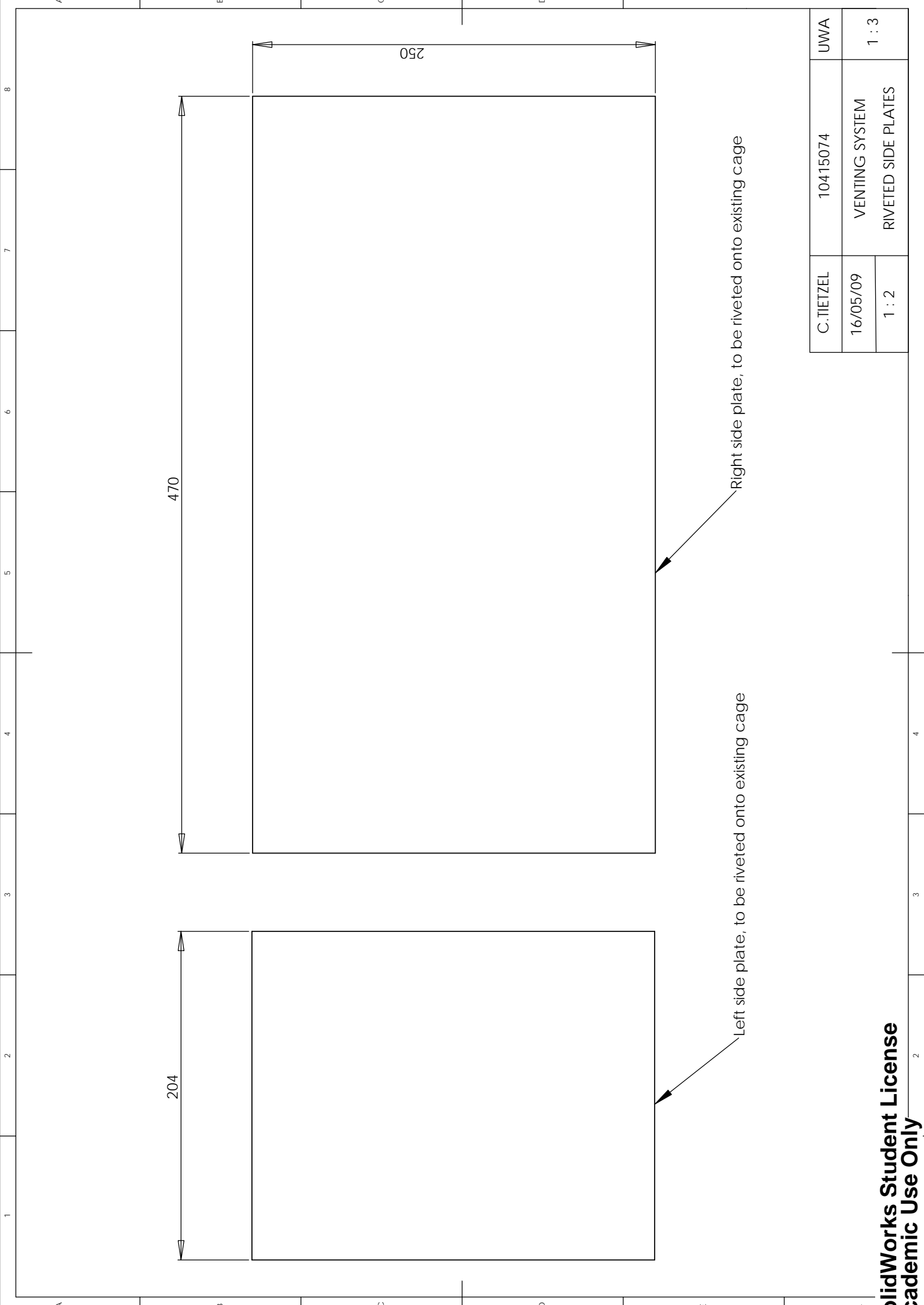
See the following 6 pages for fully dimensioned drawings of the Hyundai Getz venting system. Please note, the scaling dimensions in the bottom left corner of the details pain are only relevant when printed on A3 paper.



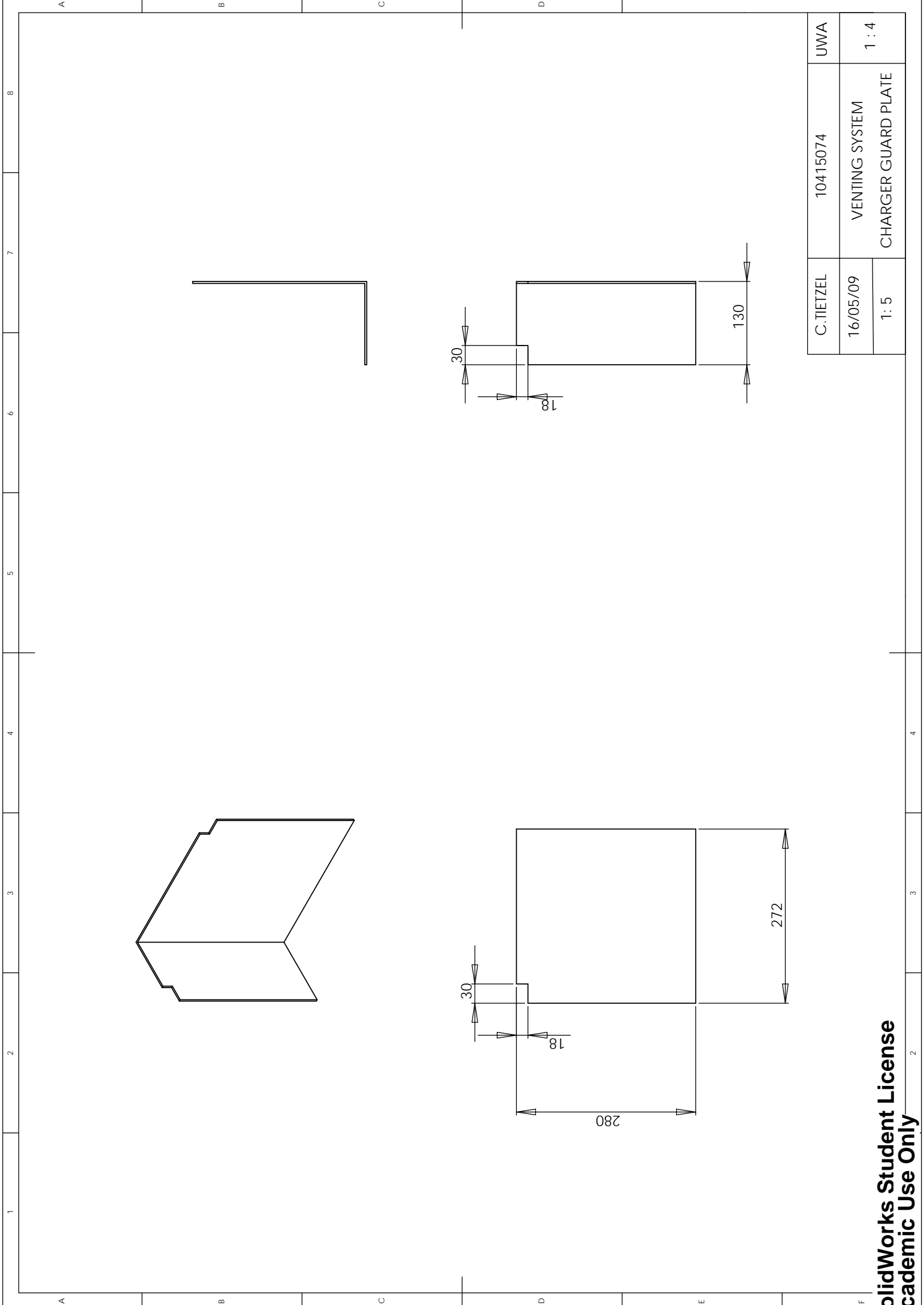
|            |                |       |
|------------|----------------|-------|
| C. TIETZEL | 10415074       | UWA   |
| 16/05/09   | VENTING SYSTEM | 1 : 1 |
| 1 : 5      | ISOMETRIC      |       |



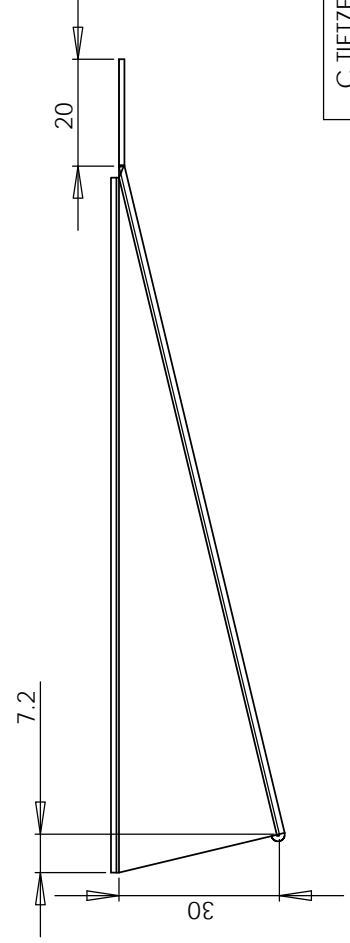
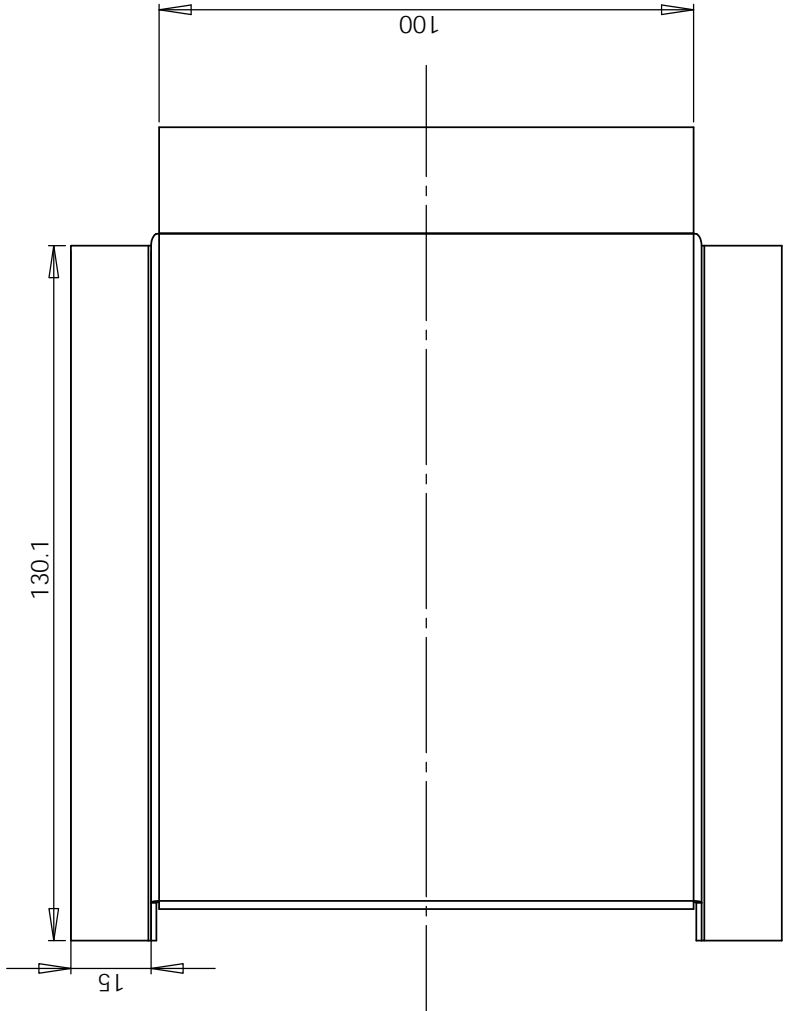
|            |                                |       |
|------------|--------------------------------|-------|
| C. TIETZEL | 10415074                       | UWA   |
| 16/05/09   | VENTING SYSTEM<br>BOTTOM PLATE | 1 : 2 |
| 1 : 5      |                                |       |



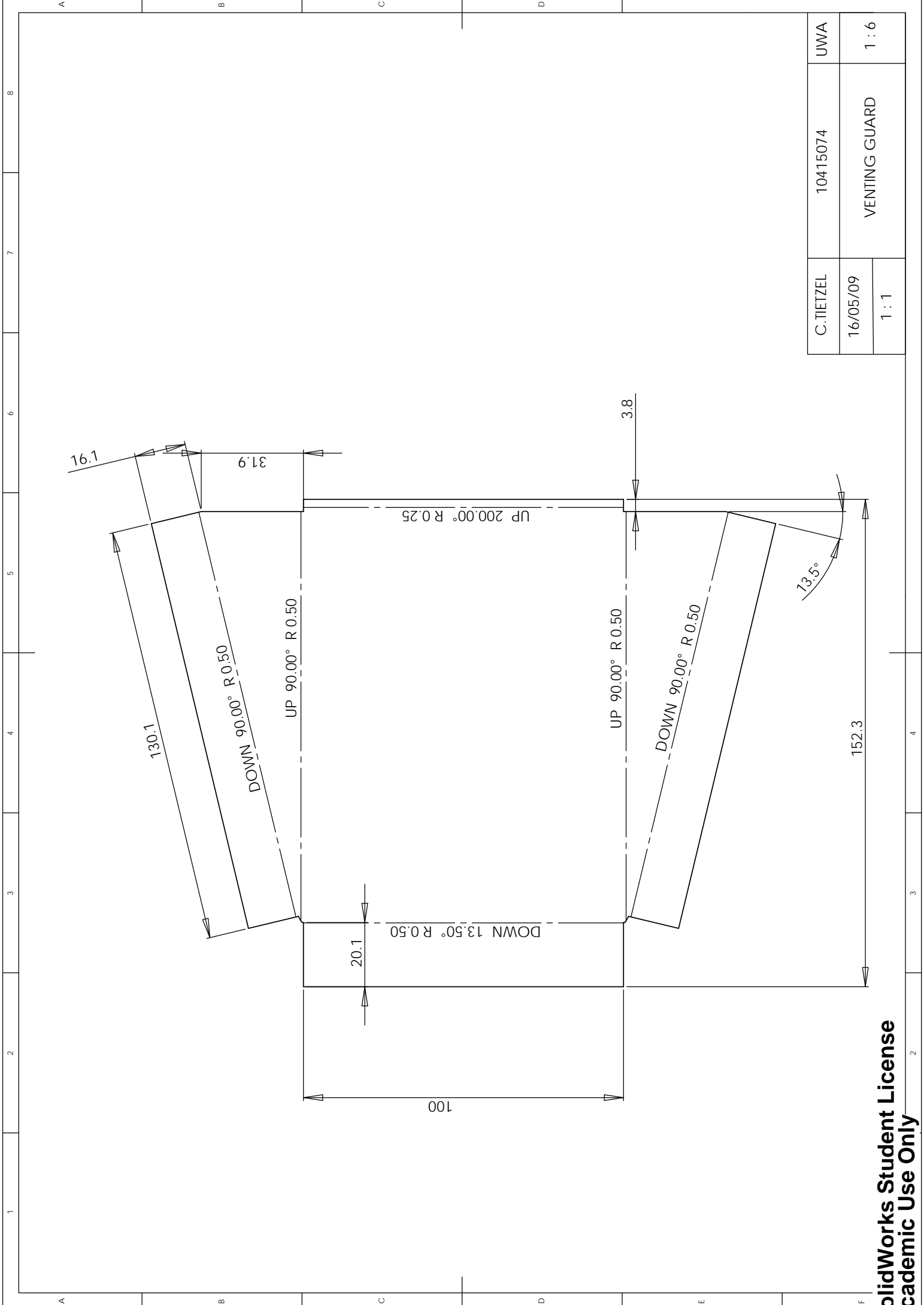
|            |                     |       |
|------------|---------------------|-------|
| C. TIETZEL | 10415074            | UWA   |
| 16/05/09   | VENTING SYSTEM      | 1 : 3 |
| 1 : 2      | RIVETED SIDE PLATES |       |



|            |                     |       |
|------------|---------------------|-------|
| C. TIETZEL | 10415074            | UWA   |
| 16/05/09   | VENTING SYSTEM      | 1 : 4 |
| 1 : 5      | CHARGER GUARD PLATE |       |



|            |               |       |
|------------|---------------|-------|
| C. TIETZEL | 10415074      | UWA   |
| 16/05/09   | VENTING GUARD | 1 : 5 |
| 1 : 1      |               |       |



|            |               |       |
|------------|---------------|-------|
| C. TIETZEL | 10415074      | UWA   |
| 16/05/09   | VENTING GUARD | 1 : 6 |
| 1 : 1      |               |       |

### 8.9 Appendix I – 2002 Model Lotus Elise Chassis Layout

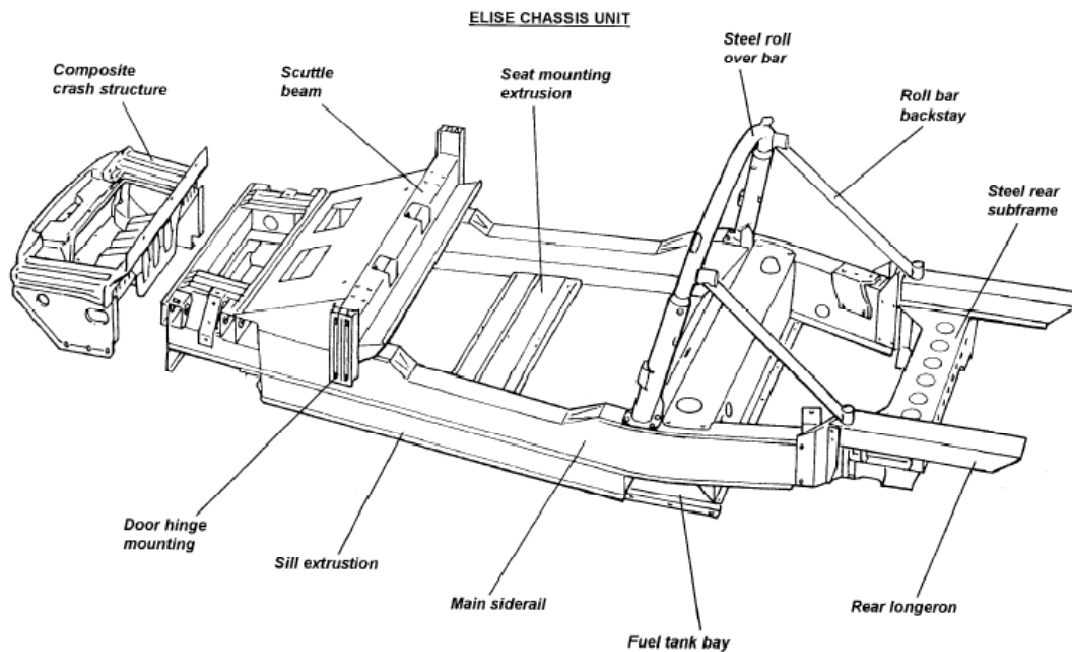
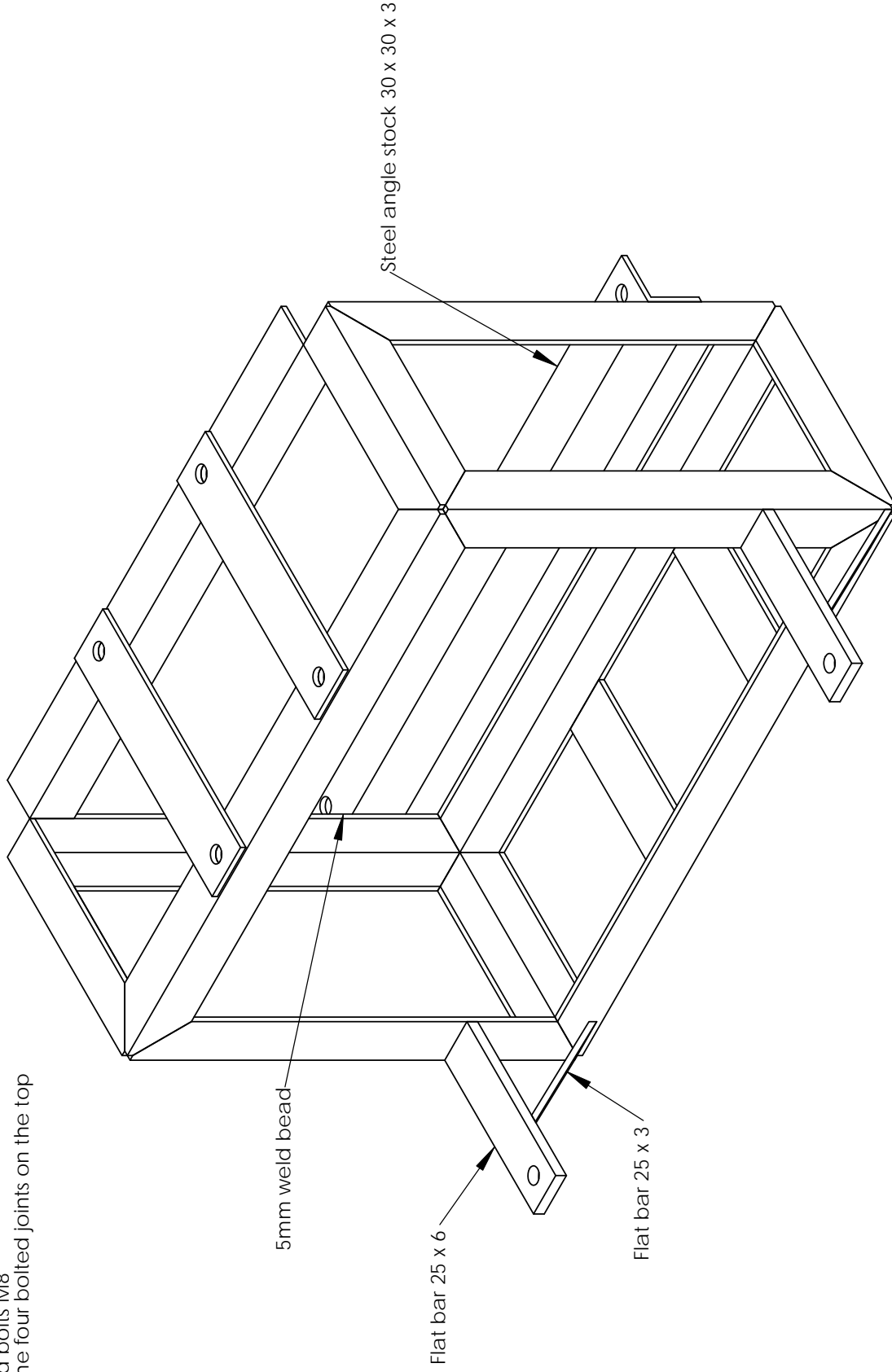


**Figure 38:** 2002 model Lotus Elise chassis layout (Lotus Cars Ltd 2001).

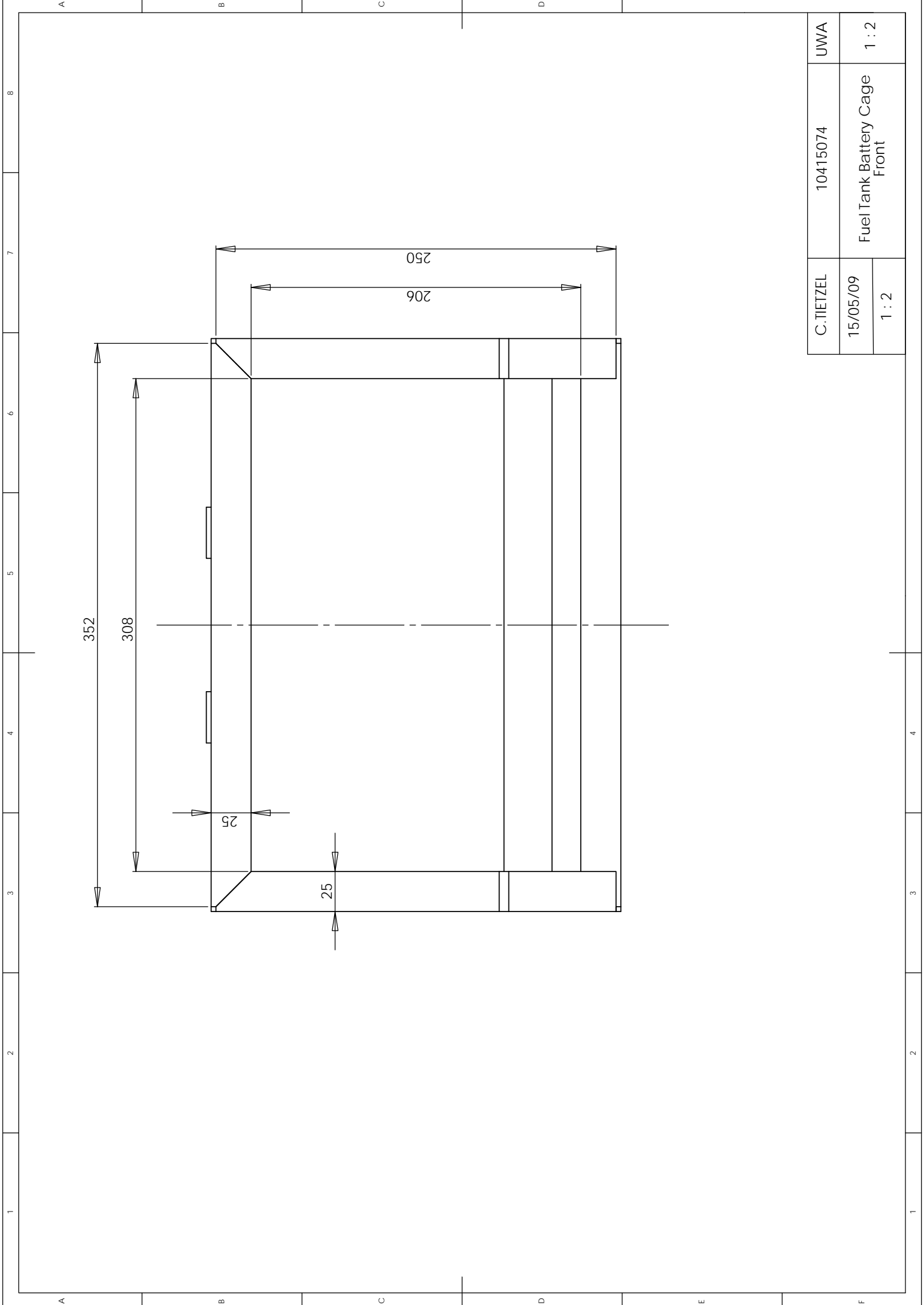
### 8.10 Appendix J – Fuel Tank Battery Cage Drawings

See the following 6 pages for fully dimensioned drawings of the Lotus Elise fuel tank battery cages. Please note, the scaling dimensions in the bottom left corner of the details pain are only relevant when printed on A3 paper.

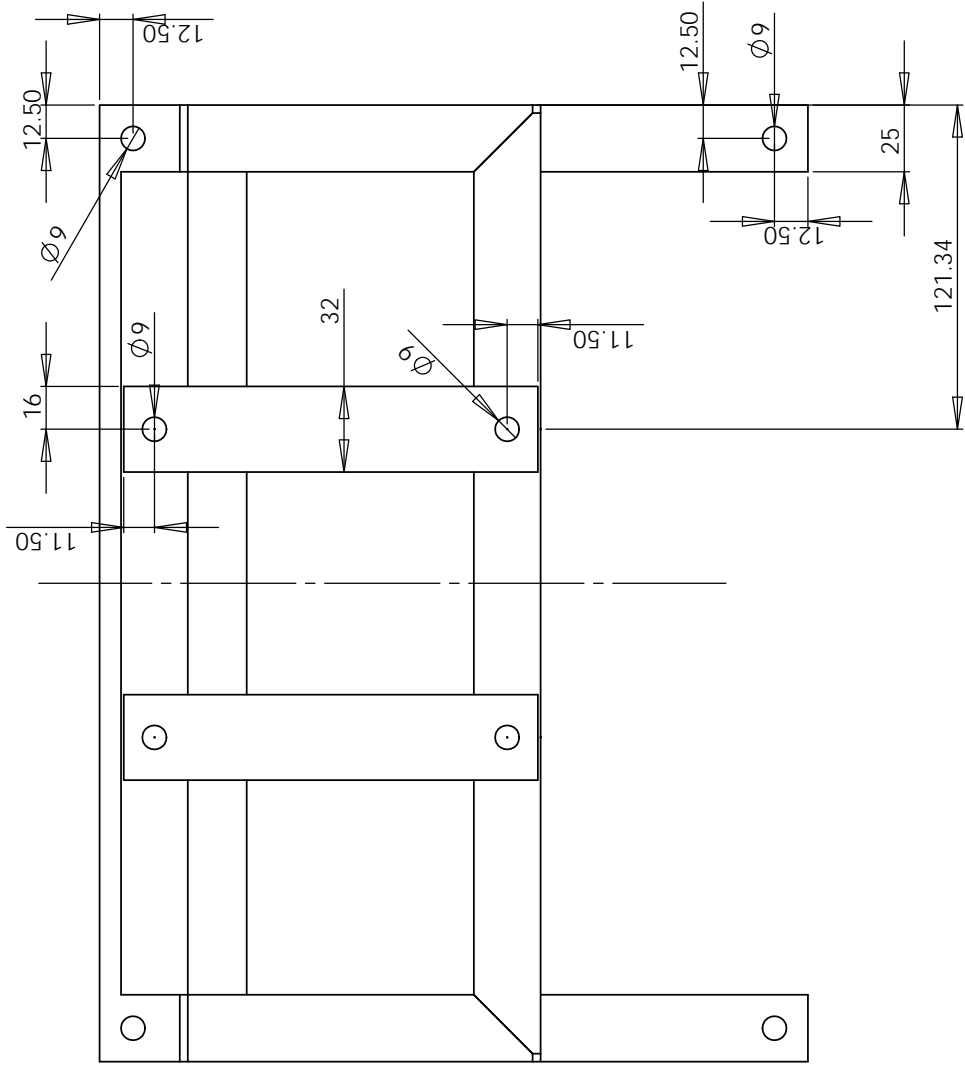
All steel angle stock is 25 x 25 x 3 unless otherwise noted  
 All flat bars are 32 x 3 unless otherwise noted  
 All holes are 9mm diameter and bolts M8  
 All joints are welded except the four bolted joints on the top



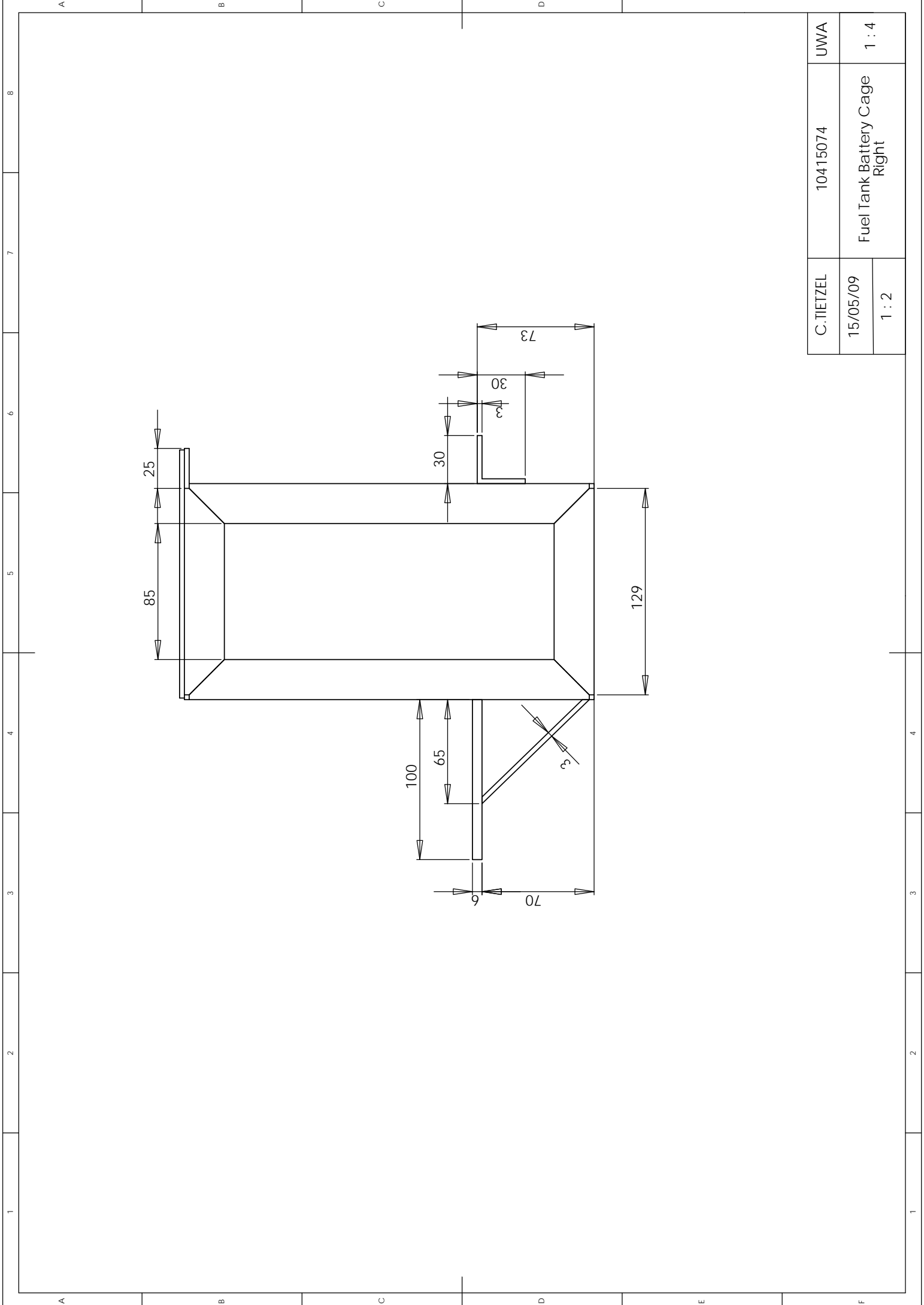
|            |                        |       |
|------------|------------------------|-------|
| C. TIETZEL | 10415074               | UWA   |
| 15/05/09   | Fuel Tank Battery Cage | 1 : 1 |
| 1 : 2      | Isometric              |       |



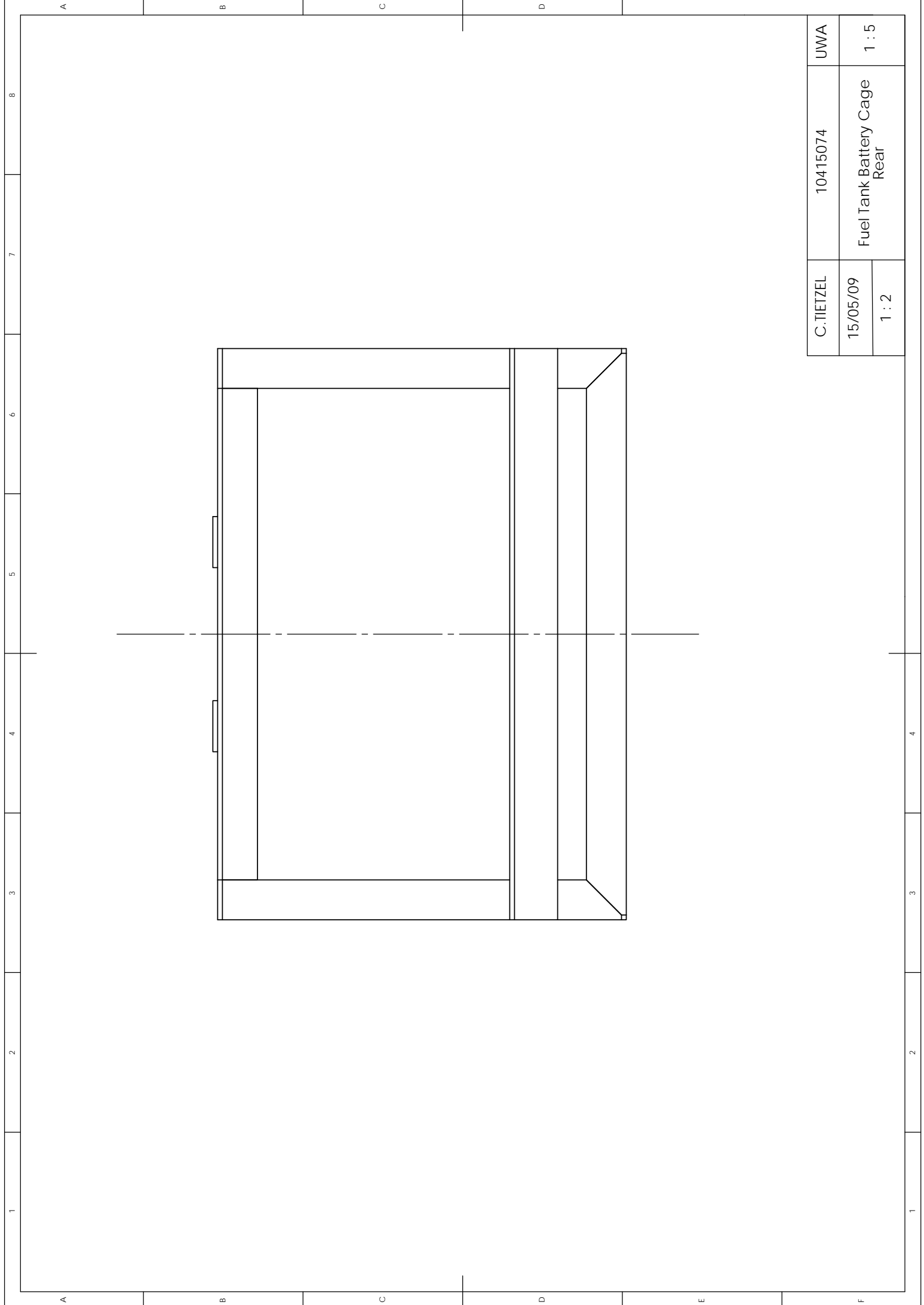
|            |                              |       |
|------------|------------------------------|-------|
| C. TIETZEL | 10415074                     | UWA   |
| 15/05/09   | Fuel Tank Battery Cage Front | 1 : 2 |
| 1 : 2      |                              |       |



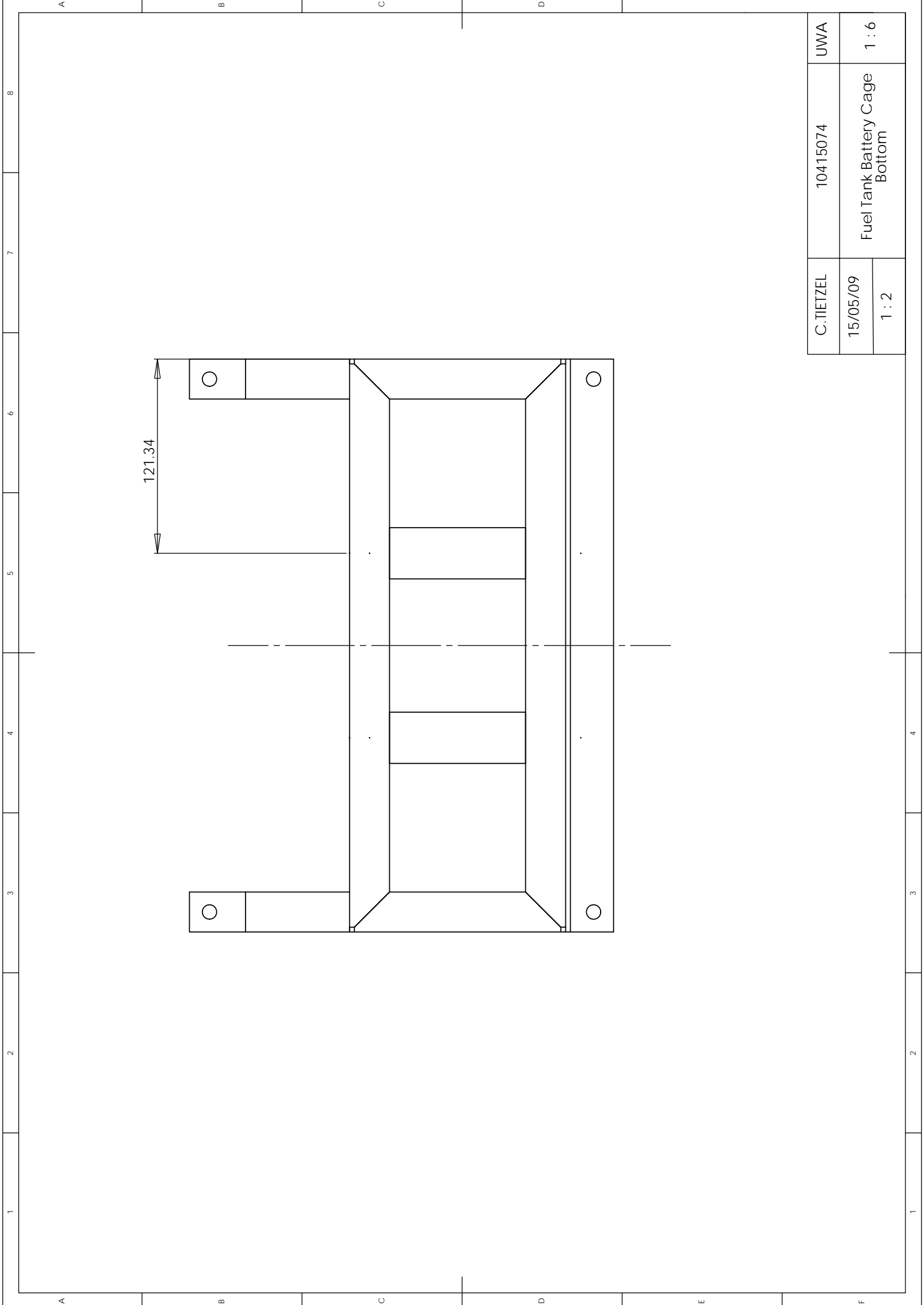
|            |                               |       |
|------------|-------------------------------|-------|
| C. TIETZEL | 10415074                      | UWA   |
| 15/05/09   | Fuel Tank Battery Cage<br>Top | 1 : 3 |
| 1 : 2      |                               |       |



|            |                                 |       |
|------------|---------------------------------|-------|
| C. TIETZEL | 10415074                        | UWA   |
| 15/05/09   | Fuel Tank Battery Cage<br>Right | 1 : 4 |
| 1 : 2      |                                 |       |



|            |                             |       |
|------------|-----------------------------|-------|
| C. TIETZEL | 10415074                    | UWA   |
| 15/05/09   | Fuel Tank Battery Cage Rear | 1 : 5 |
| 1 : 2      |                             |       |

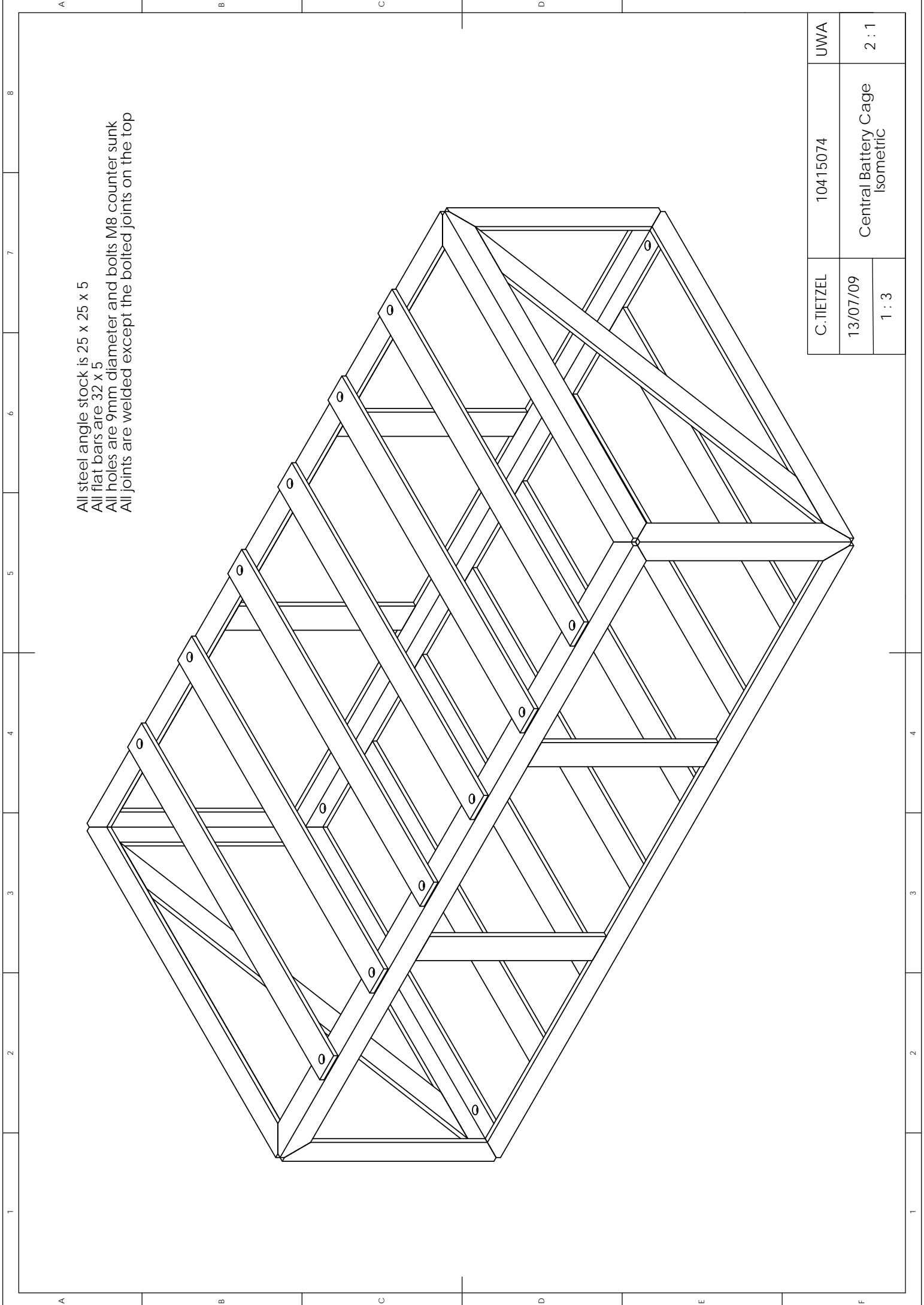


121.34

|            |                               |       |
|------------|-------------------------------|-------|
| C. TIETZEL | 10415074                      | UWA   |
| 15/05/09   | Fuel Tank Battery Cage Bottom | 1 : 6 |
| 1 : 2      |                               |       |

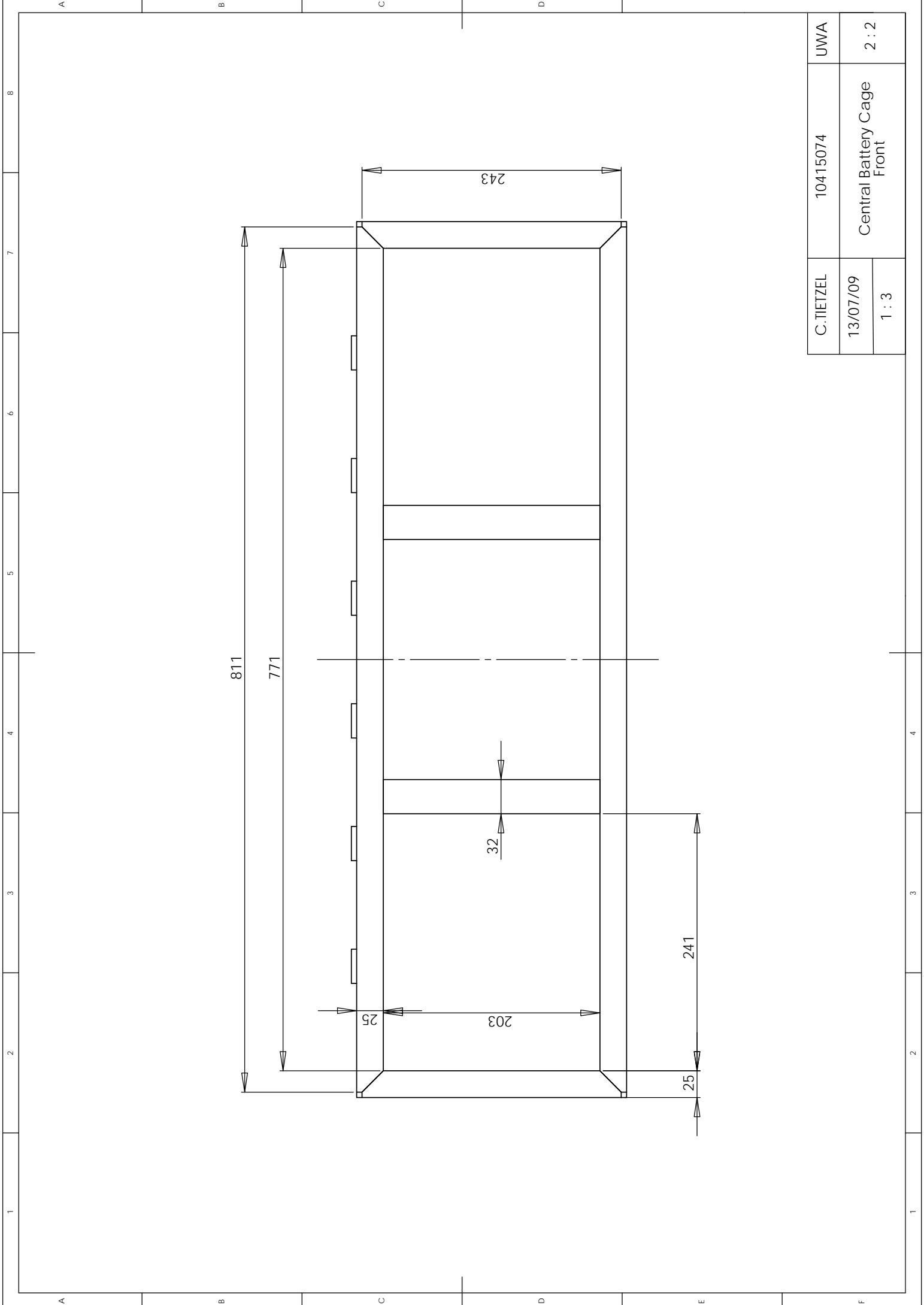
8.11 Appendix K – Central Battery Cage Drawings

See the following 5 pages for fully dimensioned drawings of the Lotus Elise central battery cage. Please note, the scaling dimensions in the bottom left corner of the details pain are only relevant when printed on A3 paper.

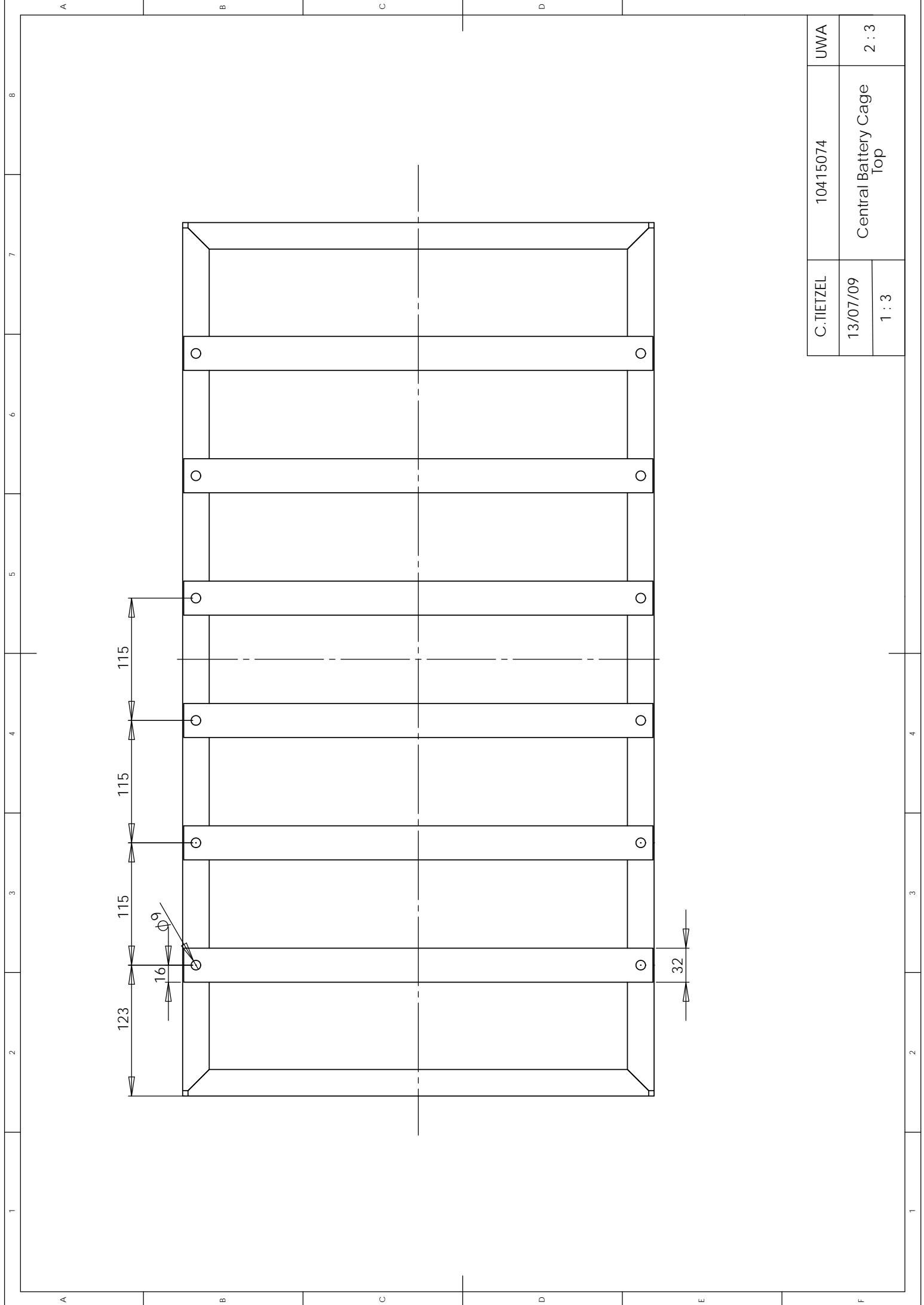


All steel angle stock is 25 x 25 x 5  
 All flat bars are 32 x 5  
 All holes are 9mm diameter and bolts M8 counter sunk  
 All joints are welded except the bolted joints on the top

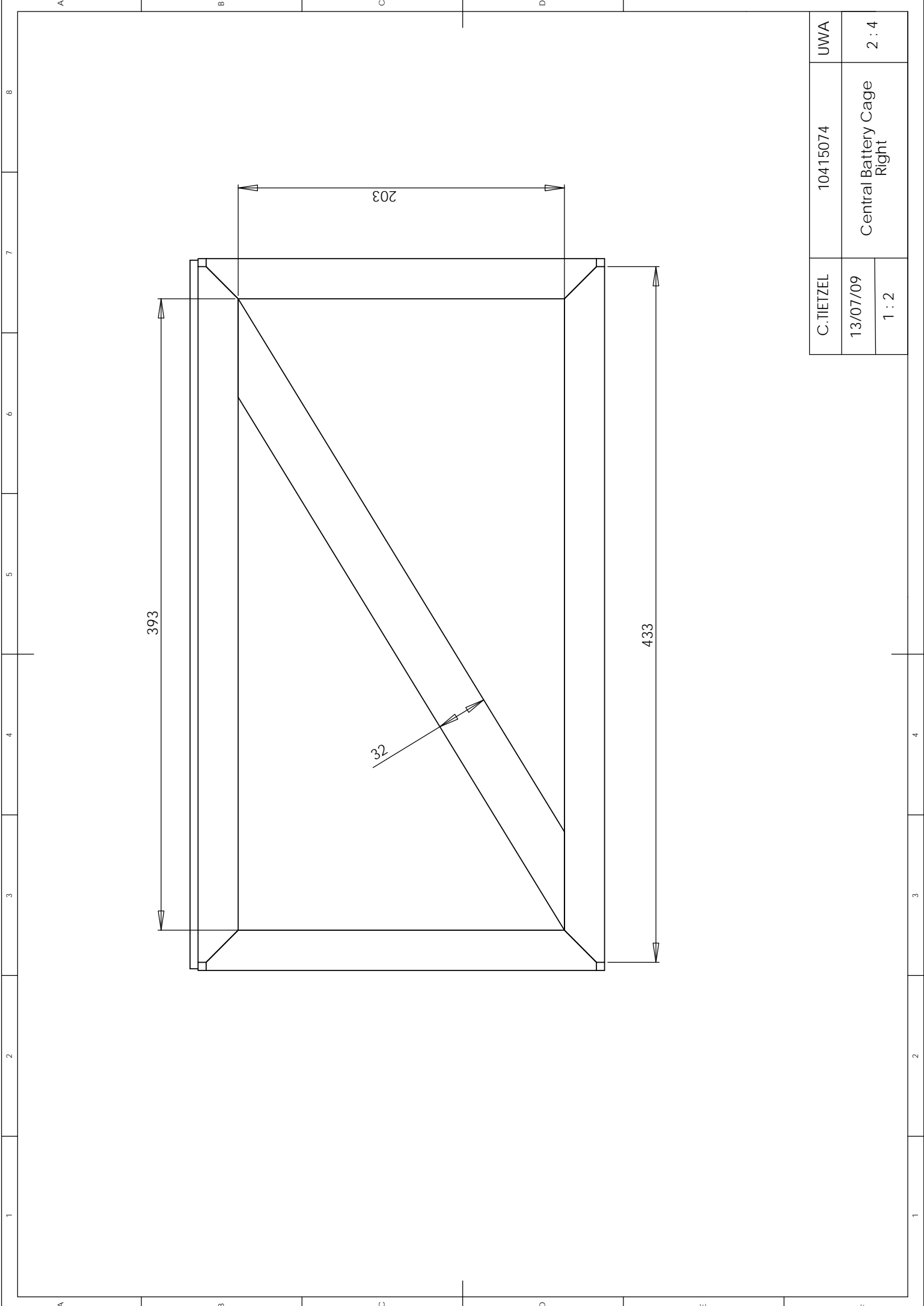
|            |                      |       |
|------------|----------------------|-------|
| C. TIETZEL | 10415074             | UWA   |
| 13/07/09   | Central Battery Cage | 2 : 1 |
| 1 : 3      | Isometric            |       |



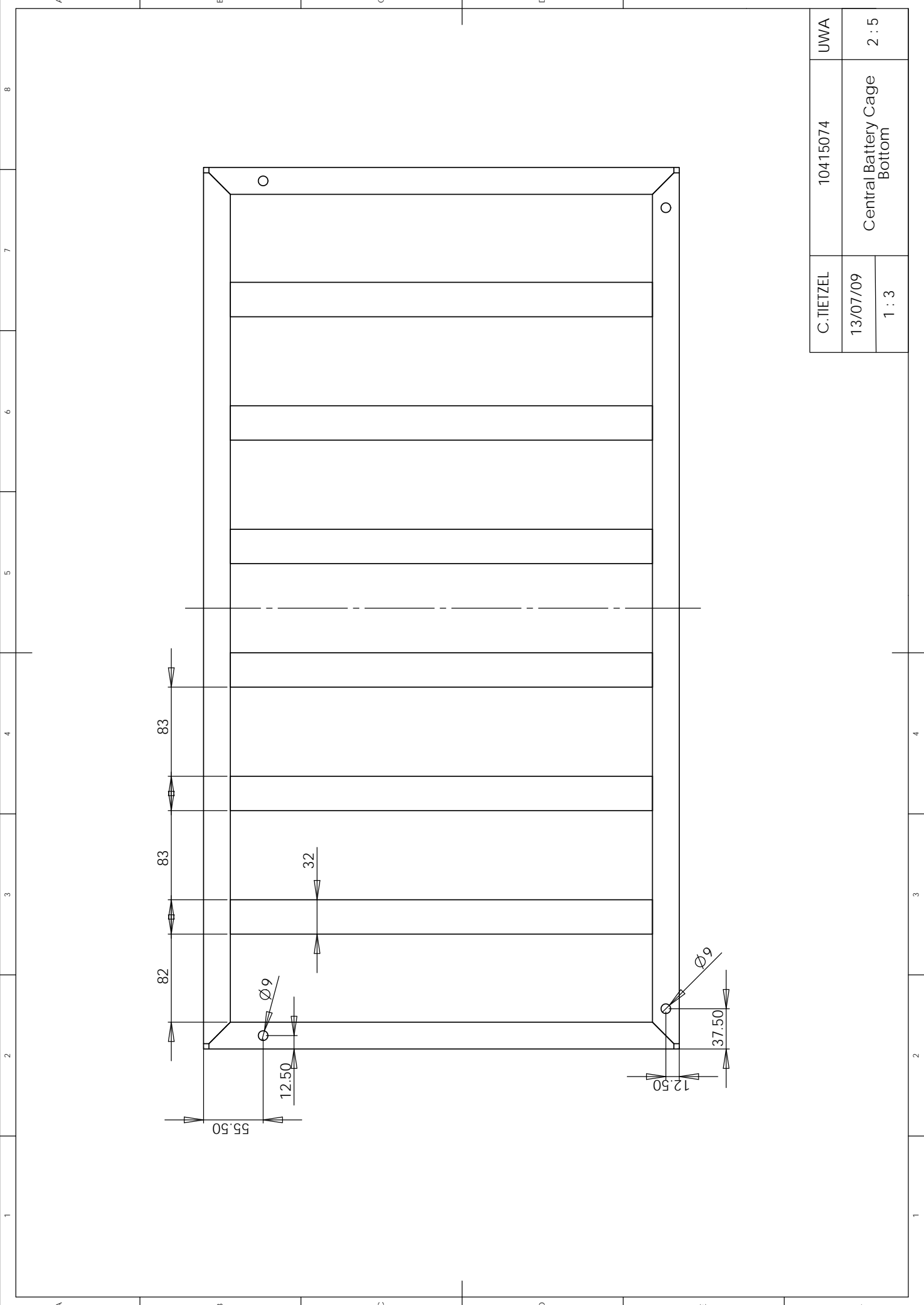
|            |                      |       |
|------------|----------------------|-------|
| C. TIETZEL | 10415074             | UWA   |
| 13/07/09   | Central Battery Cage | 2 : 2 |
| 1 : 3      | Front                |       |



|            |                             |       |
|------------|-----------------------------|-------|
| C. TIETZEL | 10415074                    | UWA   |
| 13/07/09   | Central Battery Cage<br>Top | 2 : 3 |
| 1 : 3      |                             |       |



|            |                               |       |
|------------|-------------------------------|-------|
| C. TIETZEL | 10415074                      | UWA   |
| 13/07/09   | Central Battery Cage<br>Right | 2 : 4 |
| 1 : 2      |                               |       |

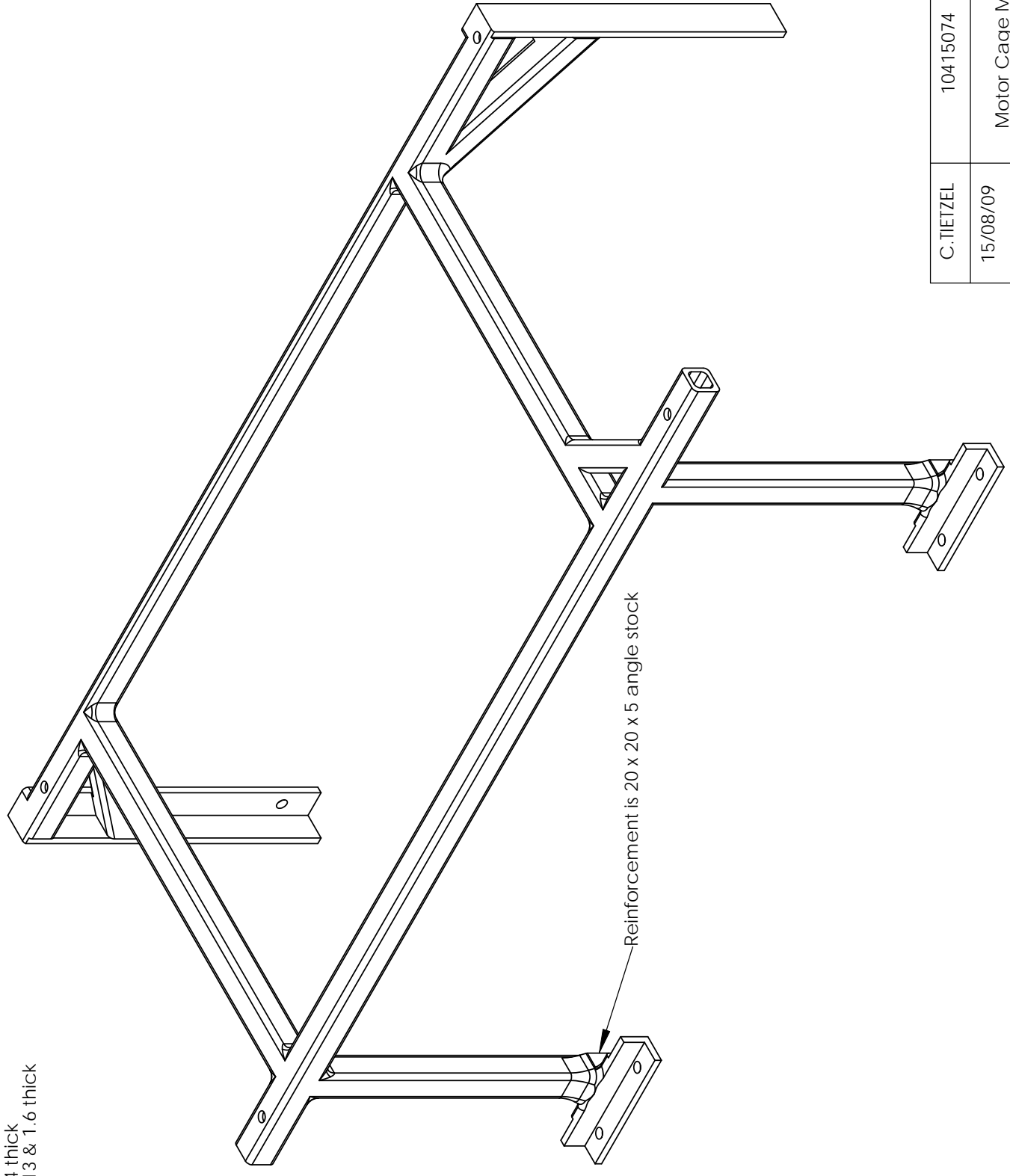


|            |                             |       |
|------------|-----------------------------|-------|
| C. TIETZEL | 10415074                    | UWA   |
| 13/07/09   | Central Battery Cage Bottom | 2 : 5 |
| 1 : 3      |                             |       |

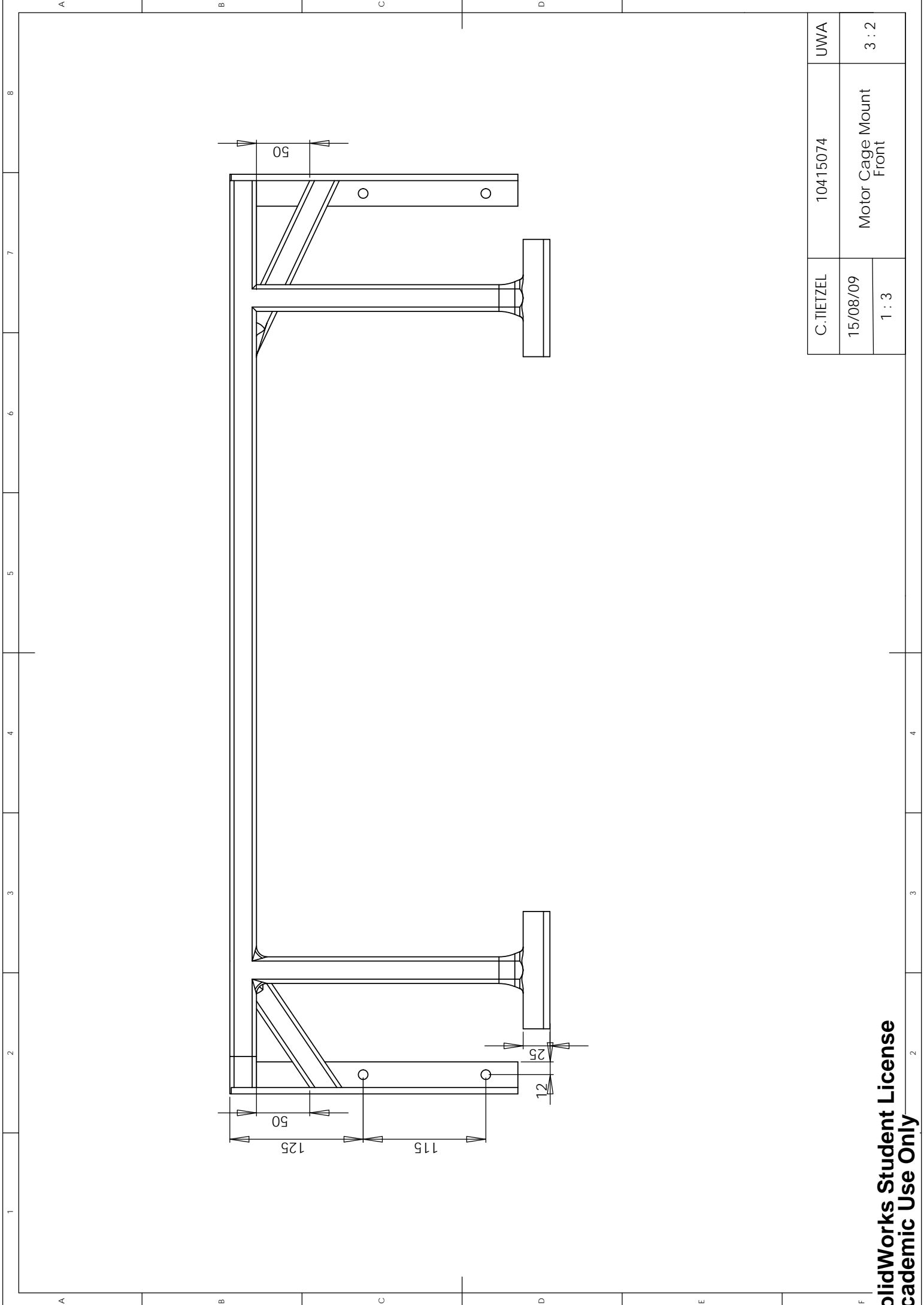
8.12 Appendix L – Central Battery Cage Mount Drawings

See the following 5 pages for fully dimensioned drawings of the Lotus Elise central battery cage mount. Please note, the scaling dimensions in the bottom left corner of the details pain are only relevant when printed on A3 paper.

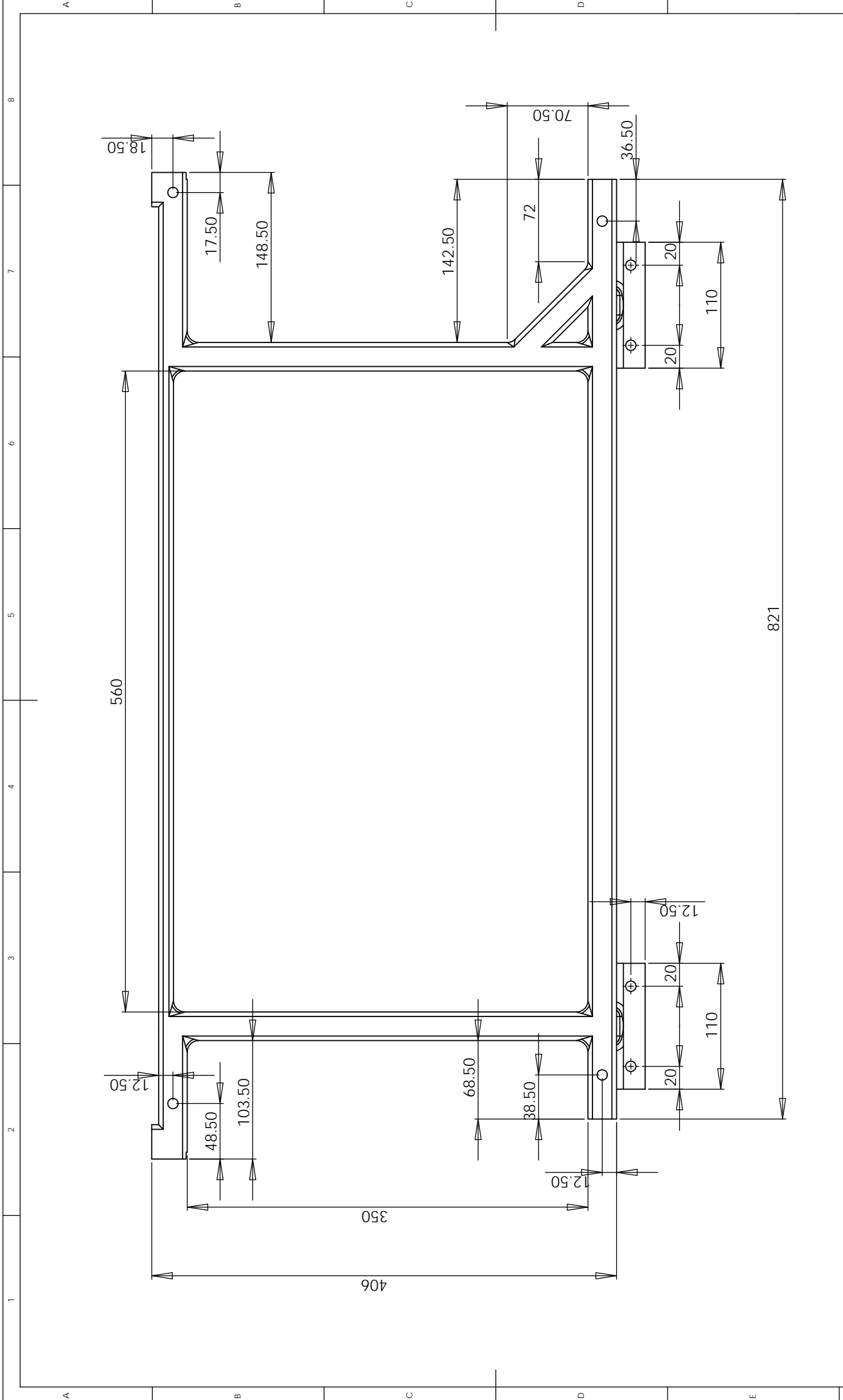
All steel angle stock is 25 x 25 x 6 unless noted  
 All square tubing is 25x25 & 4 thick  
 All rectangular tubing is 25x13 & 1.6 thick



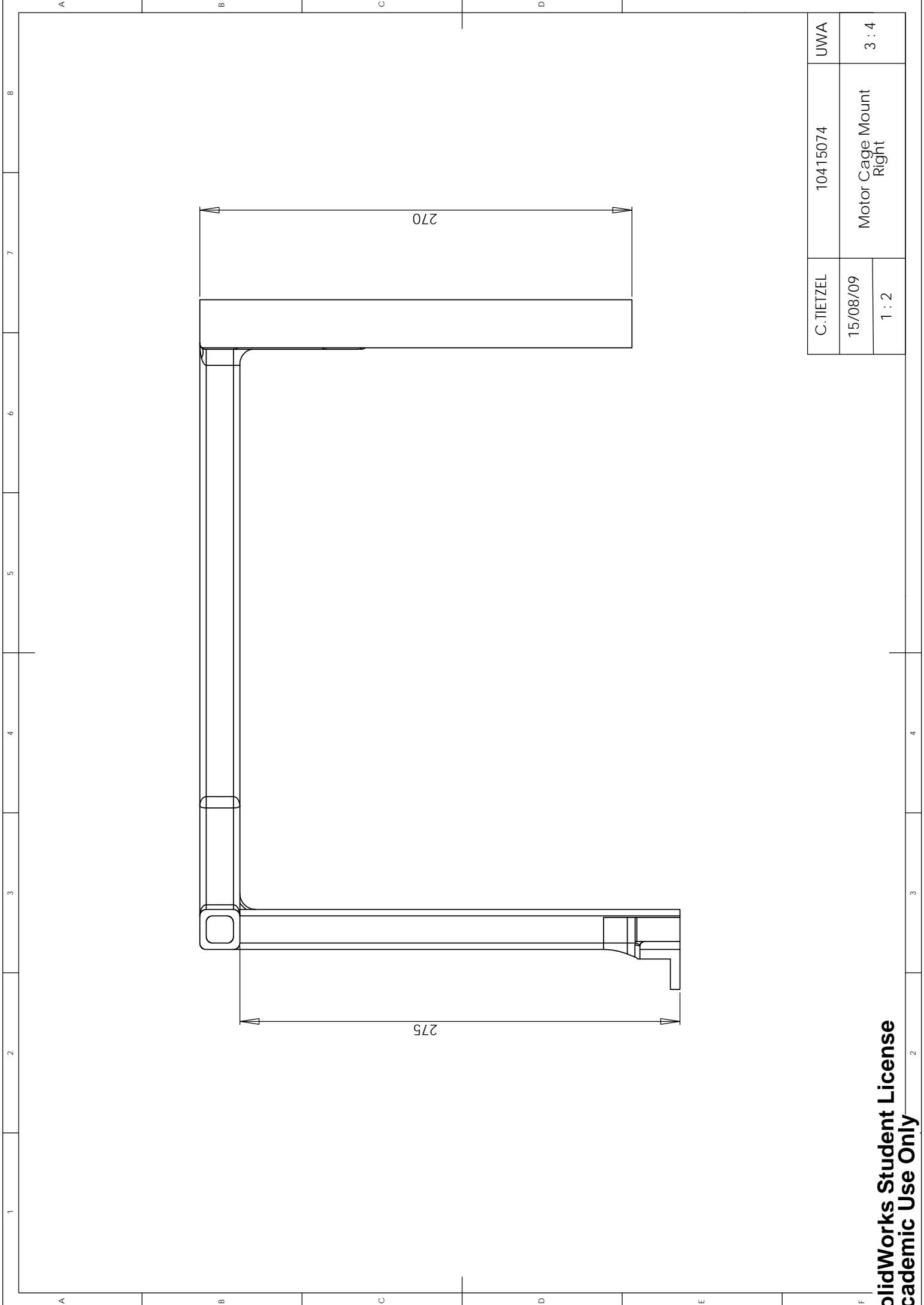
|            |                               |       |
|------------|-------------------------------|-------|
| C. TIETZEL | 10415074                      | UWA   |
| 15/08/09   | Motor Cage Mount<br>Isometric | 3 : 1 |
| 1 : 3      |                               |       |



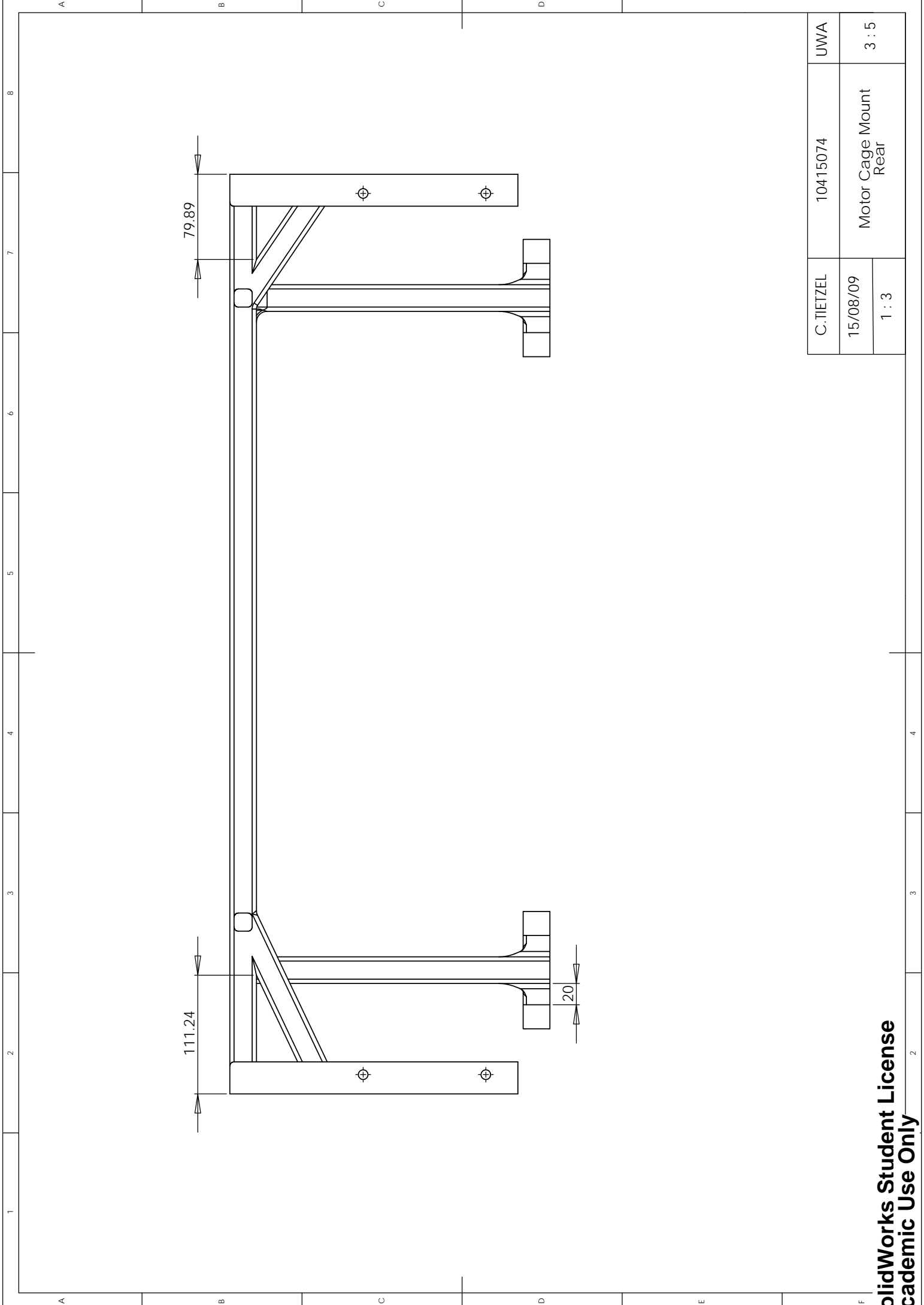
|            |                           |       |
|------------|---------------------------|-------|
| C. TIETZEL | 10415074                  | UWA   |
| 15/08/09   | Motor Cage Mount<br>Front | 3 : 2 |
| 1 : 3      |                           |       |



|            |                         |       |
|------------|-------------------------|-------|
| C. TIETZEL | 10415074                | UWA   |
| 15/08/09   | Motor Cage Mount<br>Top | 3 : 3 |
| 1 : 3      |                         |       |



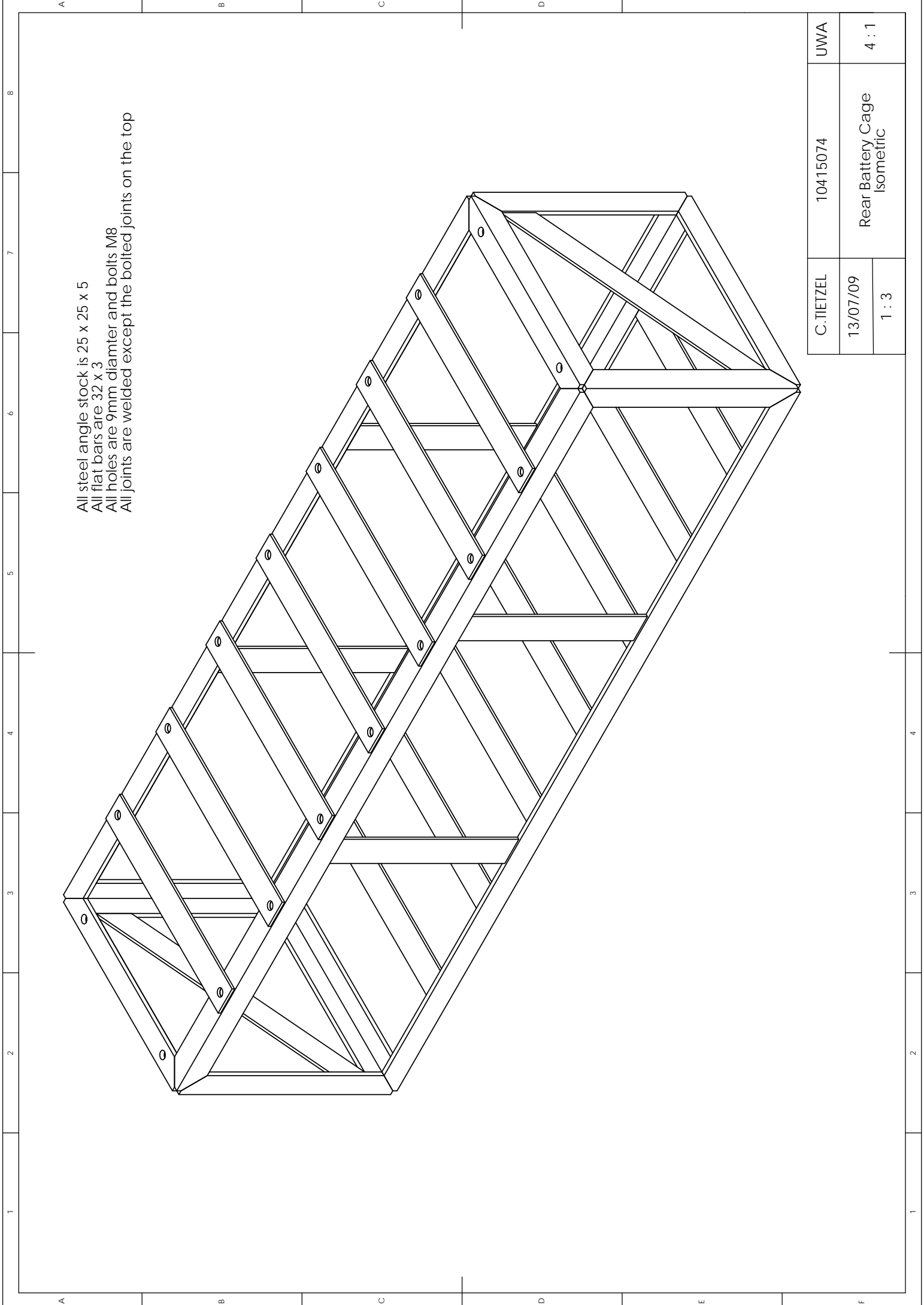
|            |                           |       |
|------------|---------------------------|-------|
| C. TIETZEL | 10415074                  | UWA   |
| 15/08/09   | Motor Cage Mount<br>Right | 3 : 4 |
| 1 : 2      |                           |       |



|            |                          |       |
|------------|--------------------------|-------|
| C. TIETZEL | 10415074                 | UWA   |
| 15/08/09   | Motor Cage Mount<br>Rear | 3 : 5 |
| 1 : 3      |                          |       |

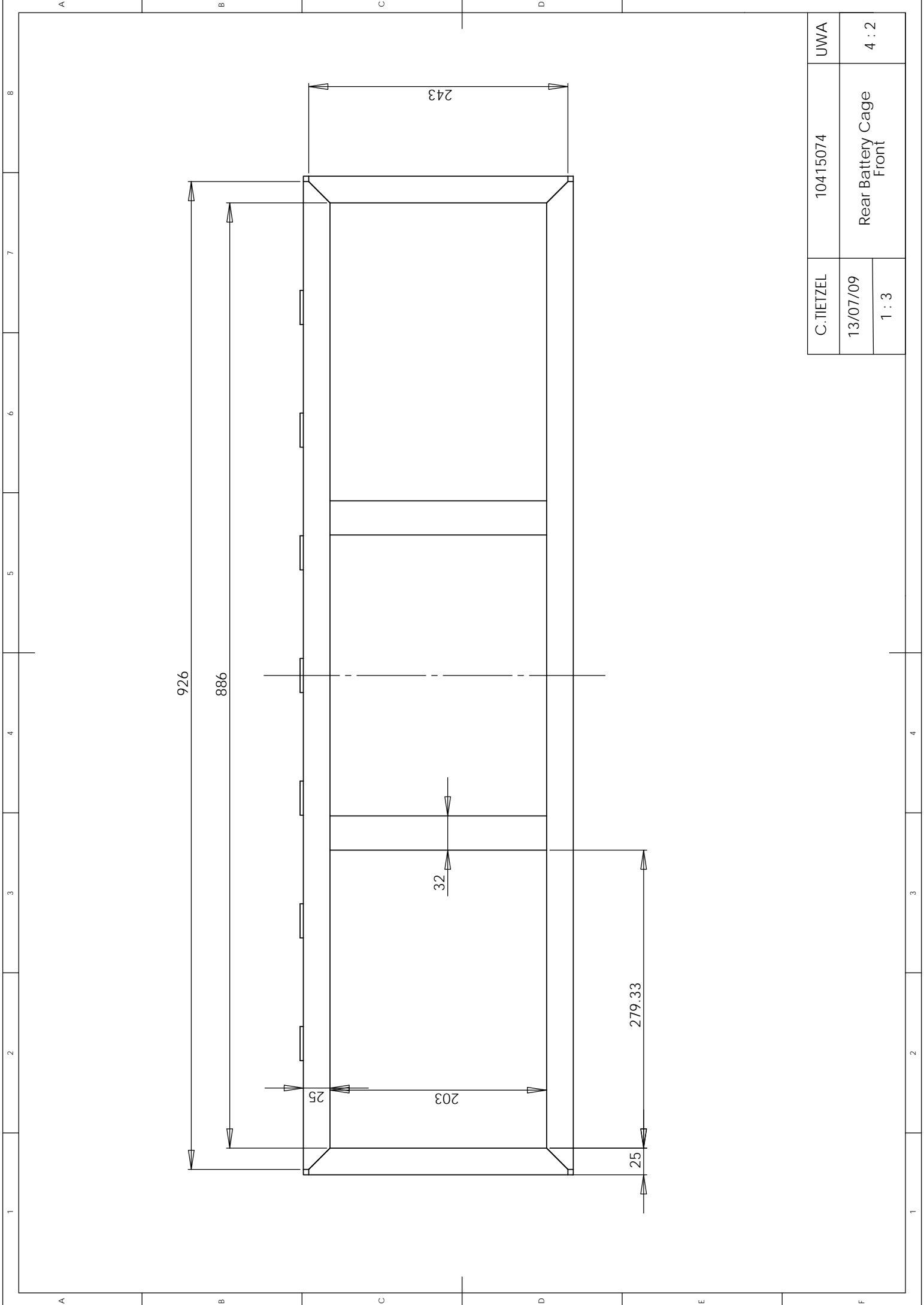
8.13 Appendix M – Rear Battery Cage Drawings

See the following 5 pages for fully dimensioned drawings of the Lotus Elise rear battery cage. Please note, the scaling dimensions in the bottom left corner of the details pain are only relevant when printed on A3 paper.

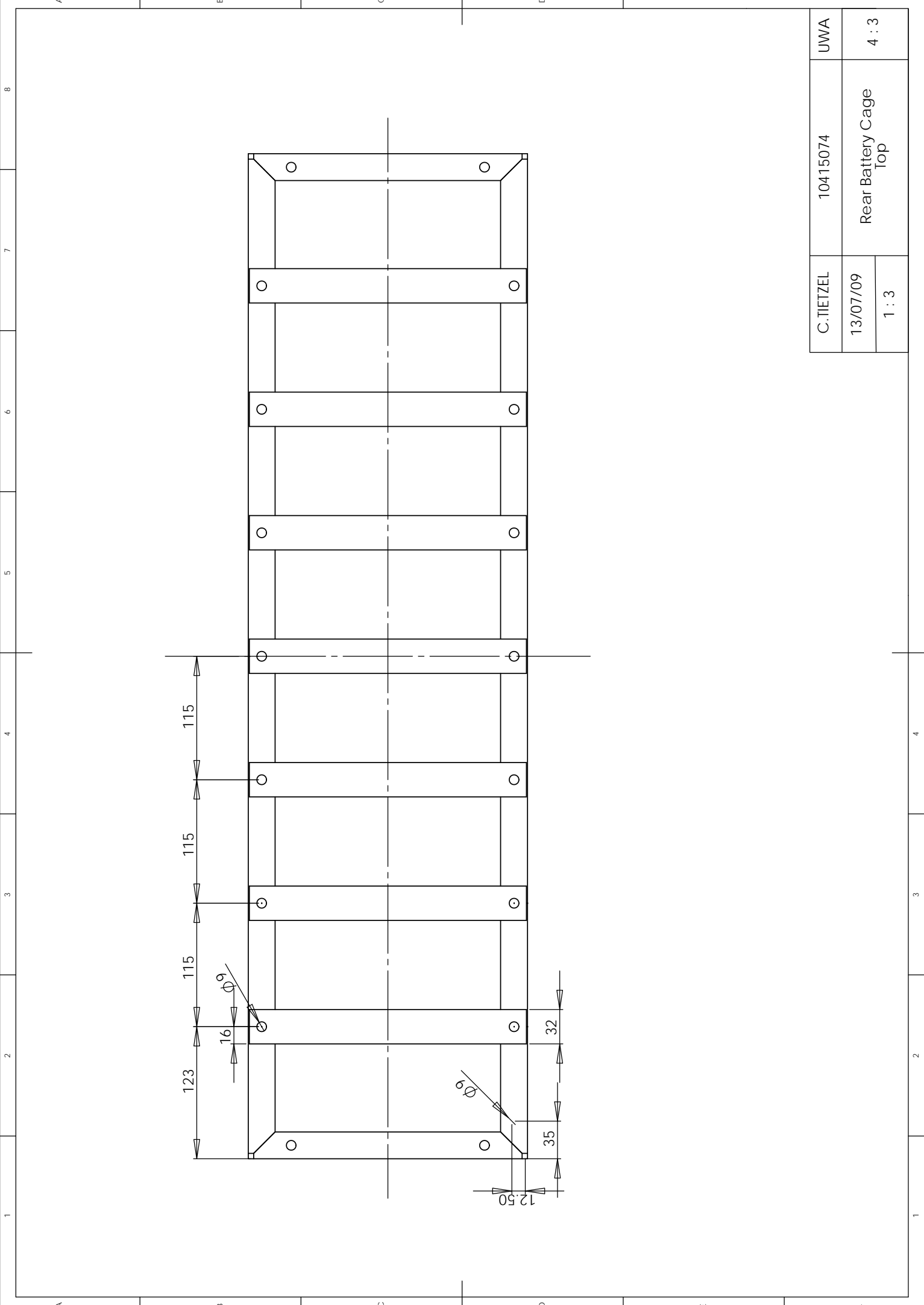


All steel angle stock is 25 x 25 x 5  
 All flat bars are 32 x 3  
 All holes are 9mm diameter and bolts M8  
 All joints are welded except the bolted joints on the top

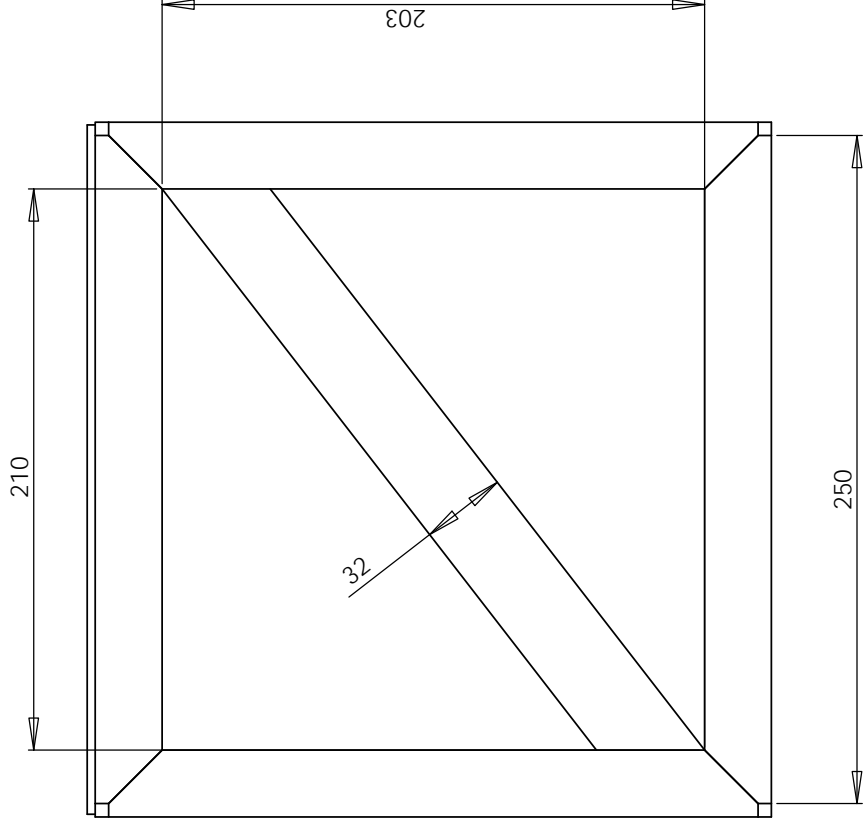
|            |                   |       |
|------------|-------------------|-------|
| C. TIETZEL | 10415074          | UWA   |
| 13/07/09   | Rear Battery Cage | 4 : 1 |
| 1 : 3      | Isometric         |       |



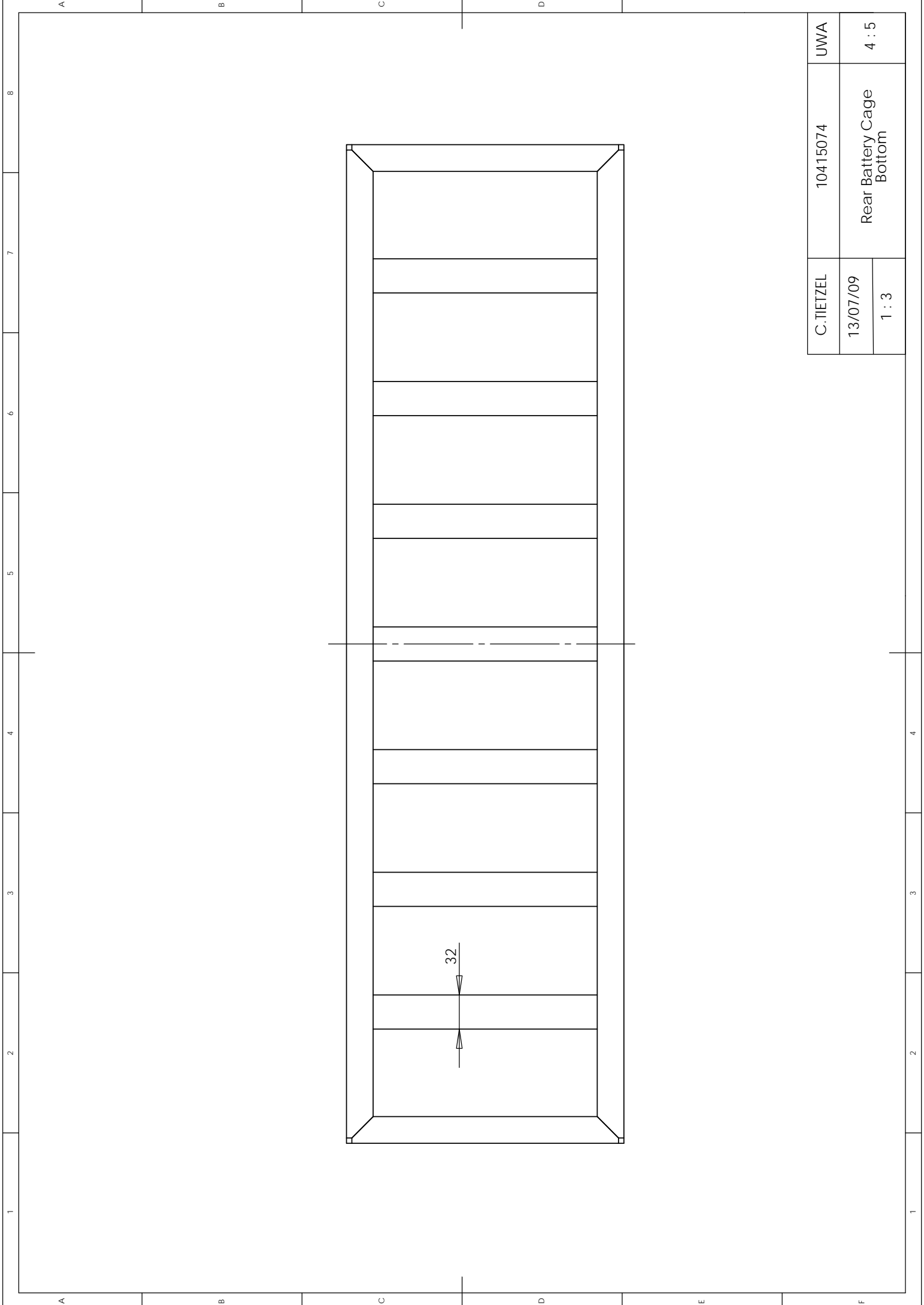
|            |                            |       |
|------------|----------------------------|-------|
| C. TIETZEL | 10415074                   | UWA   |
| 13/07/09   | Rear Battery Cage<br>Front | 4 : 2 |
| 1 : 3      |                            |       |



|            |                          |       |
|------------|--------------------------|-------|
| C. TIETZEL | 10415074                 | UWA   |
| 13/07/09   | Rear Battery Cage<br>Top | 4 : 3 |
| 1 : 3      |                          |       |



|            |                            |       |
|------------|----------------------------|-------|
| C. TIETZEL | 10415074                   | UWA   |
| 13/07/09   | Rear Battery Cage<br>Right | 4 : 4 |
| 1 : 2      |                            |       |



|            |                          |       |
|------------|--------------------------|-------|
| C. TIETZEL | 10415074                 | UWA   |
| 13/07/09   | Rear Battery Cage Bottom | 4 : 5 |
| 1 : 3      |                          |       |

#### 8.14 Appendix N – Summary of Pressures Applied to each Battery Cage

|                                     |          | <b>Fuel tank battery cage</b> | <b>Central battery cage</b> | <b>Rear battery cage</b> |
|-------------------------------------|----------|-------------------------------|-----------------------------|--------------------------|
| <b>Surface area (m<sup>2</sup>)</b> | Front    | 0.02816                       | 0.05110                     | 0.05685                  |
|                                     | Side     | 0.01701                       | 0.03220                     | 0.02305                  |
|                                     | Rear     | 0.03542                       | 0.05110                     | 0.05685                  |
|                                     | Vertical | 0.03139                       | 0.05984                     | 0.05631                  |
| <b>Pressure (N/m<sup>2</sup>)</b>   | Front    | 88,039                        | 396,216                     | 232,582                  |
|                                     | Side     | 109,311                       | 471,584                     | 430,227                  |
|                                     | Rear     | 34,997                        | 198,108                     | 116,291                  |
|                                     | Vertical | 39,490                        | 169,173                     | 117,406                  |

**Table 24:** Required pressures each battery cage must withstand.

#### 8.15 Appendix O – Safety Induction Key Points Outlined

For access to the G50 laboratory a safety induction was performed, with the major points outlining:

- Keep the laboratory clean and tidy
- Shoes must be worn at all times
- Long hair must be tied back
- Safety glasses, ear protection and gloves must be worn during appropriate operations
- No food, drink or smoking is allowed within the laboratory
- The emergency number is 2222 from the UWA telephones or 6488 2222 from any telephone
- Be aware of other people operating within your immediate area and do not distract them
- In case of a fire, activate the nearest fire alarm and do not attempt to put it out unless you know what you are doing. Proceed to the evacuation area
- The assembly area for evacuation is in the Maths building courtyard
- Be aware of the nearest first aid box within the room
- Generally double adapters, piggyback plugs and extension lead should not be used
- For heavy equipment, be sure to obtain help if needed, otherwise bend your knees and lift with your legs
- When jacking up a vehicle, adequately sign off the area
- As high voltage equipment is being used in the vehicles, do not touch high voltage electrical components without a qualified electrician

- Adequately seal and mark all electrical equipment installed in the vehicles
- If a person is shocked medical advice must be sought, even as a precaution. The WA Electrical Regulations require that all electrical accidents be reported. Notify the UWA Technical Officer on 6488 2031 or the UWA Electrical Supervisor on 6488 2016 and also complete a UWA incident/injury report form (UWA Safety & Health Manager 2007)
- Report all hazards and unsafe conditions.

The UWA workshops have their own set of general safety regulations which are conveyed during an induction and are located on the UWA website (UWA Occupational Therapist 2001). A safety induction form must be completed before operating unsupervised within the workshops (School of Mechanical Engineering 2009). The key regulations include the above mentioned with some of the additional requirements including:

- Safety glasses must always be worn at all time
- Students must have a workshop staff member present to operate within
- Advice and approval must be gained to operate all equipment within the workshop
- Machines must be used for their intended purpose.

#### 8.16 Appendix P – Safe Operating Procedures

Machinery required for operation within the workshops during fabrication includes the sheet metal cutting guillotine, drill press, lathes, and MIG welding was performed by the workshop staff. These each have their own safe operating procedures (UWA Occupational Therapist 2001) outlined further.

Safe operating procedure for sheet metal cutting guillotine:

- Ensure the cutting table is kept free of tools and clean
- Only cut materials within the capacity of the machine
- Take care when lifting and inserting the sheet metal into the machine
- Be aware of sharp edges
- Only one person should operate the machine at one time
- Hold the sheet metal firmly and ensure it has adequate support when operating the machine

- Ensure fingers are clear from the guillotine before cutting
- Using gloves, all scrap material should be put in the bin.

Safe operating procedure for drill press:

- Clean the workspace
- Ensure the drill bit is tightened with the chuck key and removed from the drill chuck
- Ensure the component to be drilled is adequately clamped or set against stop bars
- Turn on the drill and lower it at a steady rate to continually cut the material
- Never leave the drill press running unattended
- Turn off the drill press first and clean the workspace of all swarf
- Replace all drill bits, chucks and clamps to their original location.

Safe operating procedure for use on the lathes (UWA Occupational Therapist 2001):

- The isolating switch must be off while adjustments are made to the machine, for example gear changing, when removing swarf or when it is not in use
- All controls must be in the neutral position before the lathe is started
- Measuring instruments or any other components should not be kept on the moving saddle, lathe bed or head stock
- For capstan lathes, stock bar guards should be provided and kept adjusted so that the bar stock does not project beyond the limits of the guard
- The chuck face-plate or other holding devices should be effectively guarded.

Safe operating procedure for welding (UWA Occupational Therapist 2001):

- Use the least toxic material or process possible
- Ensure there is adequate ventilation in the form of a moveable exhaust hood, or use appropriate respiratory protective devices as there are toxic fumes given off from many materials and coatings
- Use the appropriate heat protection equipment including gloves for handling the material
- Use the appropriate eye protection and welding shield.